QATAR UNIVERSITY

COLLEGE OF PHARMACY

THE IMPACT OF PAMAM DENDRIMERS ON HER2-POSITIVE BREAST CANCER AND THE EARLY STAGES OF EMBRYOGENESIS

BY

HADEEL KHERALDINE

A Thesis Submitted to

the College of Pharmacy

in Partial Fulfillment of the Requirements for the Degree of

Master of Science in Pharmacy

June 2020

COMMITTEE PAGE

The members of the Committee approve the thesis of
Hadeel Kheraldine defended on 2nd of April 2020.

_____
Dr. Ousama Rachid, PhD
Thesis Supervisor

_____
Dr. Ala-Eddin Al Moustafa, PhD
Thesis Co-Supervisor

_____
Dr. Saghir Akhtar, PhD
Thesis Co-Supervisor

Approved:

_____

Mohammad Diab, Dean, College of Pharmacy

ABSTRACT

KHERALDINE, HADEEL, S., Masters: June 2020, Pharmaceutical Sciences

Title: The Impact of PAMAM Dendrimers on HER2-Positive Breast Cancer and the Early Stages of Embryogenesis

Supervisor of Thesis: Dr. Ousama M. Rachid

Poly (amidoamine) (PAMAM) dendrimers are widely used in drug delivery systems and gene transfection as drug carriers. They also exert several biological effects including modulating gene expression and interfering with transactivation of epidermal growth factor receptors, EGFR and HER2. HER2 is a major oncogene driving the proliferation of HER2-positive breast cancer cells and represents an important drug target in the treatment of breast cancer. However, it is not known whether PAMAMs can inhibit the activation of HER2 in breast carcinogenesis and whether this effect depends on the physicochemical properties of these polymers. In this study, we explored the anti-cancer effects of different generations and surface chemistries of PAMAMs on HER2-positive breast cancer cell lines. Additionally, the outcome of PAMAM dendrimers was examined in the early stages of embryogenesis.

The anti-cancer effects of PAMAMs including cell viability, colony formation, and apoptosis were studied in HER2-positive breast cancer cells; SK-BR3 and ZR-75. Additionally, the effects of PAMAMs on angiogenesis and embryogenesis were investigated using a chicken embryo model. The underlying mechanisms of action were explored by RT-PCR and Western blotting analysis.

PAMAMs exhibited significant anti-cancer effects that were more pronounced with cationic (-NH2) dendrimers, compared to neutral (-OH) or anionic (-COOH) and were greater in cationic G_6 compared to cationic G_4. Cationic G_6 PAMAMs significantly decreased the viability of HER2-positive breast cancer cell lines down to

5.1% in SK-BR3 and to 5.7% in ZR-75 cells (p<0.001), in a dose and time-dependent fashion. Cationic polymers also resulted in cell cycle deregulation as well as inhibiting colony formation in soft agar compared to controls and to other PAMAMs studied (p<0.05). Cationic PAMAMs inhibited the phosphorylation of ErbB2, EGFR, and ERK1/2 and upregulated JNK1/2/3, similar to lapatinib, a clinically used inhibitor of HER2 receptor phosphorylation. Cationic PAMAMs also inhibited the angiogenesis of the chorioallantoic membrane (CAM) of the chicken embryo model. However, they exhibited substantial toxicity to the embryos at the early stages of their normal development.

The exhibited anti-HER2 breast cancer effects of PAMAMs were generation and surface chemistry-dependent, and might be investigated further for the potential treatment of this cancer in the clinic.

Key Words: PAMAMs, G_6, G_4, $G_{5.5}$, HER2-positive breast cancer, SK-BR3, ZR-75, cell viability, cell cycle analysis, soft agar assay, chicken embryos, chorioallantoic membrane, angiogenesis, embryogenesis, apoptosis.

GRAPHICAL ABSTRACT

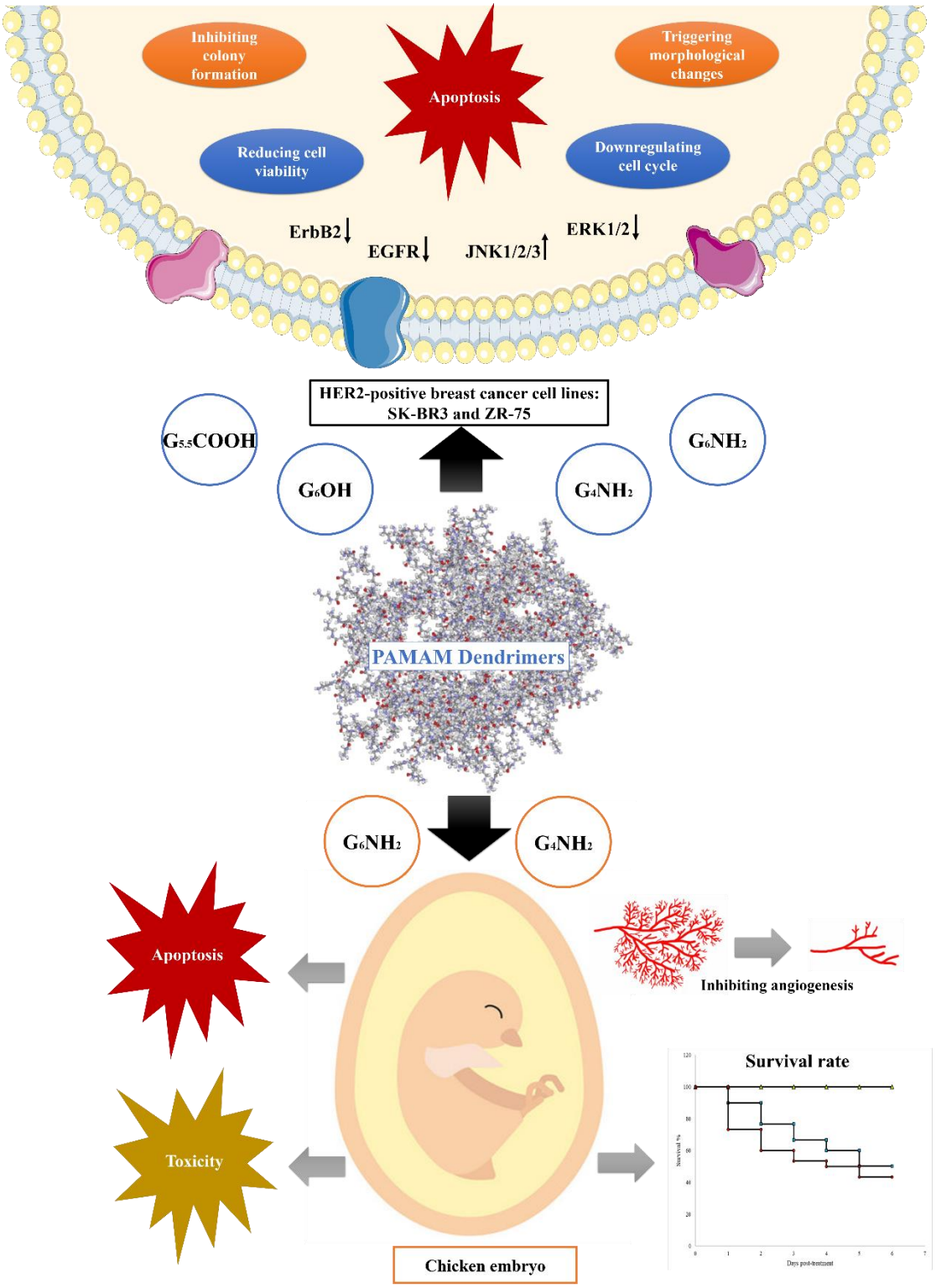

DEDICATION

This thesis is dedicated to my beloved ones, the ones who inspired me and the ones who left a good impact in my life

ACKNOWLEDGMENTS

I would like to express my sincere appreciation and gratitude to my advisor Dr. Ousama Rachid for his continuous guidance, support, and patience. I would like also to thank my co-supervisors; Dr. Ala-Eddin Al Moustafa, for sharing his experience in the lab techniques with me, and Dr. Saghir Akhtar for guiding and motivating me. I consider myself very lucky for being supervised by such a great team, as without them this work would not have been achieved. My deepest thanks to Dr. Farhan Cyprian for his valuable help in the cell cycle analysis, and Dr. Moussa Alkhalaf for his support in reviewing this work.

Also, many thanks to my lab partners, especially Ishita, Ayesha, and Hashim who taught me many lab techniques, and my colleagues at the MSc program who created the best work atmosphere which made this experience amazing.

My appreciation also extends to the College of Pharmacy faculty members, who have taught me a lot during my MSc program, and to the administrative staff and the dean, Dr. Mohammed Diab, for their continuous assistance and help. I would also like to acknowledge Qatar University for funding my project by three grants; (QUST-1-CPH-2020-12), (QUST-2-CPH-2019-18), and (QUST-1-CPH-2019-6).

Many thanks to the College of Pharmacy, College of Medicine and Biomedical Research Center lab members and staff for giving me the chance to work in their labs.

Last but not least, I would like to thank my valuable treasure in life; my family, my husband, and my friends. Thank you for believing in me, without you, I would never be the person I am today.

TABLE OF CONTENTS

LIST OF TABLES

LIST OF FIGURES

LIST OF ABBREVIATIONS

A549: A pulmonary adenocarcinoma cell line

ABCB1: ATP-binding cassette, subfamily B (MDR/TAP), member 1

ARNTL2: Aryl hydrocarbon receptor nuclear translocator like 2

ART4: ADP-ribosyltransferase 4 (Dombrock blood group)

AT1: Angiotensin receptor 1

ATCC: American type culture collection

ATF-3: AMP-dependent transcription factor 3

ATM: Ataxia-telangiectasia mutated kinase

Bax: BCL-2-associated X protein

BCL-2: B-Cell lymphoma-2

BSA: Bovine serum albumin

BTG2: B-cell translocation gene 2

C2IIa: Clostridium botulinum C2 toxin

C5orf23: Chromosome 5 open reading frame 23

Caco-2: A human colorectal adenocarcinoma cell line

CAM: Chorioallantoic membrane

CHD4: Chromodomain helicase DNA binding protein 4

CHERP: Calcium homeostasis endoplasmic reticulum protein

CHF: Congestive heart failure

CXYorf3: Homo sapiens chromosome X and Y open reading frame 3

DMSO: Dimethyl sulfoxide

DNA: Deoxyribonucleic acid

dsDNA: Double-stranded DNA

EDTA: Ethylenediaminetetraacetic acid

EGF: Epidermal growth factor

EGFR: Epidermal growth factor receptor

ELISA: Enzyme-linked immunosorbent assay

ENST00000370419: Regulating synaptic membrane exocytosis protein 1 (Rab3-interacting molecule 1) (RIM 1)

ErbB2: Erythroblastic oncogene B 2

ERK1/2: Extracellular signal-regulated protein kinase

FBS: Fetal bovine serum

FGF: Fibroblast growth factor

FOLH1: Folate hydrolase (prostate-specific membrane antigen) 1, transcript variant 1

FOXA-2: Forkhead box protein A2

G: Generation of PAMAMs

GAPDH: Glyceraldehyde 3 phosphate dehydrogenase

GIPR: Gastric inhibitory polypeptide receptor

HaCaT: A spontaneously transformed human keratinocyte cell line

HEK293: A human embryonic kidney cell line

HER2: Human epidermal growth factor receptor type 2

HeLa: An immortalized cervical cancer cell line

HepG2: A hepatocellular carcinoma cell line

HIAPP: Human islet amyloid polypeptide

HL7702: A human liver cell line

HNME-E6/E7: A human normal mammary epithelial cell line immortalized by E6/E7 gene

HPV: Human papillomavirus

HUVEC: A human umbilical vein endothelial cell line

IC50: Half maximal inhibitory concentration

IL-6: Interleukin 6

IL-β: Interleukin 1 beta

INHB-A: Inhibin beta A

J774A.1: A macrophage cell line

JNK: c-Jun N-terminal kinases

KB cells: A subline of the HeLa cell line

KCNJ10: Potassium inwardly rectifying channel, subfamily J, member 10

MAPRE-2: Microtubule associated protein RP/EB 2

MATN1: Cartilage matrix protein precursor (Matrilin-1)

MBC: Minimum bactericidal concentration

MIC: Minimum inhibitory concentration

MIP-2: Macrophage inflammatory protein 2

MIN6: A mouse insulinoma cell line

MMP: Mitochondrial membrane potential

MMP3: Matrix metalloproteinase 3

MMP9: Matrix metalloproteinase 9

MRSA: Methicillin-resistant Staphylococcus aureus

mTOR: Mammalian target of rapamycin

NAC: N-acetyl cysteine

NF-kB: Nuclear factor kappa-light-chain-enhancer of activated B cells

NFKBIA: Nuclear factor-kappa-B-inhibitor alpha

NIT-1: A mouse pancreatic beta-cell line

OR2W3: Olfactory receptor, family 2, subfamily W, member 3

P38 MAPK: P38 mitogen-activated protein kinases

PA63: Binary anthrax toxin

PAMAMs: Poly (amidoamine) dendrimers

PBECs: A primary human bronchial epithelial cell line

PC-12: A pheochromocytoma cell line

PDE11A: Phosphodiesterase 11A, transcript variant 4

PEG: Polyethylene glycol

PF: Polyfect

PHF5A: PHD-finger domain protein 5A

PI: Propidium iodide

PLC: Phospholipase C

PLHC-1: A Poeciliopsis lucida hepatocellular carcinoma-1 cell line

PTGFR: Prostaglandin F receptor (FP), transcript variant 2

PTPRR: Protein tyrosine phosphatase, receptor type, R, transcript variant 1

PVDF: Polyvinylidene fluoride

RAW 264.7: A murine macrophage-like cell line

RBCs: Red blood cells

RGS9BP: Regulator of G protein signaling 9 binding protein

RIPK-1: Receptor-interacting serine/threonine-protein kinase 1

RNA: Ribonucleic acid

ROS: Reactive oxygen species

RSU1: Ras suppressor protein 1, transcript variant

RT-PCR: Reverse transcription polymerase chain reaction

SDS: Sodium dodecyl sulfate

SERPINA-4: Serine proteinase inhibitor alpha 4

SF: Superfect

SH-SY5Y: A human neuroblastoma cell line

siRNA: Small interfering RNA

SK-BR3: A human HER2-positive breast cancer cell line

SLC8A1: Na+/Ca2+ exchanger isoform

TGFβR-1: Transforming growth factor beta receptor 1

THP-1: A human monocytic cell line

TNF-α: Tumor necrosis factor alpha

TNF-R: Tumor necrosis factor receptor

TRIM49: Tripartite motif-containing 49

U937: A histiocytic lymphoma cell line

UGT8: UDP glycosyltransferase 8 (UDP-galactose ceramide galactosyltransferase)

USP29: Ubiquitin specific peptidase 29

VEGF: Vascular endothelial growth factor

VEGFC: Vascular endothelial growth factor C

VEGFR: Vascular endothelial growth factor receptor

Vero: A monkey kidney epithelial cell line

VSMC: Vascular smooth muscle cells

WI-26 VA4: A human lung cell line

ZR-75: A human HER2-positive breast cancer cell line

zVAD-fmk: A caspase inhibitor

CHAPTER 1: INTRODUCTION

1.1. Poly (amidoamine) dendrimers (PAMAMs)

The role of polymers as active compounds for therapeutic applications has dominated the pharmaceutical polymers field. This area of research is called “polymer therapeutics”, where biologically active polymers can behave either as bioactive compounds or as inert carriers conjugated to a drug(s) (1). Most of the bioactive polymers are designed to target cancer as well as other diseases such as rheumatoid arthritis, hepatitis B and C, diabetes, and ischemia (2). Many studies were conducted on novel branched nano-sized polymeric architectures, such as dendrimers, and their biological uses are now under development.

Dendrimers are spheroidal, highly branched, cascade nano-sized polymers with a well-defined molecular architecture and a low polydispersity (3,4). They consist of an inner core that can be either hydrophobic or hydrophilic, surrounded by layers (generations) of covalently linked repeated monomers (Figure 1), and a specific number of end functional groups. The size and surface charge of dendrimers can be highly controlled during synthesis, showing their high degree of functionality (3–5).

Poly (amidoamine) dendrimers (PAMAMs) are the most studied type of dendrimers besides being the first type to be synthesized and commercialized (6). They were first introduced in 1985 by Professor Donald A. Tomalia as a new class of dendrimers, named ‘starburst polymers’ (7). Since then, PAMAM dendrimers have been used for many applications in the biomedical field and opened new doors in nanotechnology (6). Each generation of PAMAM dendrimers has a larger diameter and twice the number of terminal functional groups compared to the lower generation (Table 1) (3,4). Also, the surface chemistry of PAMAM dendrimers can be either with amine groups (cationic), carboxyl groups (anionic), or hydroxyl groups (neutral).

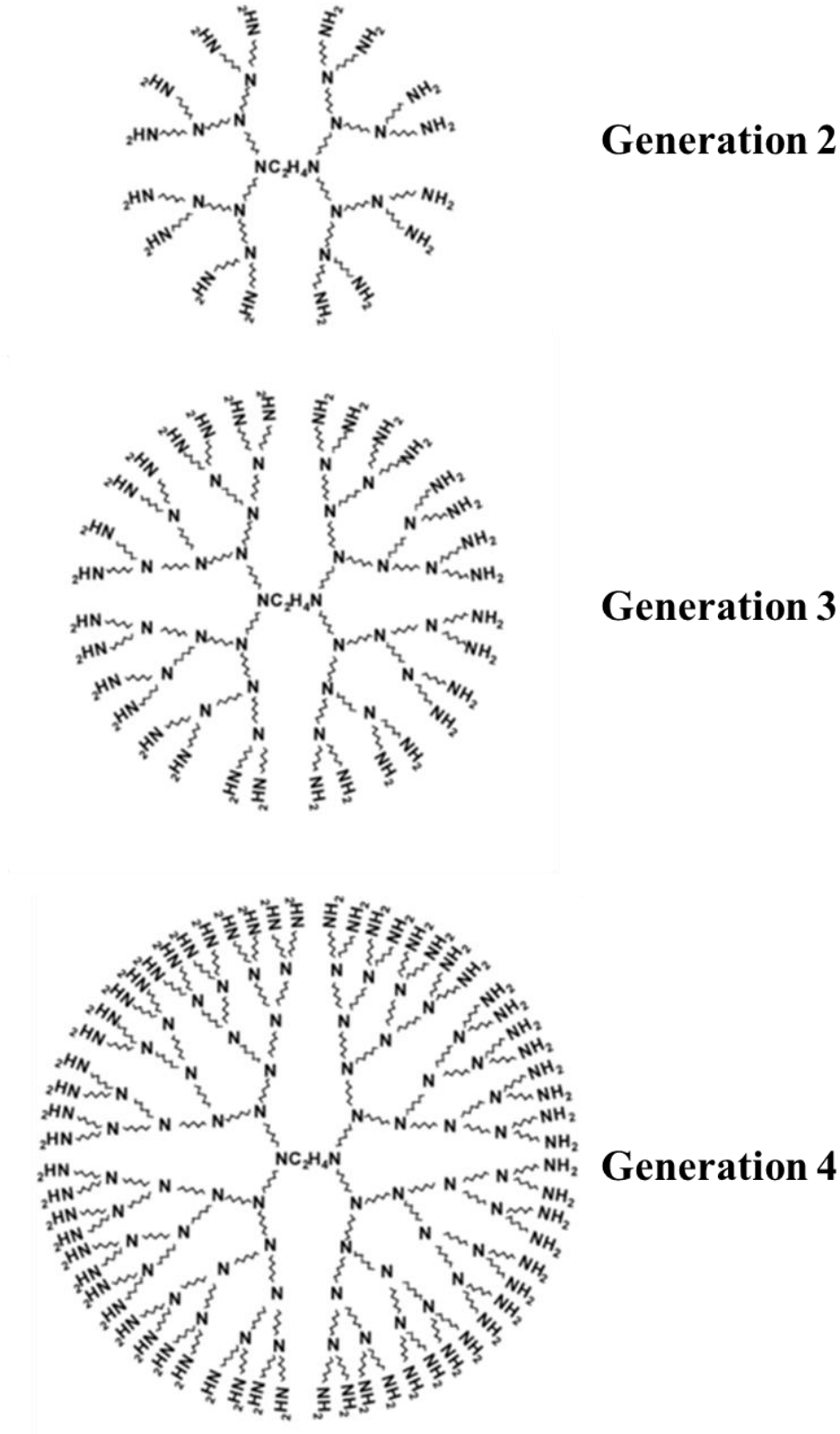

Figure 1. Amino-terminated PAMAM dendrimers generation 2, 3, and 4.

After synthesis, PAMAM dendrimers can be subjected to further modifications such as reducing branching and increasing internal volume or drug-carrying capacity, which creates fractured or "activated" dendrimers (8); for example, activated G_6 cationic PAMAMs are commercially known as Superfect (SF). On the other hand, Polyfect (PF) represents non-activated (intact) G_6 cationic PAMAMs (9).

PAMAM dendrimers serve as efficient carriers in drug delivery as they enhance drug properties. Bioconjugation of drugs and targeting moieties is possible in the interior void space (usually small molecules), which results in reducing drug toxicity and creating a controlled-release form (4). Moreover, PAMAMs surface functional groups allow molecules conjugation, as they can be modified according to specific needs and potential applications (4).

Table 1. Calculated properties of primary amino-terminated PAMAM dendrimers by generation (10).

Generation	Molecular Weight (Da)[1]	Measured Diameter (Å)[2]	Number of Surface Groups
0	517	15	4
1	1,430	22	8
2	3,256	29	16
3	6,909	36	32
4	14,215	45	64
5	28,826	54	128
6	58,048	67	256
7	116,493	81	512
8	233,383	97	1,024
9	467,162	114	2,048
10	934,720	135	4,096

[1] Dalton.

[2] Angstrom.

Surprisingly, highly sensitive assays showed that naked PAMAM dendrimers themselves are not inert, and may act as nanodrugs for several conditions. For example, they can alter gene expression patterns, interact with cellular components, and modulate inflammatory responses, indicating that they have multivalence properties (6,11,12). However, PAMAM dendrimers applications are still restricted due to their cytotoxicity, which raises concerns on these highly appreciated polymers (13).

In this introduction, we provide an overview of PAMAM dendrimers pharmacological effects in altering gene expression patterns, interfering with important cell signaling pathways, interacting with red blood cells (RBCs), interacting with cellular components, inducing cellular death, modulating inflammatory responses, and expressing antibacterial effects (Figure 2). These biological actions mostly depend on the administrated dose of PAMAMs, their surface charge, and their generation.

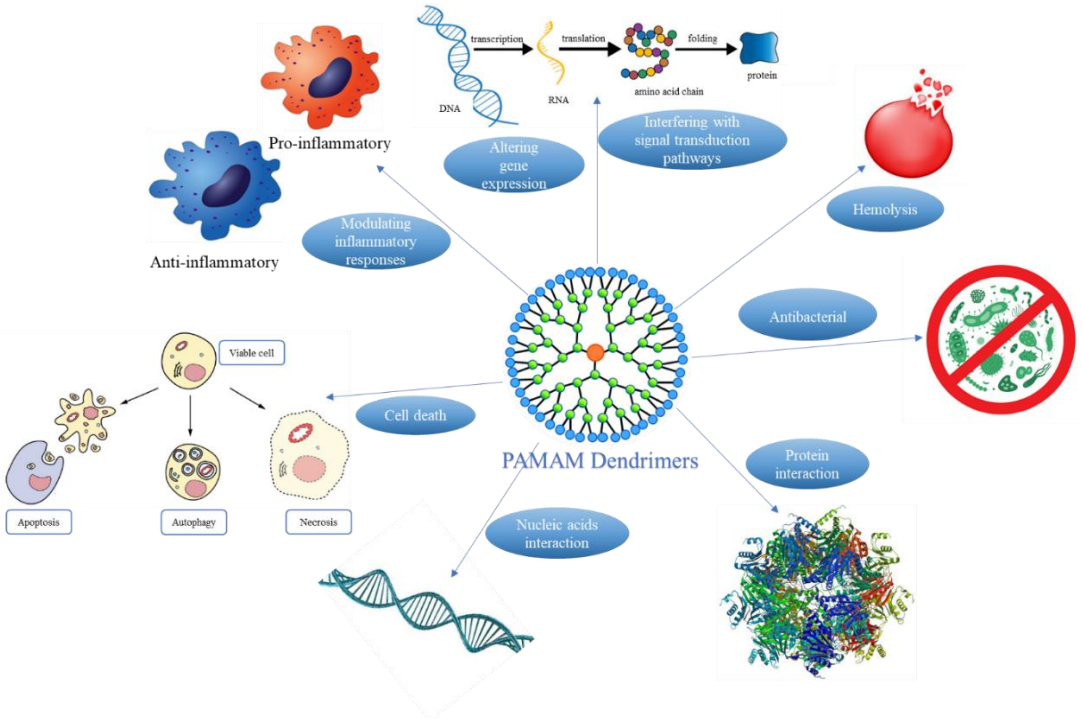

Figure 2. A summary of PAMAMs biological effects.

1.1.1. Altering gene expression pattern

Gene therapy provided a major contribution to the treatment of cancer and chronic illnesses. PAMAM dendrimers are widely used in gene therapy to carry siRNA and oligonucleotides; particularly amino PAMAMs which possess a spherical shape and a positively charged surface in the physiological pH (6). Their surface positive charge allows to create stable associations with negatively charged phosphate groups of DNA or genes and transport them into the cells or nucleus according to the needs of the experiment (14). Aside from being effective carriers for gene transfection and gene therapy, several studies revealed that different types of naked PAMAMs themselves can alter the gene expression in different models (Table 2, Figure 3) (15).

The first study that showed the importance of gene alteration induced by PAMAM dendrimers was conducted by Hollins et al, as they suggested the employment of this effect in synergizing the levels of gene alteration obtained by siRNA (15). This study found that two PAMAM-based siRNA delivery systems, PF and SF, remarkably altered gene expression in human epidermoid carcinoma A431 cell line. The same effect was noted even when complexing PF and SF with scrambled siRNA or dsDNA. Interestingly, the extent of altering gene expression was reduced by neutralization of PAMAMs positively charged surface, which indicates the impact of PAMAMs surface chemistry in this effect (15). The role of PAMAMs architecture in altering gene expression was also observed when two contradictory impacts on epidermal growth factor receptor (EGFR) gene expression appeared, as SF increased EGFR expression whereas PF inhibited it *in vitro* and *in vivo* (15,16). Furthermore, PAMAM dendrimers were able to add benefit to cancer treatment by altering gene expression in human cervical HeLa cancer cells as illustrated by Kuo et al (17). High-density microarray analysis showed that non-activated and activated G_5 cationic PAMAMs and their dendriplexes were able to modulate PHF5A, ARNTL2, and CHD4 genes, which are

implicated in cell survival and proliferation. PAMAM dendrimers were also able to modulate the expression of many other genes related to nucleic acid binding and transcription activity (Table 2, Figure 3). The extent of gene modulation depended on the architecture of non-activated and activated PAMAMs, corresponding with what was stated by Hollins et al. These findings suggest that PAMAMs role extends from being inert vectors for cancer gene therapy to potential enhancers of the anti-cancer action (17).

The previous studies stated the impact of PAMAMs architecture in altering gene expression. Further studies compared between different surface chemistries of PAMAMs with the same generation. Cationic and neutral PAMAMs were compared in terms of modulating gene expression in primary human bronchial epithelial cells, PBECs. It was stated that cationic PAMAMs can trigger specific alterations in gene expression in PBECs at relatively safe doses and without damaging the DNA (22). These gene alterations were related to cell cycle arrest; mainly triggering downregulation of genes related to cell cycle and cell division mediated by NF-κB. However, neutral PAMAM dendrimers did not affect gene transcription. It was also found that exposing PBECs to low doses of cationic PAMAMs resulted in upregulating genes implicated in immune responses, such as TNF-R and IL-1β, as well as genes involved in cell migration and disassembly of extracellular matrix, such as MMP3 and MMP9 (22). The effect of PAMAMs on inflammatory responses is further discussed in section 1.1.6. Taken together, the previous findings emphasize the impact of the physicochemical properties of PAMAM dendrimers in modulating gene expression in several cell lines (19). This can be employed to promote siRNA gene silencing action by choosing the specific type of PAMAMs which inhibits the expression of target genes (15).

Table 2. Genes upregulated and downregulated by naked PAMAM dendrimers.

Gene	Description	Effect of PAMAMs[3]	Reference(s)
ABCB1	ATP-binding cassette, subfamily B (MDR/TAP), member 1	↑	(17)
ARNTL2	Aryl hydrocarbon receptor nuclear translocator like 2	↓	(17)
ART4	ADP-ribosyltransferase 4 (Dombrock blood group)	↓	(17)
BTG2	B-cell translocation gene 2	↑	(18)
C5orf23	Chromosome 5 open reading frame 23	↑	(17)
CHD4	Chromodomain helicase DNA binding protein 4	↓	(17)
CHERP	Calcium homeostasis endoplasmic reticulum protein	↑	(17)
CXYorf3	Homo sapiens chromosome X and Y open reading frame 3	↓	(17)
EGFR	Epidermal growth factor receptor	↑↓	(9,15,16,19–21)
ENST00000370419	Regulating synaptic membrane exocytosis protein 1 (RIM 1)	↑	(17)
ErbB2	Erythroblastic oncogene B 2	↓	(19)
ERK1/2	Extracellular signal-regulated protein kinase	↓	(9,16,20,21)
FOLH1	Folate hydrolase (prostate-specific membrane antigen) 1	↑	(17)
GIPR	Gastric inhibitory polypeptide receptor	↑	(17)
IL-1β	Interleukin 1 beta	↑↓	(18,22,23)
IL-6	Interleukin 6	↓	(23)
KCNJ10	Potassium inwardly rectifying channel, subfamily J, member 10	↓	(17)
MATN1	Cartilage matrix protein precursor (Matrilin-1)	↓	(17)
MMP3	Matrix metalloproteinase-3	↑	(22)
MMP9	Matrix metalloproteinase-9	↑	(22)
NFKBIA	Nuclear factor-kappa-B-inhibitor alpha	↑	(18)
OR2W3	Olfactory receptor, family 2, Subfamily W, member 3	↑	(17)
PDE11A	Phosphodiesterase 11A, transcript variant 4	↓	(17)
PHF5A	PHD-finger domain protein 5A	↑	(17)
PTGFR	Prostaglandin F receptor (FP), transcript variant 2	↓	(17)
PTPRR	Protein tyrosine phosphatase, receptor type, R	↑	(17)
RGS9BP	Regulator of G protein signaling 9 binding protein	↓	(17)
RSU1	Ras suppressor protein 1, transcript variant	↑	(17)
SLC8A1	Na+/Ca2+ exchanger isoform	↓	(17)
TGFβR-1	Transforming growth factor beta receptor 1	↓	(23)
TNF-α	Tumor necrosis factor alpha	↑↓	(18,23)
TNF-R	Tumor necrosis factor receptor	↑	(22)
TRIM49	Tripartite motif-containing 49	↑	(17)
UGT8	UDP glycosyltransferase 8	↓	(17)
USP29	Ubiquitin specific peptidase 29	↓	(17)

[3] ↑: Gene upregulation. ↓: Gene downregulation.

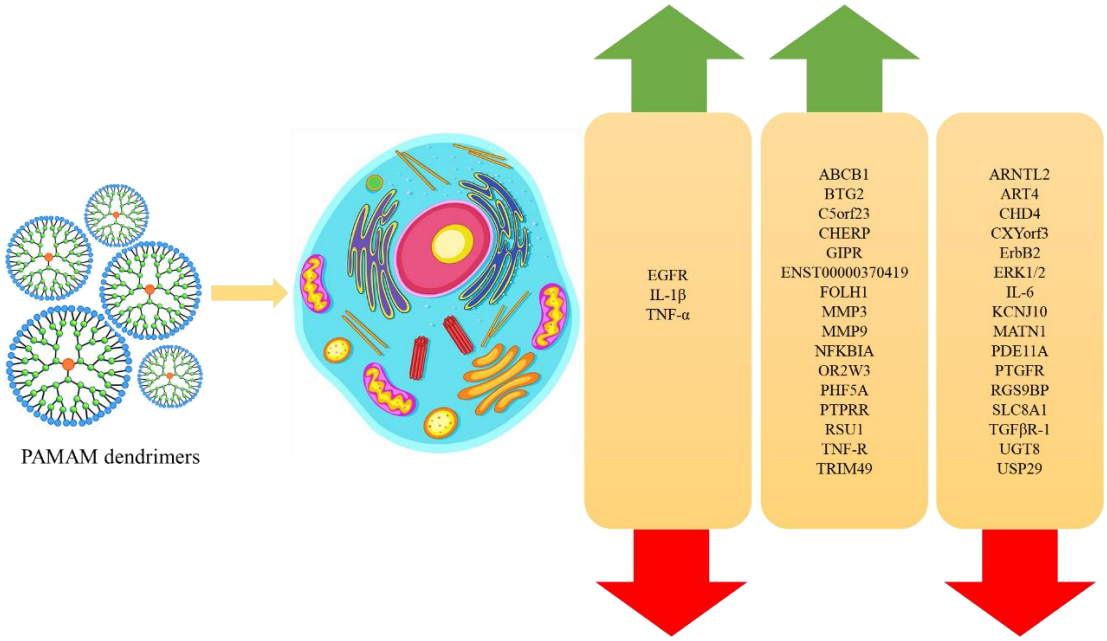

Figure 3. Genes upregulated and downregulated by naked PAMAM dendrimers.

1.1.2. Interfering with signal transduction pathways

The interaction of PAMAM dendrimers with cell signaling pathways has an essential impact on communication processes that control the basic activities of cells and organize multiple-cell actions. A study was conducted particularly on EGFR-ERK1/2 signaling pathway and p38 MAPK phosphorylation in human embryonic kidney cells, HEK293. The outcomes of this research showed for the first time that PAMAM dendrimers can alter EGFR-ERK1/2 cellular signal transduction pathway in a dose and time-dependent manner. These findings ensured that polymers used in drug delivery systems are not biologically inert, but they have intrinsic biological actions (16,20). Subsequently, *in vivo* studies in normal and diabetic male Wistar rats also revealed that both SF and PF PAMAMs can alter EGFR signaling transduction pathway, and they may act as a new group of EGFR modulators. The previous effects were dendrimer-specific, and they depended on the type of the used animal model

(normal or diabetic) with no noticeable changes in renal morphology. These findings raise hope in utilizing PAMAMs to reduce diabetes-associated vascular complications (9,16). Further, PAMAMs effects were reversible by anti-oxidants, suggesting that the mechanism of action is mediated by oxidative stress (16,20).

To gain further comprehension of the role of PAMAMs physiochemical properties in interfering with signaling pathways, a study by Akhtar et al. explored the role of different generations (G_4, G_5, G_6, and G_7) and different surface chemistries (cationic, anionic, and neutral PAMAMs) of PAMAMs on renin-angiotensin system signaling through Angiotensin II-mediated transactivation of EGFR and ErbB2 (EGFR2). Primary aortic vascular smooth muscle cells, VSMC, were used for this purpose, and results showed that G_5 cationic PAMAM dendrimers inhibited Angiotensin II/AT1 receptor-mediated transactivation of EGFR and ErbB2 in a dose and time-dependent fashion. Additionally, downstream signaling via ERK1/2 was inhibited. PAMAMs generation was linearly correlated with these effects, as the effects increased upon treatment with higher generations (G_7>G_6>G_5>G_4) (9,19). Furthermore, cationic PAMAMs exhibited the highest impact on cell signaling, followed by anionic and neutral PAMAMs. The mechanism behind G_5 PAMAMs suppression of Ang II-mediated transactivation of EGFR and ErbB2 was found to be through inhibiting the non-receptor tyrosine kinase (Src) (9,19).

1.1.3. Interaction with red blood cells and platelets

PAMAM dendrimers cytotoxicity has been widely investigated (24–26), demonstrating a general trend that cationic PAMAMs exhibit a concentration and generation-dependent cytotoxicity compared to anionic and neutral PAMAMs, which are less toxic or even non-toxic (26,27). A similar trend was found in the effect of PAMAMs on red blood cells (RBCs), as they can cause hemolysis and induce

morphological changes in RBCs, mainly because the positively charged surface of PAMAMs can interact with the negatively charged cell membrane of RBCs (28). Therefore, investigating PAMAMs blood compatibility is very important to ensure the safe application of these compounds.

In order to understand the role of PAMAMs surface chemistry in interacting with RBCs, a study tested the effect of cationic PAMAMs (G_3, G_4, G_5, and G_6), anionic PAMAMs ($G_{1.5}$, $G_{2.5}$, $G_{3.5}$, and $G_{4.5}$), and neutral PAMAMs (G_3, G_4, and G_5) on RBCs suspensions (2% hematocrit) (29). The results of this study revealed that cationic PAMAM dendrimers caused a significant and serious hemolysis compared to the anionic and neutral PAMAMs, which caused much less hemolytic effect. Induction of hemolysis by cationic PAMAMs was time, concentration, and generation-dependent, as it increased gradually from G_3 to G_6. Furthermore, the onset of hemolysis was faster upon using cationic PAMAMs compared to anionic and neutral ones at similar concentrations and generations. On the other hand, a compound with the same amino surface chemistry and different polymeric structure also caused hemolysis in RBCs. This is a strong evidence on the role of surface amino groups of cationic PAMAMs in causing RBC lysis and aggregation (29). Another investigation also suggested that RBCs hemolysis induced by PAMAM dendrimers is mainly due to changing the mobility and arrangement of fatty acid chains in the bilayer of RBCs cellular membrane (27).

Different studies examined the impact of cationic PAMAM dendrimers (G_2, G_3, and G_4) on RBCs morphology and membrane integrity in human blood samples. Results revealed that PAMAM dendrimers can interact with RBCs causing various morphological changes (27,30). The nature of these changes was subjected to the used concentration of cationic PAMAMs, i.e. a concentration of 1 nM induced echinocytic

transformation, using 10 nM elongated the cells and created spindle-shaped forms, and finally, using 100 nM created drepanocyte-like cells. In addition, higher concentrations were needed to cause similar shape transitions upon using lower generations of PAMAMs (G_2 and G_3), showing the generation-dependency of this action (27). Similar results were obtained from another study, as G_4 cationic PAMAMs induced echinocytic transformation at a concentration of 10 nM, and a small number of RBCs were elongated and turned to a spindle-shaped cells (Figure 4). Spherocyte-like cells were formed when higher concentrations of PAMAMs were used (100 nM) (30). Together, it can be stated that PAMAMs interaction with RBCs is dose-dependent.

Other studies looked into the effect of G_7 cationic PAMAMs on platelets. They concluded that these cationic polymers can alter platelet morphology and function, accompanied by an increase in their aggregation. In addition, PAMAMs triggered blood clot in zebrafish embryos *in vivo* (31,32). Another study used different types of PAMAMs with different surface chemistries to investigate the impact of PAMAMs on platelets, and found that only cationic PAMAMs and not anionic or neutral ones can induce platelet aggregation (33). In rodents, administering cationic PAMAMs intravenously produced a disseminated intravascular coagulation-like condition, resulting in rapid mortality (34). Altogether, these data support that the trend of PAMAMs toxicity towards RBCs and platelets is surface chemistry, generation, and dose-dependent.

Interestingly, the antigen-antibody reaction was impaired after applying $G_{4.5}$ anionic PAMAMs on RBCs, while similar concentration of G_5 cationic and neutral PAMAMs did not cause a visible impact on the RBCs agglutination. This may indicate that this effect is not caused by the dendrimer itself, but by the interaction between the surface of RBCs and $G_{4.5}$ anionic PAMAMs (35).

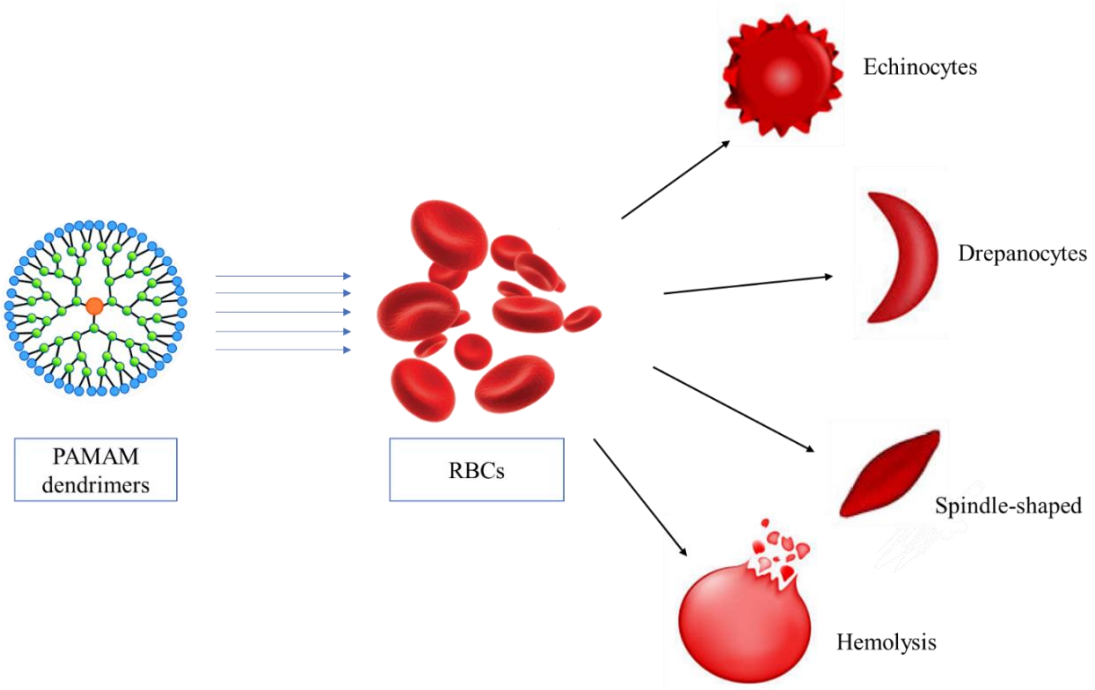

Figure 4. Effect of PAMAMs on RBCs morphology.

1.1.4. Interactions with cellular components

PAMAM dendrimers were found to interact with cellular and subcellular structures depending on the surface chemistry of the used PAMAMs. These interactions may change the function of the substrate in a desired manner or even induce cellular toxicity (13). For example, G_3 neutral PAMAMs were found to bond strongly with human islets amyloid polypeptide (hIAPP) monomers in pancreatic MIN6 and NIT-1 cells in mouse islets. This resulted in inhibiting hIAPP aggregation and thus, shutting down its toxicity and contributing to the treatment of type-2 diabetes (36). It was also found that PAMAM dendrimers prevented the generation of hIAPP by stopping its polymerization, mainly due to reducing the formation of interpeptide contacts and hydrogen bonds (36). Another study compared between similar sizes of PAMAMs with opposite surface charges to see the role of surface chemistry in PAMAMs biological actions. In that study, the impact of G_4 cationic and $G_{3.5}$ anionic PAMAM dendrimers

on the assembly and function of tight junctions in human colorectal adenocarcinoma cell line (Caco-2) was assessed. For this purpose, PAMAMs effect on transporting a small marker of permeability (mannitol) was investigated. Results revealed that tight junctions were not opened upon using anionic PAMAMs, whereas cationic PAMAMs changed tight junctions allowing mannitol transportation. The mechanism behind this effect was linked partially with the PLC-dependent signaling pathway. Further, cationic PAMAMs released intracellular calcium stores and opened tight junctions which allowed small molecules transport and calcium signaling. Besides, PAMAMs charge density resulted in additional intracellular interactions that need further investigation (37).

Furthermore, cationic PAMAM dendrimers were able to block the pore-forming B components of the binary anthrax toxin (PA63) and clostridium botulinum C2 toxin (C2IIa) at low concentrations, presenting a novel biological action. Therefore, by blocking these pores, cationic PAMAMs inhibited transporting the A components from endosomes to the cytosol of target cells. As a result, HeLa and Vero cell lines were protected from intoxication. These data show a novel potential effect of PAMAM dendrimers which can protect human target cells from the toxicity of binary toxins from pathogenic bacteria (38).

1.1.5. Triggering cellular death

PAMAM dendrimers' unique architecture and special properties make them useful in several applications in different fields. However, despite all their benefits in science and nanotechnology, several disadvantages exist, which limit their use (13). Similar to most polymeric delivery systems, PAMAM dendrimers show some extent of toxicity. This toxicity usually depends on the type of dendrimers, generation, dose, and surface chemistry. Positively charged PAMAMs are often the most toxic (13,39). Thus,

it is critical to study the potential cytotoxic behaviors of PAMAM dendrimers and their underlying mechanisms of action. We will discuss a few studies that investigated mechanisms of cellular death induced by PAMAM dendrimers: autophagy, apoptosis, and necrosis (Figure 5).

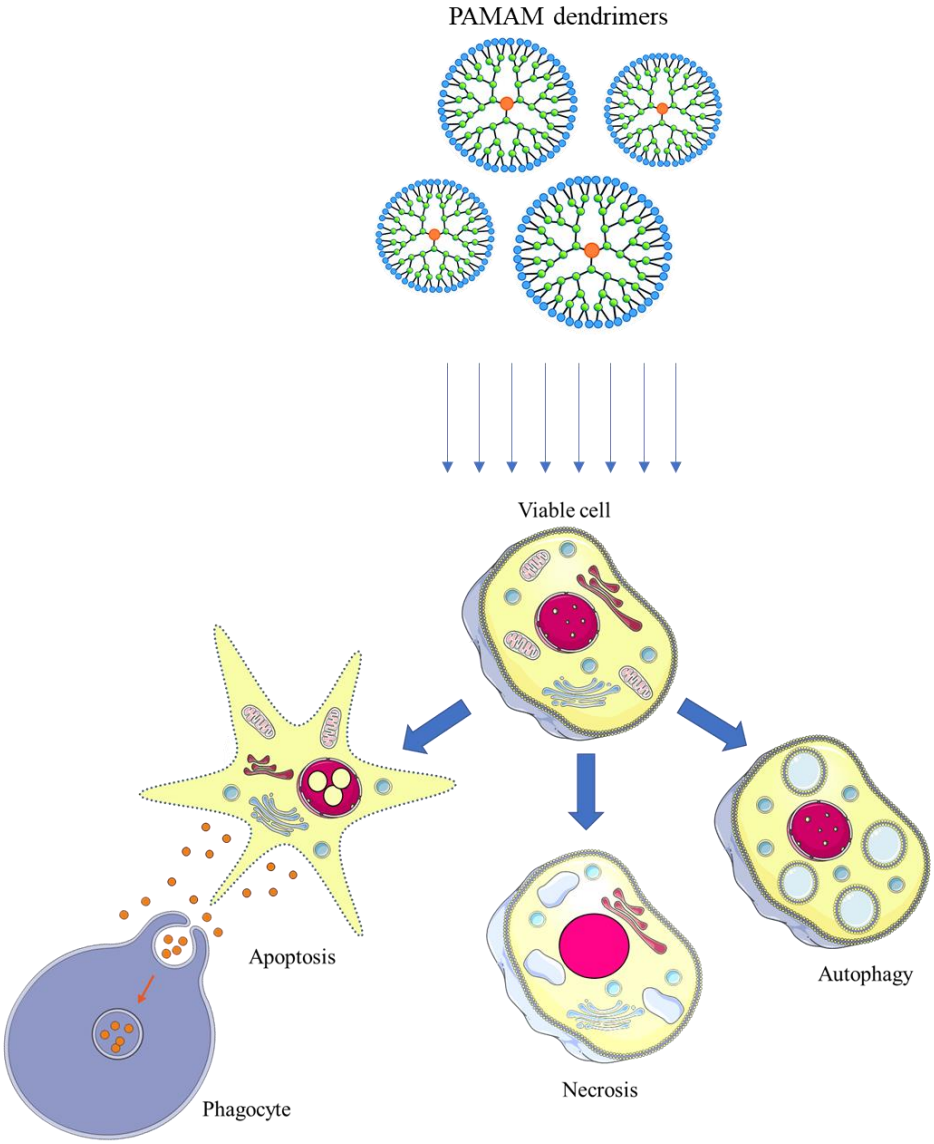

Figure 5. Induction of cell death by PAMAM dendrimers.

1.1.5.1.Autophagy

Cationic PAMAM dendrimers were proven to trigger autophagy in different cell lines. G_3 cationic PAMAMs specifically induced the accumulation of autophagosomes in human lung adenocarcinoma A549 cells. However, when hallmarks of apoptosis were assessed (DNA fragmentation and Caspase-3 activity), no apoptosis was observed in the studied cells upon treatment with G_3 cationic PAMAMs (40). Another study stated that cationic G_5 PAMAMs could trigger autophagy in HepG2 hepatocellular carcinoma cells and thus, may contribute to hepatocellular carcinoma therapy (41). Cationic G_5 PAMAMs also induced both growth inhibition and autophagy in human glioma cell lines and human liver cells, HL7702 (42,43). The mechanism of autophagy induced by PAMAMs was through decreasing phosphorylation of Akt/mTOR signaling pathway and activating ERK1/2 signaling in a dose and time-dependent manner (40–43). PAMAMs induction of autophagy was also mediated by producing reactive oxygen species, ROS (41,42,44). Further investigation was conducted regarding the association between oxidative stress and autophagy in neurotoxicity triggered by G_5 cationic PAMAMs in rat pheochromocytoma cell line, PC-12, and human neuroblastoma cell line, SH-SY5Y. It was found that inhibiting ROS production resulted in a decrease in the autophagic effects produced by PAMAM dendrimers on neuronal cells. Moreover, the application of antioxidants such as NAC, lipoic acid, and tocopherol was suggested by this study to enhance the security of PAMAM dendrimers against neuronal cell. Suppression of autophagy reversed cell death caused by PAMAMs as well in a significant-manner, which emphasizes that autophagy plays a major role in PAMAM dendrimers-induced cytotoxicity. These findings might lead to the use of antioxidants and autophagy inhibitors to alleviate PAMAMs neurotoxicity in the clinic (44).

1.1.5.2. Apoptosis and necrosis

Many studies discussed the apoptosis and necrosis incidences caused by PAMAM dendrimers, as different surface chemistries and generations were investigated. G_4 cationic PAMAMs induced strong necrotic and weak apoptotic cell death in human acute T-cell leukemia Jurkat cells, mediated by disruption of mitochondrial membrane potential (MMP) and activation of ATM-mediated DNA damage (45). In another study, G_4 cationic PAMAMs induced apoptosis in human lung cells, WI-26 VA4, in a dose-dependent manner, mediated by MMP disruption as well (46). Also, G_5 cationic PAMAMs were found to induce apoptosis and necrosis in both KB cells and RAW 264.7 murine macrophage-like cells (47,48). In KB cells, this effect was mediated by lysosomal/mitochondrial pathways, as PAMAMs were localized in the lysosomal compartment causing an increase in lysosomal pH and cytotoxicity (47). On the other hand, induced apoptosis and necrosis in RAW 264.7 cells was inhibited upon pre-treatment with Caspase inhibitor zVAD-fmk, indicating that the mechanism is Caspase-dependent. Moreover, PF and SF G_6 PAMAM dendrimers triggered apoptosis in HEK 293 cells, mediated by oxidative stress-dependent mechanisms (16).

Furthermore, an increased production of intracellular ROS was detected in mammalian cells (49) and fish hepatocellular carcinoma cells, PLHC-1 (50), after treatment with G_4, G_5, and G_6 cationic PAMAMs. ROS production has led to DNA damage, apoptosis, and even necrosis at higher levels, in a PAMAMs concentration and generation-dependent manner ($G_4<G_5<G_6$) (49–51). Additionally, G_7 cationic PAMAMs induced significant apoptosis incidences in human umbilical vein endothelial cells, HUVEC, accompanied by necrosis at higher concentrations. A release of extracellular vesicles was detected as G_7 cationic PAMAMs interacts strongly with plasma and mitochondrial membrane (52).

The cationic surface chemistry of PAMAM dendrimers is the major contributor in inducing cell death. Compared to anionic PAMAMs, apoptosis was induced only by cationic PAMAMs in zebrafish embryos and it was concentration-dependent (53). PAMAMs with other surface chemistries (anionic and neutral) did not exhibit cytotoxicity, suggesting the safety of these compounds in comparison with cationic PAMAMs (52,54)**.** Therefore, we can conclude that amino terminated PAMAM dendrimers induce cellular death in the different discussed models. This effect was correlated with concentration, generation, and the number of surface amine groups (55).

1.1.6. Modulation of the inflammatory responses

Surprisingly, PAMAM dendrimers exhibit two contradictory effects on inflammation (Table 3). It was demonstrated that they produce an anti-inflammatory effect, which makes them drug candidates for the treatment of several inflammations (56). However, other studies revealed that some PAMAMs (even the same PAMAMs which have been stated as anti-inflammatory agents) induce inflammatory responses and secretion of pro-inflammatory cytokines in non-diseased animal models (56).

1.1.6.1. Anti-inflammatory effects

The anti-inflammatory effects of naked PAMAMs were accidentally discovered *in vivo* by Chauhan et al. PAMAMs with 1,2-diaminoethane core and different surface chemistries were administered to male albino rats, and three *in vivo* assays were used to study the anti-inflammatory effect; the carrageenan-induced paw edema model, the cotton pellet test, and the adjuvant-induced arthritis assay. G_4 cationic PAMAMs exhibited a more significant anti-inflammatory effect compared to $G_{4.5}$ anionic PAMAMs in a dose-dependent manner. Moreover, the combination of PAMAMs and indomethacin showed a higher anti-inflammatory effect than each compound alone

(57). PAMAM dendrimers were also able to protect from pancreas injury in caerulein-induced acute pancreatitis mouse model. $G_{4.5}$ anionic PAMAMs and G_5 neutral PAMAMs significantly and dose-dependently reduced pathological alterations in the pancreas by reducing the inflammatory responses. In addition, PAMAMs inhibited the gene expression of pro-inflammatory cytokines (IL-1β, IL-6, TNF-α, and TGFβR-1) in pancreatic tissues *in vivo* and *in vitro* (mouse peritoneal macrophages). Anionic PAMAMs protective effects for acute pancreatitis *in vivo* were more significant than neutral PAMAMs. The total number of plasma white blood cells and monocytes was also significantly reduced by PAMAMs *in vivo*. The mechanism behind the anti-inflammatory action was associated with inhibiting the nuclear translocation of NF-κB in macrophages (23).

1.1.1.1.Pro-inflammatory effects

Cationic PAMAM dendrimers generations G_3, G_4, G_5, and G_6 were tested *in vitro* in THP-1, U937, and mouse J774A.1 macrophage cell lines (18,51). The measured indicators of inflammatory response and oxidative stress were reactive oxygen species (ROS) and subsequent cytokine production. PAMAMs increased intracellular ROS production, concentration, and time-dependently. ROS production was also correlated linearly with PAMAMs generation, as it increased upon treatment with higher generations. In addition, cytokine assay indicated an increase in the pro-inflammatory mediators' secretion (IL-6, TNF-α, and MIP-2) upon exposing cells to PAMAMs in a concentration, generation, and time-dependent manner (51). Moreover, PAMAM dendrimers activated signal transduction related to NF-κB and thus, increased the expression of NFKBIA, BTG2, IL1 β, and TNFα (18). Furthermore, an *in vivo* study in female CD-1 mice revealed that G_0, G_1, G_2, and G_3 cationic PAMAMs exhibit pro-

inflammatory actions using murine air pouch model. PAMAM dendrimers attracted leukocytes into air pouches; mainly neutrophils. In addition, an increase in local production of several cytokines/chemokines was also noted, and it was generation-dependent (58).

Table 3. Effects of PAMAM dendrimers on inflammatory responses.

Generation	Model	Study Type	Effect	Reference
Cationic PAMAM Dendrimers				
0	Female CD-1 mice	*In vivo*	Pro-inflammatory	(58)
1	Female CD-1 mice	*In vivo*	Pro-inflammatory	(58)
2	Female CD-1 mice	*In vivo*	Pro-inflammatory	(58)
3	THP-1 and U937 cells	*In vitro*	Pro-inflammatory	(18)
	Female CD-1 mice	*In vivo*	Pro-inflammatory	(58)
4	HaCaT cells	*In vitro*	Pro-inflammatory	(59)
	J774A.1 macrophage cell	*In vitro*	Pro-inflammatory	(51)
	THP-1 and U937 cells	*In vitro*	Pro-inflammatory	(18)
	Male albino rats	*In vivo*	Anti-inflammatory	(57)
5	HaCaT cells	*In vitro*	Pro-inflammatory	(59)
	J774A.1 macrophage cell	*In vitro*	Pro-inflammatory	(51)
	Male Sprague-Dawley rats	*In vivo*	None	(60)
6	HaCaT cells	*In vitro*	Pro-inflammatory	(59)
	J774A.1 macrophage cell	*In vitro*	Pro-inflammatory	(51)
Anionic PAMAM Dendrimers				
4.5	Male albino rats	*In vivo*	Anti-inflammatory	(57)
	Caerulein-induced acute pancreatitis mice	*In vivo*	Anti-inflammatory	(23)
Neutral PAMAM Dendrimers				
5	Caerulein-induced acute pancreatitis mice	*In vivo*	Anti-inflammatory	(23)

Surprisingly, another study *in vivo* using male Sprague-Dawley rats as a model stated that G_5 cationic PAMAMs did not stimulate an inflammatory response themselves, as they did not elevate the pro-inflammatory cytokines (IL-1β and TNFα) as shown by a bio bead-based ELISA system. Thus, further investigation of PAMAMs inflammatory responses and cytotoxicity *in vivo* should be carefully established (60).

The difference in the reported behavior of similar types of PAMAM dendrimers in modulating inflammatory responses is probably due to using different models, different concentrations, and different routes of administration. Moreover, the pro-inflammatory effect was mainly found in non-diseased models (56). Therefore, a deeper investigation of this area is needed before the therapeutic use of PAMAMs for anti/pro-inflammatory purposes.

1.1.2. Antimicrobial effects

PAMAM dendrimers have been widely investigated for their antimicrobial effects, particularly cationic PAMAMs, which have a promising future in this area (61). Their antimicrobial effects are mainly as a result of the electrostatic interaction between the positively charged surface of PAMAMs and the negatively charged bacterial cell wall, causing disruption and disintegration of the lipid bilayer and releasing of electrolytes and nucleic acids, which cause cell death eventually (61,62).

The antimicrobial effects of G_5 PAMAMs were studied in Gram-negative pathogen Pseudomonas aeruginosa. PAMAM dendrimers exhibited a high toxicity towards Pseudomonas aeruginosa in a concentration-dependent manner. Besides, their antimicrobial effects were diminished upon PEG-coating of PAMAMs; showing the role of surface chemistry in mediating this effect (63). Another study used isolated bacteria from various clinical specimens (urine, blood, sputum, wounds, and burns) to evaluate the antimicrobial effects of G_6 cationic PAMAM dendrimers. The following

bacteria were assessed; Gram-negative bacteria (Pseudomonas aeruginosa, Escherichia coli, Acinetobacter baumannii, Salmonella typhimurium, Shigella dysenteriae, Klebsiella pneumoniae, Proteus mirabilis) and Gram-positive bacteria (Staphylococcus aureus and Bacillus subtilis). It was found that G_6 PAMAM dendrimers inhibited the growth of standard Gram-negative, Gram-positive, and isolated bacteria in a concentration-dependent manner, with a higher effect against standard strains (61). The inhibition zone size increased upon increasing the concentration of PAMAMs, and the most sensitive bacteria were Proteus mirabilis, Salmonella typhimurium, Shigella dysenteriae, and Staphylococcus aureus. On the other hand, the least sensitive bacteria were Acinetobacter baumannii at the same used concentration of PAMAMs. The highest values of minimum inhibitory concentration (MIC) and minimum bactericidal concentration (MBC) were found in isolated Escherichia coli and Acinetobacter baumannii, while the minimum MIC and MBC were found in Salmonella typhimurium (61). Furthermore, G_7 cationic PAMAM dendrimers showed remarkable antibacterial activities against a wide range of Gram-negative and Gram-positive bacteria; Pseudomonas aeruginosa, Escherichia coli, Acinetobacter baumannii, Shigella dysenteriae, Klebsiella pneumoniae, Proteus mirabilis, Staphylococcus aureus, and Bacillus subtilis. All bacterial strains were collected from clinical samples and identified using microbiological tests. In addition, the following strains were used as standard strains; Escherichia coli, Pseudomonas aeruginosa, Acinetobacter baumannii, Shigella dysenteriae, Klebsiella pneumoniae, Proteus mirabilis, Staphylococcus aureus, and Bacillus subtilis. Similar to previous studies, the antibacterial effects of G_7 PAMAM dendrimers were concentration-dependent. However, they were higher in isolated bacteria compared to standard ones. Proteus mirabilis, Shigella dysenteriae, and Staphylococcus aureus were the most sensitive strains to G_7 PAMAMs, whereas

Acinetobacter baumannii was the least sensitive at the same dendrimer concentration. Moreover, Escherichia coli, Acinetobacter baumannii, Pseudomonas aeruginosa and Staphylococcus aureus clinical isolates had the highest values of MIC50, MIC90 MBC50, and MBC90, while the least MIC50 and MIC90 values belonged to Shigella dysenteriae and Proteus mirabilis. The least MBC50 and MBC90 values were found in Shigella dysenteriae. In conclusion, the higher antibacterial activity of G_7 PAMAM dendrimers compared to lower generations of PAMAMs is mainly due to the highly branched structure, large molecular weight, and number of terminal amino groups, as G_7 PAMAMs contain 512 surface amino groups (62).

Another study explored the effect of different surface chemistries of PAMAMs; cationic and anionic PAMAMs in terms of expressing antimicrobial actions. Several bacterial types were tested; Staphylococcus aureus, Bacillus subtilis, Escherichia coli, Pseudomonas aeruginosa, Methicillin-resistant Staphylococcus aureus (MRSA), Candida albicans, and Aspergillus niger. The antimicrobial activity was estimated by measuring the diameter of inhibition zones. Results revealed that PAMAMs showed a successful effect against Gram-positive, Gram-negative bacteria, yeast strains, and fungal strains. Gram-positive bacteria were more sensitive than Gram-negative bacteria for all PAMAMs, mainly due to differences in the bacterial cell wall structure (64). Additionally, G_2, G_3, G_4, and G_5 cationic and $G_{3.5}$ anionic PAMAMs showed a generation, concentration, and surface functional groups-dependent antimicrobial effect against Gram-positive and Gram-negative skin pathogens; Staphylococcus aureus and Escherichia coli. The higher the generation, the less the MIC50 was, which confirms the role of PAMAMs size in this antimicrobial effect. Escherichia coli was more sensitive to PAMAMs with lower MIC50 than Staphylococcus aureus, and the antibacterial effect increased upon increasing the number of surface amino groups of

PAMAMs. On the other hand, a study assessed the bacterial membrane integrity following treatment with PAMAMs, and found a significant correlation between PAMAMs effect on membrane disruption and their antimicrobial effects, which may be one of their mechanisms of action (65). Moreover, G_4 neutral PAMAM dendrimers were effective against Escherichia coli induced ascending uterine infection *in vivo* in guinea pig model cervix. It was also found that levels of TNFα, IL-6, and IL-1β in the placenta of treated animals were higher compared to healthy animals. By comparing the antimicrobial effects of G_4 cationic, anionic, and neutral PAMAMs, cationic PAMAMs exhibited superior antibacterial activities but their toxicity was higher. Neutral PAMAMs changed the permeability of the bacterial cellular membrane, while cationic and anionic PAMAMs damaged the membrane causing bacterial lysis (66).

In conclusion, the variety of the biological applications of PAMAM dendrimers raises hopes for the future development of these compounds as new nanotherapeutic agents, either to act solely or to add benefit to other therapies. These reported behaviors follow a similar trend in most cases, as they were more significant in PAMAMs with higher generations, higher concentrations, and higher number of surface amino groups. However, safety considerations regarding the application of cationic PAMAMs need to be addressed, and further research is warranted to ensure the safe and effective employment of these compounds.

1.2. HER2-positive breast cancer: Introduction and problem statement

Breast cancer is one of the leading causes of death in women worldwide and the second common type of cancer, with increased incidence rates. It has major negative impacts on patients' physical, mental, emotional and social status (67). Breast cancer has a high prevalence in Qatar, with a high morbidity of 31% of total cancer cases in women. According to the Qatar Cancer Registry, 56 women out of every 100,000 have

a high risk of promoting breast cancer (68). Therefore, huge efforts are devoted in conducting more research to gain further understanding of the cellular and molecular aspects related to the initiation and progression of this disease.

Breast cancer has various types that mainly differ in prognosis and response to therapy. Knowing the type provides key information about how the cancer may behave. One of the challenging subtypes is HER2-positive breast cancer, which overexpresses human epidermal growth factor receptor 2 (HER2). In this type, an overexpression of the HER2 receptor or amplification of the HER2 gene occurs, which results in making an excess of the HER2 protein. This protein belongs to transmembrane receptor tyrosine kinases and it promotes cell growth, survival, and differentiation (69,70). In addition, HER2-positive breast cancer is seen in about 15-20% of total breast cancers (71), and it forms around 15% of all invasive breast cancers, with an increased incidence of lymph node metastasis (72). This type presents many challenges, including early relapse, poor prognosis and aggressive behavior in the tumor due to fast tumor growth. Its response to hormonal therapy and chemotherapy is not satisfying, although the latter was effective in some cases (73–75). Mortality in early-stage disease occurs at high rates in this type as well (70,71). Furthermore, it was found that overexpression of HER2 in human tumor cells is closely related to increased angiogenesis and gene expression of vascular endothelial growth factor (VEGF), which is mainly responsible for the formation of new blood vessels.

Currently, trastuzumab (a monoclonal antibody) and lapatinib (a tyrosine kinase inhibitor) are considered the first line anti-HER2 therapies that have shown significant clinical benefits, in addition to multiple drugs (Table 4) (78–80). However, they express major limitations, such as non-specific toxicity, patient relapsing, low bioavailability, and intolerable side effects (81,82). For instance, most patients who initially respond to

trastuzumab develop resistance within one year, and treatment with lapatinib also faces acquired and intrinsic resistance developed by cancer cells (83–85). To overcome this resistance, extensive studies found that combination therapy resulted in improved clinical outcomes, which increase the overall survival and reduce disease progression (86–89).

For advanced cases of HER2-positive breast cancer, it is recommended to treat patients with "dual HER2 blockade", which is consisted of trastuzumab and pertuzumab in addition to a Taxane. Unfortunately, HER2-positive breast cancer metastasis is still an incurable disease (80,90).

The other issue related to anti-HER2 drugs is the cardiotoxicity. Severe congestive heart failure (CHF) incidences were reported upon treatment with trastuzumab, along with higher incidence rates of left ventricular dysfunction (91–93). On the other hand, lapatinib express a lower toxicity as stated by multiple trials, as it shows a favorable cardiac safety profile compared to trastuzumab (94–96). Altogether, the limitations of anti-HER2 drugs emphasize the urgent need to investigate new compounds as potential drugs in order to avoid the undesired side effects and overcome drug resistance.

Table 4. Current treatments of HER2-positive breast cancer.

Treatment	Brand Name
Ado-Trastuzumab Emtansine	Kadcyla
Lapatinib	Tykerb
Neratinib	Nerlynx
Pertuzumab	Perjeta
Trastuzumab	Herceptin

Current research interests in the area of HER2-positive breast cancer aim at finding new treatment strategies in order to overcome the limitations of current therapies and increase survival rates (97). Plenty of promising options that target HER2 were proposed, for example, novel anti-HER2 antibodies such as margetuximab, MCLA-128, and ZW-25 that are now being investigated in clinical trials (90,97–99). These antibodies showed an ability to specifically target HER2, either alone or combined with other anti-HER2 therapies (97,100,101). Another group is novel tyrosine kinase inhibitors, which are currently under development, including neratinib, tucatinib, poziotinib, and pyrotinib (90,97–99). Other novel treatment approaches are proposed, such as immunotherapy and combination therapy. However, some of these options still express certain toxic effects (97).

1.3. Angiogenesis

Angiogenesis is a vital function, defined as a physical process of forming new blood capillaries out from pre-existed vessels, which allows exchanging oxygen and metabolites in all tissues (102). It is also necessary for cell growth, development and wound healing. It starts in the embryonic stages and keeps occurring throughout life (102). The process of angiogenesis is regulated by endogenous local or systemic chemical signals in the body which also determine the ability of a certain tissue to activate angiogenesis. Endothelial cells proliferation and migration are controlled by various stimulating or inhibiting factors that represent the essence of vessel formation; mainly vascular endothelium growth factors family (VEGF) and their receptors, along with other signaling pathways (103). Furthermore, angiogenesis plays an essential role in cancer development, as tumors need nutrition and oxygen in order to grow and disseminate (Figure 6) (104). In the early 1970s, the first one who related cancer development to angiogenesis was Judah Folkman, as he described cancer cells to be "hot and bloody" (105). Ever since, interrupting this pathway became a target to inhibit

cancer growth and progression by cutting off the supplies and starving the tumor. Angiogenesis is also related to the transition of tumors from a benign state to a malignant one (104). In addition, abnormality in HER2 activation, particularly in breast cancer, was found to be associated with high rates of angiogenesis and VEGF expression, and thus, increasing metastasis (106). This emphasizes the importance of targeting this process in order to contribute to the treatment of cancer.

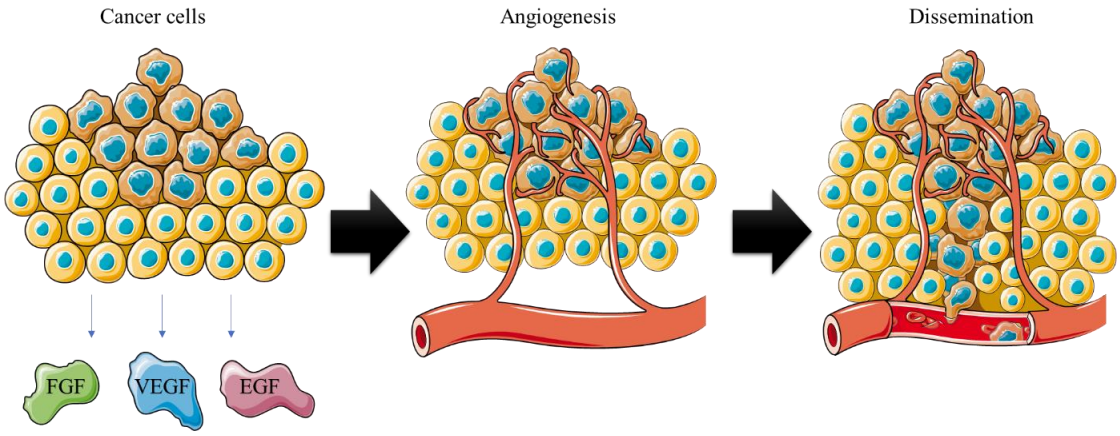

Figure 6. Angiogenesis in cancer.

FGF, fibroblast growth factor; VEGF, vascular endothelium growth factor; EGF, epidermal growth factor.

1.4. Embryogenesis:

Embryogenesis is a complex highly-controlled process of development and formation of the embryo throughout pregnancy (107). In the biomedical field, different models are used to study embryogenesis; mostly mouse, rats, chicken, and zebrafish models. In particular, chicken and zebrafish models are favored, as they are easy to maintain, reliable, cost-effective, and fast (108). The purpose of studying

embryogenesis is mainly to predict drug safety profiles on the embryos in case they were administrated during pregnancy. Thus, a clear idea regarding drug toxicity is gained by investigating embryogenesis (109–111). Interestingly, different studies reported that tumorigenesis is significantly similar to the early stages of embryogenesis regarding their biological behaviors. These two processes are comparable in terms of proliferation, differentiation, migration, and so on (112–115). However, unlike tumorigenesis, embryogenesis is a strictly regulated process that happens in an organized manner (112).

1.5. Study rationale and objectives

The limitations in HER2-positive breast cancer treatments require further investigation of new potential therapies, either to act solely or to synergize other anti-HER2 agents. Combining effective anti-cancer compounds with anti-HER2 treatments will likely result in overcoming drug resistance, improving clinical outcomes, and diminishing undesired side effects. As PAMAM dendrimers express several biological effects aside from being drug carriers, their effects on cancer should be taken into consideration. Their ability to modulate gene expression patterns and interfere with cell signaling pathways, particularly EGFR and ErbB2 (HER2) signaling pathways, raises the question of whether these polymers have a beneficial anti-HER2 effect in HER2-positive breast cancer. However, this area has not been studied before. Thus, the aims of this research are summarized as follows:

1. Evaluating the potential anti-cancer activity of different generations and surface chemistries of PAMAM dendrimers in HER2-positive breast cancer cells.
2. Exploring the underlying mechanisms of action responsible for PAMAM dendrimers' anti-cancer effects.
3. Investigating the impact of PAMAM dendrimers on angiogenesis using the chorioallantoic membrane (CAM) of the chicken embryo model (*in ovo*).

4. Predicting the safety profile of PAMAMs during early embryonic stages using the chicken embryo model.

CHAPTER 2: MATERIALS AND METHODS

2.1. PAMAM dendrimers

Four types of PAMAM dendrimers were synthesized by Dendritech and purchased from Sigma Aldrich Chemical Company (USA) (Table 5). As instructed by the manufacturer, they were stored at 4° C. PAMAM dendrimers stock solutions were prepared in pre-filtered (0.45 µm membrane) distilled water with concentrations of 1, 10, 100 mg/mL. The stock solutions were stored at 4° C for no longer than 3 weeks (116).

2.2. Lapatinib

Lapatinib (N-[3-chloro-4-[(3-fluorophenyl) methoxy] phenyl]-6- [5- [(2-methylsulfonyl ethyl amino) methyl]-2-furyl] quinazolin-4-amine) was purchased from LC Laboratories, Massachusetts, USA (L-4804). It was dissolved in DMSO and stored at 4° C as instructed per manufacturer. Several stock solutions were prepared, ranging from 10 µg/mL to 10 mg/mL. The percentage of DMSO in the treatment did not exceed 0.1%.

Table 5. Types of PAMAM dendrimers used in this study.

Type	Catalog Number	Vendor	Surface Chemistry	Stock Solution	G[4]	MW[5] (g/mol)
PAMAM dendrimers ethylenediamine core	412449	Sigma Aldrich (USA)	-NH2	10 wt. % in methanol	4.0	14,214.17
PAMAM dendrimers ethylenediamine core	536717	Sigma Aldrich (USA)	-NH2	5 wt. % in methanol	6.0	58,046.11
PAMAM-OH dendrimer	536822	Sigma Aldrich (USA)	-OH	5 wt. % in methanol	6.0	58,298.21
PAMAM dendrimer ethylenediamine core	536784	Sigma Aldrich (USA)	-COOH	5 wt. % in methanol	5.5	52,900.21

[4] Generation.
[5] Molecular weight.

2.3. Cell culture

Two different breast cancer cell lines which overexpress HER2; SK-BR3 (ATCC® HTB-30™) and ZR-75-1 (ATCC® CRL-1500™) were purchased from the American Type Culture Collection (ATCC). Cells were grown and expanded in 1X Gibco® RPMI 1640 media (Thermo Fisher Scientific, USA) supplemented with 10% fetal bovine serum (FBS; Invitrogen, Life Technologies) and 1% PenStrep antibiotic (Thermo Fisher Scientific, USA). As a control in this study, we used human normal mammary epithelial cells immortalized by the E6/E7 gene by HPV type 16 (HNME-E6/E7) (117). HNME-E6/E7 cells were grown in 1X Gibco® Keratinocyte-SFM media (Thermo Fisher Scientific, USA) supplemented with 1% PenStrep antibiotics (Thermo Fisher Scientific, USA). Cells were incubated at 37° C in a 5% CO2 incubator. Cells were maintained by routine sub-culturing in T-75 filtered tissue culture flasks (Thermo Fisher Scientific, USA). Cells media was replaced with a fresh one every 48 hours; 10 mL during the week and 12 mL in the weekends.

2.3.1. Cell viability

Around 8,000 - 10,000 cells/well of the studied cell lines (HNME-E6/E7, SK-BR3, and ZR-75) were seeded in 96-well plates (Thermo Fisher Scientific, USA), and were left to adhere overnight. After 24 hours, fresh media was added instead of the old one, and cells were treated with different concentrations of PAMAM dendrimers, ranging from 0.1 to 100 µM. Additionally, lapatinib; a well-known anti-HER2 drug, was used as a positive control in the concentrations of 10 to 100 nM in SK-BR3, and 1 to 100 µM in ZR-75. After several time points post-treatment (24, 48 and 72 hours) media was discarded, and fresh media with 2% Alamar Blue dye (Thermo Fisher Scientific, USA) was added to cells. Plates were incubated for 3-4 hours in 5% CO2 at 37° C incubator. After that, fluorescence was recorded at a wavelength of 560 nm using Infinite m200 PRO microplate reader (TECAN, Switzerland) (Figure 7). Percentage of

viable cells was calculated using the following formula:

$$\%\, Viability = \frac{Fluorescence\ of\ treated\ wells}{Fluorescence\ of\ control\ wells} \times 100$$

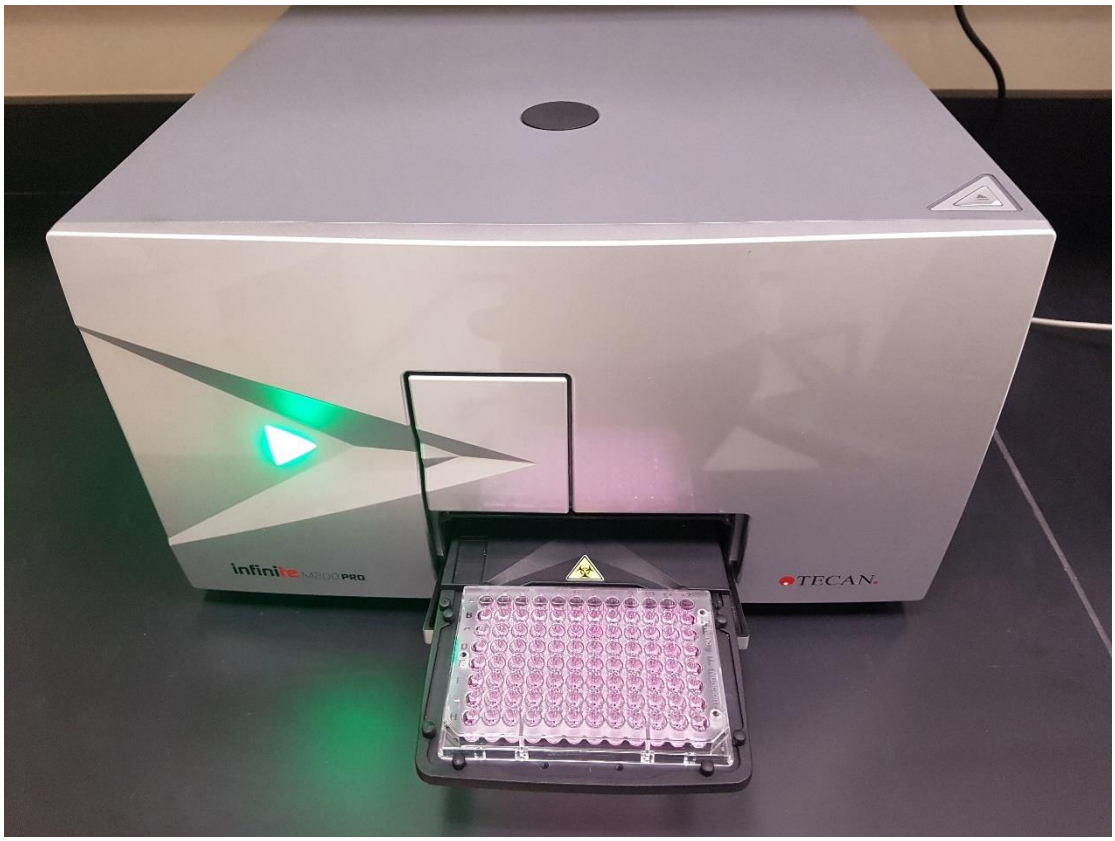

Figure 7. TECAN machine used in cell viability assay and protein quantification.

2.3.2 Morphological examination

Around 200,000 - 300,000 cells/well of the studied cell lines (HNME-E6/E7, SK-BR3, and ZR-75) were seeded in 6-wells plates (Thermo Fisher Scientific, USA) and left to adhere overnight. After 24 hours, old media was substituted with a fresh one, and PAMAM dendrimers were used to treat cells at concentrations equal to the corresponding IC50 of G_6NH_2. In addition, SK-BR3 and ZR-75 cell lines were treated

with the corresponding IC50 of lapatinib which was reported in the literature (118–120). The morphological changes were observed after 48 hours using a DMi8 inverted microscope (Leica, Germany) connected to Leica EC4 digital camera. Images were taken using Leica LAS EZ software.

2.3.3. Cell cycle analysis

Around 300,000 - 400,000 cells/well of the studied cell lines (HNME-E6/E7 and SK-BR3) were seeded in Low Attachment Surface Polystyrene 6-wells plates (Costar, USA) and were incubated overnight. After 24 hours, PAMAM dendrimers were used to treat cells at concentrations equal to the corresponding IC50 of G_6NH_2. After 48 hours, floating cell populations were harvested and counted by Neubauer counting chamber. Then, cells were washed with ice-cold PBS and centrifuged at 4° C (200 x g for 15 minutes). The supernatant was discarded, and cells were fixed with 2 mL added ice-cold 70% ethanol drop-wisely with gentle vortexing. Then, the samples were kept at -20° C for at least 24 hours. On the day of measurement, ethanol was discarded by centrifuging samples at 4° C (800 x g for 15 minutes), and cells were washed with ice-cold PBS twice. After that, 500 µL of FxCycle PI/RNase staining solution® (Thermo Fisher Scientific, USA) were added to each sample. Then, samples were incubated at 37° C in a shaking water bath for 50 minutes in dark. Samples were run in Accuri C6 flow cytometry (BD Biosciences, USA), and results were analyzed by the FlowJo V10 software. A number of 50,000 cells was considered statistically significant.

2.3.4. Colony formation assay

This experiment was used to evaluate whether cancer cells can form colonies in agar upon treatment with PAMAM dendrimers. A stock of 2% Agar solution was prepared for the soft agar assay by dissolving noble agar (Sigma-Aldrich, USA) in sterile DPBS (Thermo Fisher Scientific, USA) through heating and mixing. Agar

solution (0.4 %) was prepared by diluting agar stock with 10 % RPMI media, and 1 mL was poured in each well of 6-well plates to create the first layer. While the first layer was solidifying, the second layer solution was prepared by mixing agar solution (0.3 %) with RPMI media, 1500 cells/well of SK-BR3 and ZR-75 cells, and treatment. PAMAM dendrimers were used to treat cells at concentrations equal to the corresponding IC50 of G_6NH_2. Then, 1 mL of the mixture was poured above the first layer. Colony formation was monitored for three weeks in terms of size and number, and microscopic pictures were recorded from different zones using Leica EC4 digital camera and Leica LAS EZ software. After three weeks of treatment, colonies in each well were counted and categorized into small or large colonies.

2.3.5. RT-PCR of SK-BR3, ZR-75, and HNME-E6/E7 cells lines

2.3.5.1. RNA extraction:

RNA extraction kit (QIAGEN Canada Inc., ON, Canada) was used according to the manufacturer's protocol to extract total RNA from SK-BR3, ZR-75, and HNME-E6/E7 cells treated with PAMAM dendrimers at a concentration equal to the corresponding IC50 of G_6NH_2. Briefly, cells were collected, and RLT buffer was added and mixed well. The lysate was centrifuged at 13,000 x g for 3 minutes, and the supernatant was carefully transferred to an Eppendorf tube (Eppendorf, Germany). Then, ethanol (70%) was added and mixed well, which creates conditions that allow specific binding of RNA to the RNeasy membrane. This mixture was transferred to RNeasy Mini spin columns placed in collection tubes, then it was centrifuged. After discarding the flow-through from the spin column, RW1 buffer was added and again centrifuged, followed by discarding the flow-through. The mixture then was washed twice with RPE Buffer, and the flow-through was discarded. To dry the membrane, the RNeasy spin column was placed in a new collection tube and centrifuged. Finally,

RNase-free water (QIAGEN, CA, USA) was added to the spin column membrane and centrifuged for 1 minute to elute the RNA. RNA concentrations were quantified using the nanodrop reader (Thermo-Fisher Scientific, USA) at 260/280 nm to guarantee a ratio of >1.7, which indicates that the RNA is free of contaminants. The samples were stored at -80° C for further analysis.

2.3.5.2. Reverse-Transcription Polymerase Chain Reaction (RT-PCR)

RNAs from cell lines (SK-BR3, ZR-75, and HNME-E6/E7) were used for RT-PCR to analyze the effect of PAMAM dendrimers on vascular endothelial growth factor ligand (VEGF) and apoptotic markers (Table 6). List of primers used in this experiment is shown in (Table 7). One-Step RT-PCR kit was performed using The SuperScript® III One-Step RT-PCR System with Platinum® *Taq* DNA Polymerase (Invitrogen, USA). The components of the kit (2X Reaction Mix, SuperScript® III RT/Platinum Taq Mix and Nuclease-free water) were allowed to thaw on ice. A 1X RT master mix (Table 8) was also prepared in ice.

Table 6. List of mRNA of interest detected by RT-PCR in SK-BR3, ZR-75, and HNME-E6/E7 cell lines.

No.	Gene	Description
1	VEGF	Vascular endothelial growth factor ligand
2	Bax	BCL-2-associated X protein; an apoptosis regulator
3	BCL-2	B-Cell lymphoma-2; an anti-apoptotic marker
4	Caspase-3, 8, 9	Caspase proteins that contribute to initiating the apoptosis signal
5	p53	Tumor protein p53; a tumor suppressor gene
6	GAPDH	Glyceraldehyde 3 phosphate dehydrogenase

In PCR tubes (Eppendorf, Germany), the appropriate volumes of the master mix were dispensed; RT Master Mix (Table 8) (1X, Thermo-Fisher Scientific, USA) with template RNA (1µg). RT-PCR was then carried out in the Veriti 96 well-plate thermal cycler (Applied Biosystems, Austin, TX) using the following program: cDNA synthesis and initial denaturation at 60°C for 15 minutes and 94°C for 2 minutes, respectively, followed by 40 cycles of denaturation at 94°C for 15 seconds, annealing at the specific temperatures mentioned in table 7 for 30 seconds, and elongation at 68°C for 60 seconds. Finally, the PCR reaction mixtures were held at 68°C for 5 minutes for the final elongation and then at 4°C until they were removed from the machine. The PCR product from each exon was visualized using 1.5% agarose gel (Promega, USA) run at 110 V, 400 mA for 40 minutes.

Table 7. List of primers used in RT-PCR of SK-BR3, ZR-75, and HNME-E6/E7 cell lines.

Gene	Forward Primer (5'-3')	Reverse Primer (5'-3')	Annealing Temperature (^{0}C)
BCL-2	GGATGCCTTTGTGGAATTGT	GTCCAAGATAAGCGCCAAGA	42
p53	AGAGACCGCCGTACAGAAGA	GCATGGGCATCCTTTAACTC	53
Caspase-3	GCAGCAAACCTCAGGAAAC	TGTCGGCATACTGTTTCAGCA	50
Caspase-8	TCCTCTTGGGCATGACTACC	TGTCAATCTTGCTGCTCACC	56
Caspase-9	AGCCAGATGCTGTCCCATAC	CAGGAGACAAAACCTGGGAA	50
VEGF	TGCAGATTATGCGGATCAAACC	TGCATTCACATTTGTTGTGCTGTAG	56

Table 8. RT-PCR master mix.

Component	Volume (μL)
2X Reaction Mix	25
Forward Primer (10μM)	1
Reverse Primer (10μM)	1
SuperScript® III RT/Platinum Taq Mix	2
Nuclease-free Water	20
Total	49

2.3.5.3. Agarose Gel Electrophoresis

After RNA extraction, the integrity of RNA was analyzed using agarose gel electrophoresis. An agarose gel with a concentration of 1.5% (Invitrogen, USA) was prepared in 1X TBE buffer solution. The gel was poured in a tray after adding SYBR Safe DNA Gel Stain (Invitrogen, USA). After that, the gel was covered with TBE buffer (1X). RT-PCR product along with TriTrack DNA loading dye (6X) (Thermo Scientific, USA) were loaded into the wells. Gene Ruler 100 bp Plus DNA ladder (BIO-RAD) was used as an indicator of the size of PCR products. The gel was run at 110 V, 400 mA for approximately 40 minutes. Gels were imaged using the iBright CL1000 imaging system (Figure 8).

2.3.6. Western blotting analysis

SK-BR3 and ZR-75 cells were seeded in 100 mm petri dishes (Thermo Fisher Scientific, USA) at a concentration of 2,000,000 – 3,000,000 cells/dish, then incubated and left to adhere overnight. On the next day, cells were treated with PAMAM dendrimers at concentrations equal to the IC50 of G_6NH_2 PAMAMs and incubated for 48 hours. In addition, SK-BR3 and ZR-75 cell lines were treated with the corresponding IC50 of lapatinib which was reported in the literature (118–120). To collect protein samples, media with floating cells were harvested and centrifuged at 1000 RPM for 5 minutes. Then, the supernatant was discarded, and the cell palette was resuspended in SDS lysis buffer. As for the cells attached to the plate, an adequate amount of SDS lysis

buffer was added, and cells were scraped gently by a scrapper. Samples were stored at -20° C for further analysis. Protein quantification was conducted using Pierce BCA Protein Assay Kit (Thermo Scientific, USA) according to the manufacturer protocol.

Figure 8. iBright machine used for imaging in RT-PCR and Western blotting.

NuPAGE® Bis-Tris Electrophoresis System was used to run Western blotting. Stained protein samples were boiled at 95° C for 10 minutes. After that, proteins were loaded at a concentration of 50 µg per well in NuPAGE® Novex® Bis-Tris Gels (4-12 %). PageRuler™ Prestained Protein Ladder (Thermo Scientific, USA) was used as an indicator of the size of proteins in the samples. Running phase was performed in two steps, starting with 60 V for 10 minutes then 120 V for 1:45 hours in order to separate proteins based on their molecular weight. Afterward, proteins were transferred into PVDF membranes at 35 V for 1:10 hours. Following the transfer, the PVDF blots were blocked with 3% BSA (Thermo Fisher Scientific, USA) for 1 hour with gentle shaking. The PVDF membranes then were incubated with previously prepared primary antibodies overnight (Table 9) with gentle shaking at 4° C.

Table 9. List of the used antibodies in Western blotting analysis.

No.	Antibody	Source	MW of Target Protein (kDa)	Manufacturer
1	Anti-Mouse	Goat	NA	Cell Signaling Technology, Inc., USA
2	Anti-Rabbit	Goat	NA	Cell Signaling Technology, Inc., USA
3	GAPDH	Rabbit	37	Abcam, USA
4	ErBb2	Mouse	138	Abcam, USA
5	P-ErbB2	Rabbit	185	Abcam, USA
6	EGFR	Rabbit	134	Abcam, USA
7	P-EGFR	Rabbit	170	Abcam, USA
8	ERK 1/2	Rabbit	44, 42	Abcam, USA
9	P-ERK1/2	Rabbit	44, 42	Cell Signaling Technology, Inc., USA
10	Cleaved Caspase-3	Rabbit	17	Abcam, USA
11	BCL-2	Mouse	26	Abcam, USA
12	BAX	Mouse	23	Invitrogen, USA
13	JNK1, JNK2, JNK3	Rabbit	54	Abcam, USA

On the next day, primary antibodies were removed, and membranes were washed for 10 minutes three times with 1X TBST buffer, and incubated with the respective secondary antibodies for 2 hours at room temperature with gentle shaking. Proteins were detected using Pierce™ ECL Western Blotting Substrate by chemiluminescence. Blots were imaged using the iBright CL1000 imaging system (Figure 8).

2.4. Chicken embryos

Fertilized White Leghorn chicken eggs were purchased from Arab Qatari for Poultry Production in Qatar. Eggs were incubated at 37° C and 60% humidity in MultiQuip incubator. They were rotated hourly to prevent adhesions between the embryo and its membranes (121). All procedures were approved by Qatar University-Institutional Bio-safety committee. Briefly, the eggshell was opened, and the shell membrane was removed carefully after adding 500 µL of PBS 1X (Sigma-Aldrich, UK). Round glass coverslips (Sigma-Aldrich, UK) were used to carry the treatment, then they were placed directly on the embryo (Figure 9). In control embryos, empty coverslips were placed. Subsequently, eggs were closed and incubated.

2.4.1. Angiogenesis analysis

Chicken embryos were treated with 5, 10 and 20 µM of G_6NH_2 PAMAMs, and 20 µM of G_4NH_2, G_6OH, and $G_{5.5}COOH$ PAMAMs at embryonic day 6, and were compared to untreated controls. The effect of PAMAMs on chicken embryos was evaluated 48 hours post-treatment using the CAM of the chicken embryos, as two areas were compared within the same embryo; the area under the coverslip (exposed area) and the area surrounding it (unexposed area). Microscopic images of exposed areas and unexposed areas were analyzed using AngioTool software version 0.6a as described by Zudaire et al. (122). The images had the same size and magnification with unified

AngioTool inputs; vessel diameter thresholds at [10,255], vessel thickness at 4 and 5, removed small particles at 200 and filled holes at 150. Two blood vessel parameters were quantified for each experimental group and controls; total number of junctions and average vessel length.

2.4.2. Effect of PAMAMs on embryogenesis

The effect of cationic PAMAM dendrimers on early stages of embryogenesis was evaluated as chicken embryos were treated with 20 µM of G_4NH_2 and G_6NH_2 PAMAMs at embryonic day 3, then they were incubated for 5 days. Death incidences were recorded during this period. On embryonic day 8, embryos were sacrificed, and autopsied, as small parts of the brain, liver and heart tissues were taken for RNA extraction and RT-PCR analysis (Figure 10).

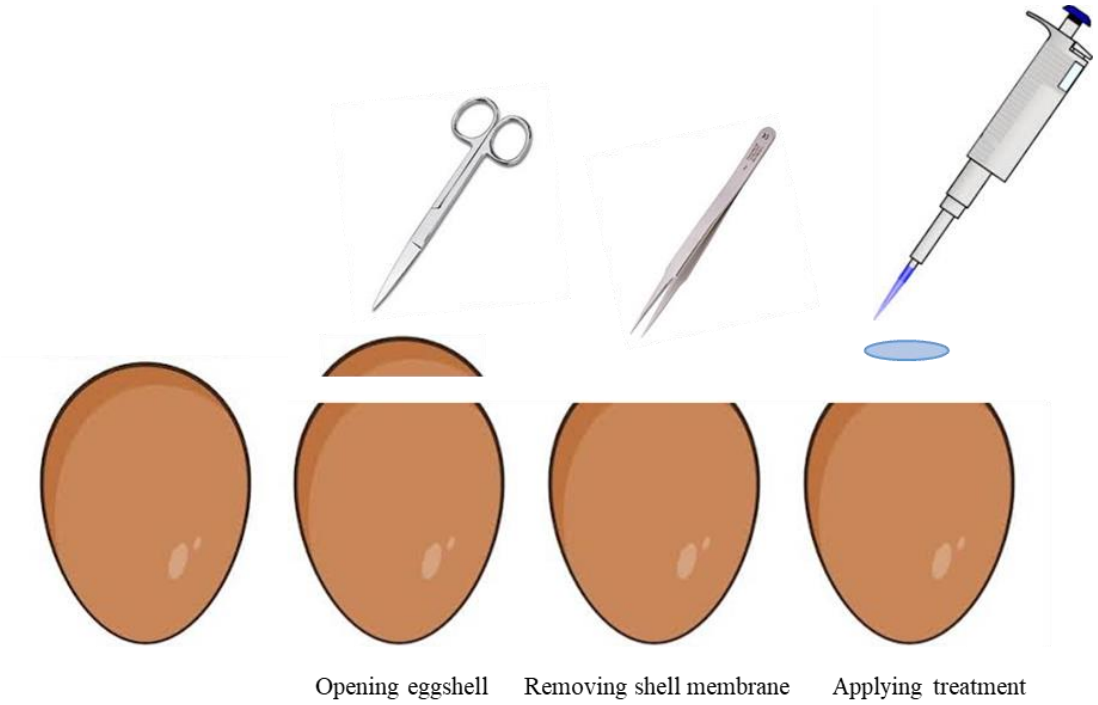

Figure 9. Chicken embryos treatment protocol.

Figure 10. 8-day old chicken embryo.

2.4.3. RT-PCR of tissues derived from chicken embryos

2.4.3.1. RNA extraction

RNA was extracted from the collected chicken embryos tissues samples (brain, heart, and liver). Before starting the RNA extraction, β-Mercaptoethanol (β-ME) (Sigma-Aldrich, USA) was added to RLT buffer for the extraction of RNA from tissues. Briefly, RNAlater (Ambion, US)-stabilized frozen fresh tissue was disrupted in liquid nitrogen and ground very well using a mortar and pestle. The resulting powder tissue and liquid nitrogen were poured into an RNase-free, liquid-nitrogen-cooled, micro-centrifuge tube (Fisher Scientific, USA), not allowing the tissue to thaw. RLT buffer was added and homogenized by pushing the lysate not less than 5 times through a blunt 20-gauge needle fitted to an RNase-free syringe. The lysate was spun at 13,000 x g for

3 minutes and the supernatant was carefully moved to an Eppendorf tube (Eppendorf, Germany). A similar procedure as mentioned in the above section 2.3.5.1. was carried out. RNA concentrations were quantified using the nanodrop reader (Thermo-Fisher Scientific, USA) at 260/280 nm to guarantee a ratio of >1.7, which indicates that the RNA is free of contaminants. The samples were stored at -80°C for further analysis.

2.4.3.2. Reverse-Transcription Polymerase Chain Reaction (RT-PCR)

Primers used in this experiment are listed in table 10. The gene expression of mRNA of interest (Table 11) in tissues of treated embryos was calculated relative to untreated embryos tissue mRNA levels, as they were used as a control. RT-PCR kit was performed as described in section 2.3.5.

2.5. Statistical analysis

The data were shown as an average of mean ± SEM (standard error of the mean). Each experiment was repeated at least three times (n=3). Statistical analysis of the data was performed using Microsoft Excel. Differences between treated groups and controls were determined one-way ANOVA followed by Tukey's post-hoc test. In AngioTool analysis for blood vessel parameters, student's T-test was used. Results were considered statistically significant when $p<0.05$.

Table 10. List of primers used in RT-PCR of tissues derived from chicken embryos.

Gene	Forward Primer (5'-3')	Reverse Primer (5'-3')	Annealing Temperature (^{0}C)
FOXA-2	GACCTCTTCCCCTTCTACCG	AGGTAGCAGCCGTTCTCAAA	56
MAPRE-2	CAAAGGAGCCTTCCACAGAG	GTCACTTCTGATGGCAGCAA	56
RIPK-1	CCGTACAGAATTGCAGCAGA	TTCCATTAGCACACGAGCTG	56
INHB-A	GCCACCAAGAAACTCCATGT	GCAACGTTTTCTTGGGTGTT	46
ATF-3	AAAAGCGAAGAAGGGAAAGG	ATACAGGTGGGCCTGTGAAG	50
SERPINA-4	CCAGCAAAAGGGAAAATGAA	CACCACTGATGCCAGAGAGA	50
VEGF-C	AGGGAACACTCCAGCTCTGA	CTCCAAACTCTTTCCCCACA	50
GAPDH	CCTCTCTGGCAAAGTCCAAG	CATCTGCCCATTTGATGTTG	56

Table 11. List of mRNA of interest detected by RT-PCR in tissues isolated from chicken embryos.

No.	Gene	Description
1	FOXA-2 (123)	- This protein is a member of the forkhead class of DNA-binding proteins. - It is an important transcription factor for different genes such as albumin and transthyretin, which are specific to the liver. - They have a role in dopamine neuron development.
2	MAPRE-2 (124)	- This protein is microtubule-associated. - It is important for spindle symmetry during mitosis. - It may contribute to the tumorigenicity of colorectal cancers and in controlling the proliferation of normal cells.
3	RIPK-1 [provided by RefSeq, Aug 2017]	- This protein contributes to inflammatory responses and cellular death in response to tissue damage.
4	INHB-A [provided by RefSeq, Aug 2016]	- This protein contributes to regulating hormone secretion from the pituitary gland. - It plays a role in eye, tooth and testis development. - It also regulates gonadal stromal cell proliferation.
5	ATF-3 [provided by RefSeq, Apr 2011]	- This protein contributes to activation variety of transcription factors, such as CREB protein family. - It also plays a role in cellular stress response.
6	SERPINA-4 (125)	- SERPINA-4 gene encodes Kallistatin protein, which has multiple biological functions, such as anti-inflammatory, vasodilation, angiogenesis, oxidative stress and cancer progression.
7	VEGF-C [provided by RefSeq, Apr 2014]	- This protein is a member of the vascular endothelial growth factor (VEGF) family. - It induces angiogenesis and triggers the growth of endothelial cells, and can modulate the permeability of blood vessels as well.
8	GAPDH (126)	- GAPDH is a housekeeping gene that is widely used as the internal control for comparisons of gene expression data.

CHAPTER 3: RESULTS

3.1. Anti-cancer screening

3.1.1. Cell viability

3.1.1.1. Dose response

The main purpose of studying cell viability is to explore the anti-cancer effects of our compounds in different cell lines. It can also show the time and dose response of a specific cell line to different treatments. Alamar blue is considered a reliable and easy method to quantify cell viability of a large number of samples (127). It is mainly based on the reduction of resazurin; a non-toxic compound that can enter the cells through the cellular membrane. After being reduced, its color changes from blue to pink, resulting in a high fluorescence (128,129).

The effect of different doses of PAMAM dendrimers on cell viability was assessed after exposing SK-BR3, ZR-75, and HNME-E6/E7 cell lines to different concentrations for 48 hours. The cell viability was calculated relative to the controls. In SK-BR3 cells, the most significant reduction of viability was seen in wells treated with G_6NH_2 PAMAMs, starting from 0.1 µM ($p<0.05$). Upon increasing the dose of G_6NH_2 PAMAMs, the cell viability gradually decrease down to 5.1%±2.14 ($p<0.001$) at 10 µM, showing the dose-dependency of this effect. On the other hand, G_6OH and $G_{5.5}COOH$ PAMAMs were less effective compared to G_6NH_2 PAMAMs, reducing the cell viability to 26%±7.21 and 38%±4.73 at a concentration of 100 µM, respectively ($p<0.001$). Additionally, treatment with G_4NH_2 PAMAMs didn't show a significant reduction in cell viability at concentrations below 5 µM, and the highest used concentration (100 µM) inhibited viability down to 48.6%±0.96 ($p<0.01$) (Figure 11).

To confirm the ability of G_6NH_2 PAMAMs in reducing HER2-positive breast cancer cell viability, their impact on another breast cancer cell line which overexpresses

HER2; ZR-75 was examined. Similar to SK-BR3 cells, our results revealed that the G_6NH_2 reduced the viability of ZR-75 cells in a dose-dependent manner. This action was significant upon treatment with 1 µM of G_6 cationic PAMAMs, reaching down to 5.75%±0.87 at 10 µM (p<0.01) (Figure 12).

In addition, G_6NH_2 PAMAMs were able to reduce HNME-E6/E7 cell viability significantly starting from a concentration of 0.5 µM, in a dose-dependent fashion. The cell viability was decreased reaching down to 5%±2.74 (p<0.001) after 48 hours of exposure at the highest used dose of G_6NH_2 PAMAMs (10 µM) (Figure 13).

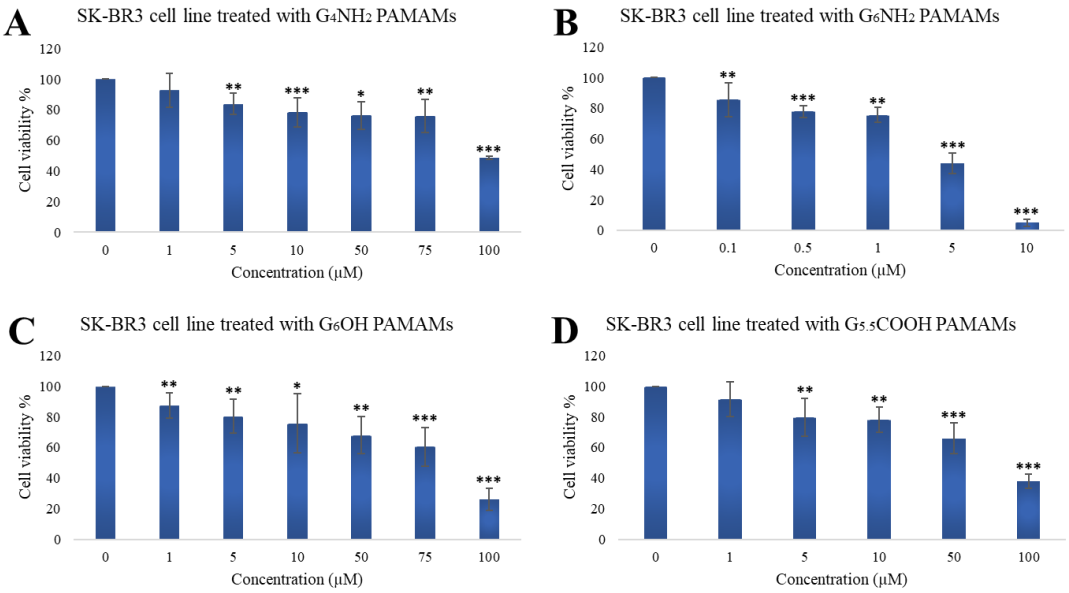

Figure 11. Effect of different doses of PAMAM dendrimers on the viability of SK-BR3 cell line.
Cells were treated with: A) G_4NH_2 PAMAMs (1 to 100 µM), B) G_6NH_2 PAMAMs (0.1 to 10 µM), C) G_6OH (1 to 100 µM) and D) $G_{5.5}COOH$ (1 to 100 µM). Cell viability was assessed after 48 hours of treatment. Data are presented as percentage of treatment relative to the control (Mean ± SEM; n=3). Statistical analysis was performed using one-way analysis of variance (ANOVA). Tukey's post-hoc test was conducted to compare treatment groups and results were stated as *statistically significant when p<0.05 compared to the control. * *p<0.05, **p<0.01, and *** p<0.001.*

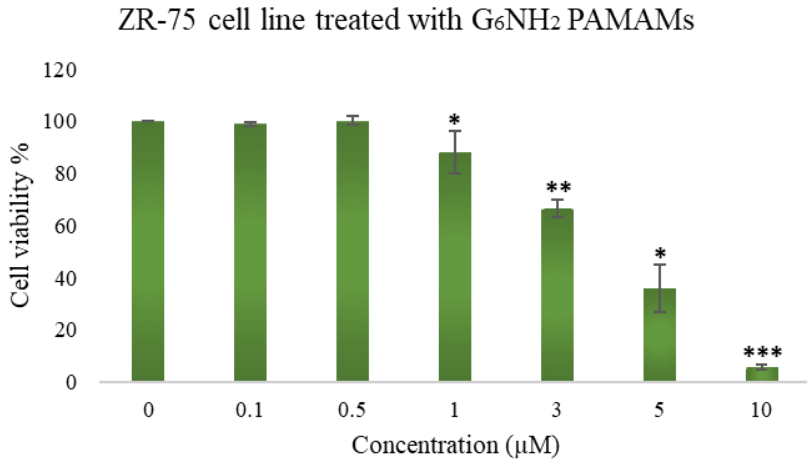

Figure 12. Effect of different doses of PAMAM dendrimers on the viability of ZR-75 cell line.
Cells were treated with G_6NH_2 PAMAMs (0.1 to 10 µM). Cell viability was assessed after 48 hours of treatment. Data are presented as percentage of treatment relative to the control (Mean ± SEM; n=3). Statistical analysis was performed using one-way analysis of variance (ANOVA). Tukey's post-hoc test was conducted to compare treatment groups and results were stated as *statistically significant when $p<0.05$ compared to the control. ** $p<0.05$, **$p<0.01$, and *** $p<0.001$.*

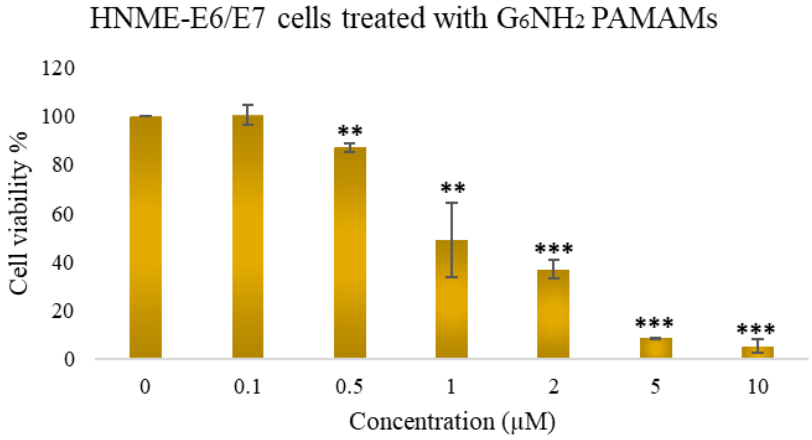

Figure 13. Effect of different doses of PAMAM dendrimers on the viability of HNME-E6/E7 cell line.
Cells were treated with G_6NH_2 PAMAMs (0.1 to 10 µM). Cell viability was assessed after 48 hours of treatment. Data are presented as percentage of treatment relative to the control (Mean ± SEM; n=3). Statistical analysis was performed using one-way analysis of variance (ANOVA). Tukey's post-hoc test was conducted to compare treatment groups and results were stated as *statistically significant when $p<0.05$ compared to the control. ** $p<0.05$, **$p<0.01$, and *** $p<0.001$.*

Furthermore, the positive control, lapatinib, reduced cell viability of HER2-positive breast cancer cell lines significantly starting from low doses; 10 nM (68.55%±4.12, $p<0.001$) and 1 µM (86.06%±7.97, $p<0.001$) in SK-BR3 and ZR-75 cell lines, respectively. Viable cell percentage was reduced down to 40% at higher doses of lapatinib in both cell lines with SK-BR3 cells being more sensitive to lapatinib compared to ZR-75 cells (Figure 14).

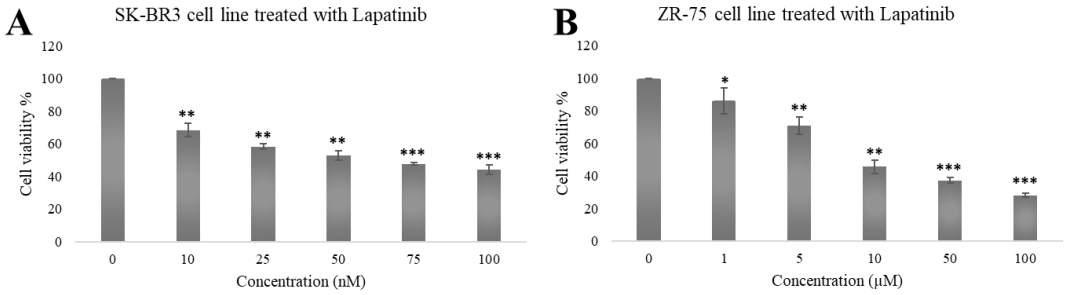

Figure 14. Effect of different doses of lapatinib on the viability of SK-BR3 and ZR-75 cell lines.
A) SK-BR3 cells were treated with lapatinib (10 to 100 nM), B) ZR-75 cells were treated with lapatinib (1 to 100 µM). Cell viability was assessed after 48 hours of treatment. Results are presented as percentage of treatment relative to the control (Mean ± SEM; n=3). Statistical analysis was performed using one-way analysis of variance (ANOVA). Tukey's post-hoc test was conducted to compare treatment groups and results were stated as *statistically significant when $p<0.05$ compared to the control. * *$p<0.05$, **$p<0.01$, and *** $p<0.001$*

3.1.1.2. Time response

SK-BR3, ZR-75, and HNME-E6/E7 cell lines were treated with PAMAM dendrimers at either 10 µM or 100 µM depending on the dose response results. Their effects on cell viability were monitored at several time points (0, 24, 48, 72 hours).

As expected, all PAMAMs showed a time-dependent inhibition of cell viability in the used cell lines (p<0.001) (Figure 15). The highest inhibitory effects of PAMAMs were found upon treatment with G_6NH_2 PAMAMs, as it reached down to 6.87%, 2.64%, and 2.61% in SK-BR3, ZR-75, and HNME-E6/E7, respectively after 72 hours of exposure.

3.1.1.3. Calculating the IC50

In order to calculate the IC50 of PAMAM dendrimers in SK-BR3, ZR-75, and HNME-E6/E7 cell lines, different concentrations were used, ranging from 0.1 µM to 100 µM. Cells were treated with PAMAMs up to 48 hours, and viability values produced by Alamar blue results were plotted as a function of concentrations.

It was found that G_6NH_2 PAMAMs produced the lowest IC50 in SK-BR3 cells (4.62±0.29 µM), while G_6OH and G5.5 PAMAMs had much higher IC50s, ranging from 47 to 83 µM. However, a lower IC50 was produced by G_4NH_2 PAMAMs in SK-BR3 cell line compared to G_6NH_2 PAMAMs (98.02±1.42 µM).

Moreover, the calculated IC50 of G_6NH_2 in ZR-75 cells was approximately similar to what was found in SK-BR3 (4.21±0.38 µM), confirming its effect on HER2-positive breast cancer cells viability. Further, in HNME-E6/E7 cells, the IC50 produced by G_6NH_2 PAMAMs was less than what was found in cancer cells (1.5±0.86) (Table 12).

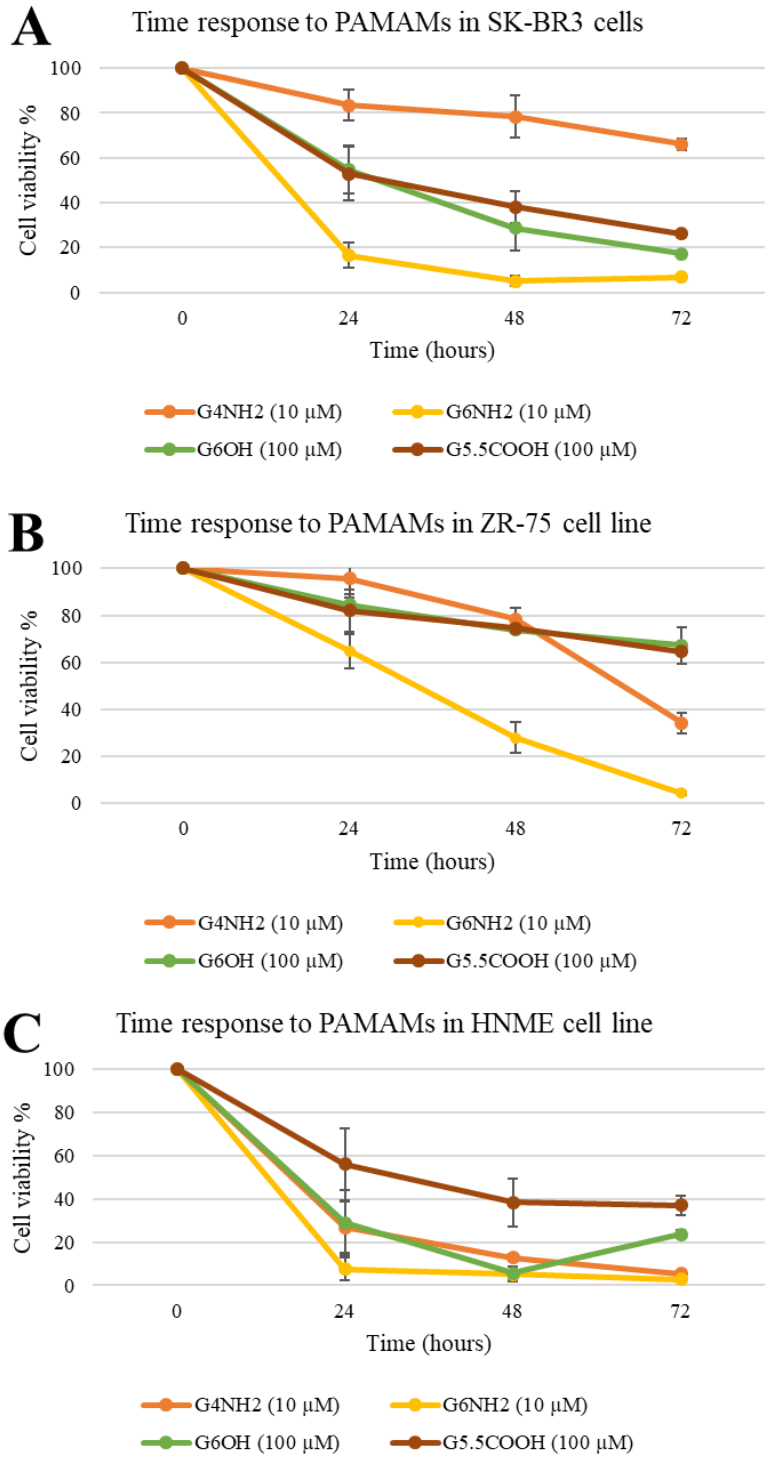

Figure 15. Time response to treatment with PAMAM dendrimers.
Time response to PAMAM dendrimers was investigated in A) SK-BR3, B) ZR-75, and C) HNME-E6/E7 cells. Cells were treated with G_4NH_2 (10 µM), G_6NH_2 (10 µM), G_6OH (100 µM) and $G_{5.5}COOH$ (100 µM). Cell viability was assessed after 48 hours of treatment. Data are presented as percentage of treatment relative to the control (Mean ± SEM; n=3). Statistical analysis was performed using one-way analysis of variance (ANOVA). Tukey's post-hoc test was conducted to compare treatment groups and results were stated as *statistically significant when $p<0.05$ compared to the control.

Table 12. The calculated IC50 of PAMAM dendrimers in the examined cell lines; SK-BR3, ZR-75, and HNME-E6/E7.
Values are expressed as the average IC50 calculated from 3 experiments (Mean ± SEM; n=3x3).

PAMAM Dendrimers	SK-BR3	ZR-75	HNME-E6/E7
G_4NH_2	98.02 ± 1.42 µM	-	-
G_6NH_2	4.62 ± 0.29 µM	4.21 ± 0.38 µM	1.5 ± 0.86 µM
G_6OH	83.4 ± 8.13 µM	-	-
$G_{5.5}COOH$	81.46 ± 5.51 µM	-	-

3.1.2. Morphological examination

Monitoring cell morphological alteration upon treatment is an effective technique that can provide important information about cell differentiation processes, survival, adhesion and alterations in gene expression. Thus, SK-BR3, ZR-75, and HNME-E6/E7 cell morphology was evaluated through microscopic examination following 48 hours of treatment with PAMAM dendrimers at a concentration of 4.62, 4.21, and 1.5 µM (IC50s of G_6NH_2), respectively.

Corresponding with cell viability assay results, the morphological changes induced by PAMAMs were the most significant following the treatment with G_6NH_2 PAMAMs, as cells lost their shape, cellular membrane integrity, and cell-cell adhesion compared to controls. There was also a smaller number of cells and a higher cell death. In addition, G_4NH_2 PAMAMs induced morphological alterations to a less extent only in HNME-E6/E7 cells, while the other types of PAMAMs did not induce a noticeable effect on cell morphology as cells appeared similar to controls (Figure 16).

Lapatinib was used as a positive control in SK-BR3 (50 nM) and ZR-75 (9.9 µM), and it induced morphological changes to a less extent comparing with G_6NH_2 PAMAMs. Furthermore, a combination of lapatinib and G_6NH_2 PAMAMs was used to treat breast cancer cells, and it induced morphological changes higher than lapatinib alone but not G_6NH_2 PAMAMs alone (Figure 17).

In controls, cell shape and behavior did not change for 48 hours from usual. SK-BR3 and HNME-E6/E7 cells usually have a spindle-like shape, while ZR-75 cells appear as round cells clotted together in colonies.

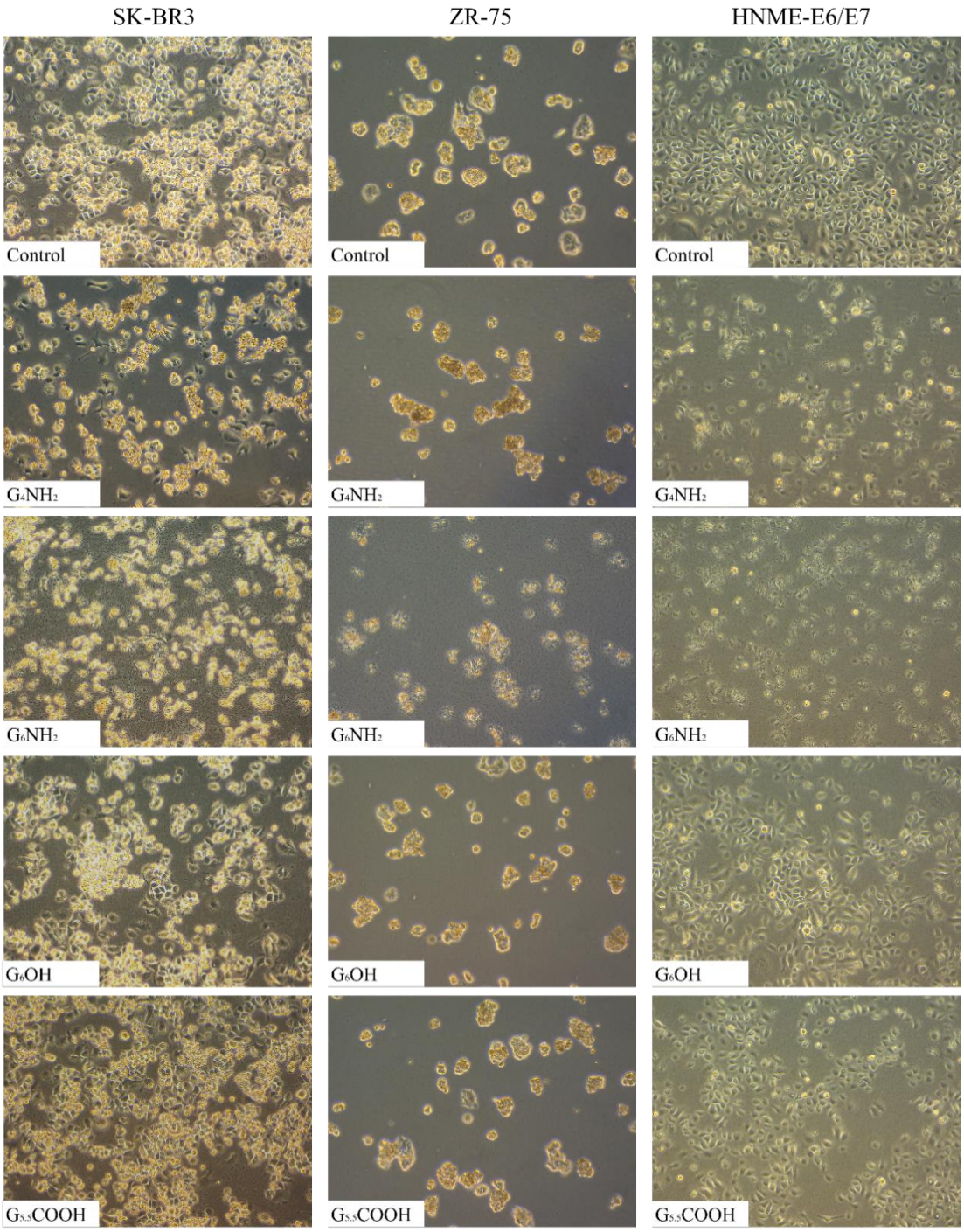

Figure 16. Morphological changes induced by PAMAM dendrimers.
Cells were treated with concentrations equal to the IC50 of G_6NH_2 PAMAMs. Images were taken at a magnification scale of 10X following 48 hours of treatment (N=3).

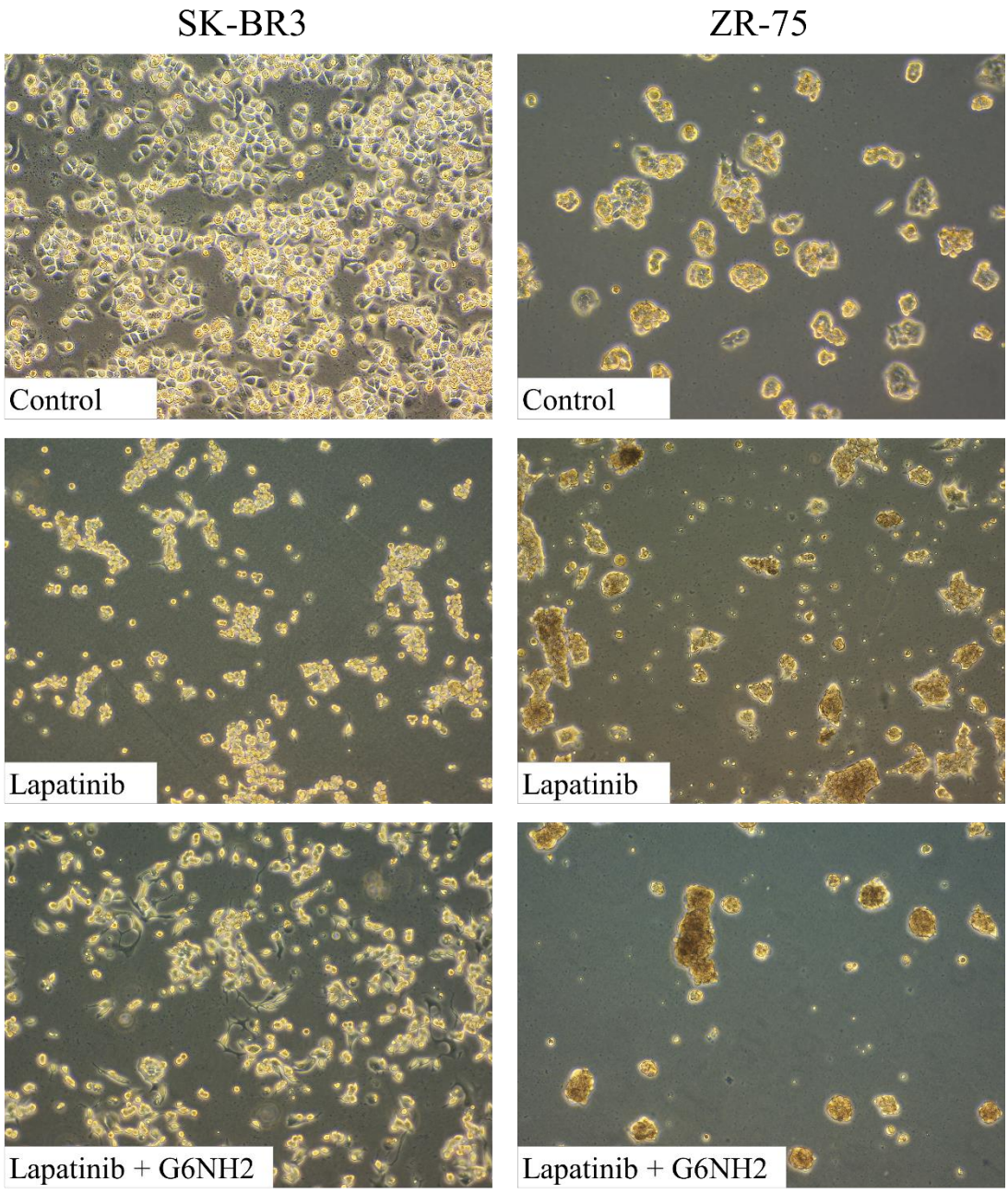

Figure 17. Morphological changes induced by lapatinib and a combination of lapatinib and G_6NH_2 PAMAMs.
Cells were treated with concentrations equal to the IC50 of lapatinib and G_6NH_2 PAMAMs. Images were taken at a magnification scale of 10X following 48 hours of treatment (N=3).

3.1.3. Cell cycle analysis

This experiment was performed to examine the effects of PAMAM dendrimers on cell cycle progression in two cell lines (SK-BR3 and HNME-E6/E7). Flow cytometer was used to quantify the DNA content in each phase of the cell cycle. The resulting figures generally show three peaks each one is assigned to the amount of the DNA in each phase of cell cycle. The first peak represents cells that are arrested at the G1/G0 phase of the cell cycle. The second one denotes cells at the S phase, and the last one is assigned to cells at the G2/M phase.

Our results showed that both G_4NH_2 and G_6NH_2 PAMAMs triggered a statistically significant cell cycle arrest in the sub G0 phase of the cell cycle in SK-BR3 (36.1±1.9 and 37.2±3.54, $p<0.05$) and HNME-E6/E7 cells (10.8±1.83 and 24.6±3.61, $p<0.05$) after 48 hours of treatment. Moreover, a statistically significant cell cycle deregulation in the G1/G0 phase was also observed upon treatment with cationic PAMAMs; G_4NH_2 and G_6NH_2 in both cell lines; SK-BR3 (47.1±3.73 and 50.9±2.19, $p<0.05$) and HNME-E6/E7 (66±3.6 and 55.4±2.42, $p<0.05$) compared to the control. Cationic G_4 and G_6 PAMAMs also induced a significant cell cycle arrest in the S phase significantly in HNME-E6/E7 cells but not in SK-BR3 cells (11.7±1.52% and 11.1±1.04%, $p<0.05$). Further, other types of PAMAMs did not affect the cell cycle control significantly ($p>0.05$) (Figures 18 and 19).

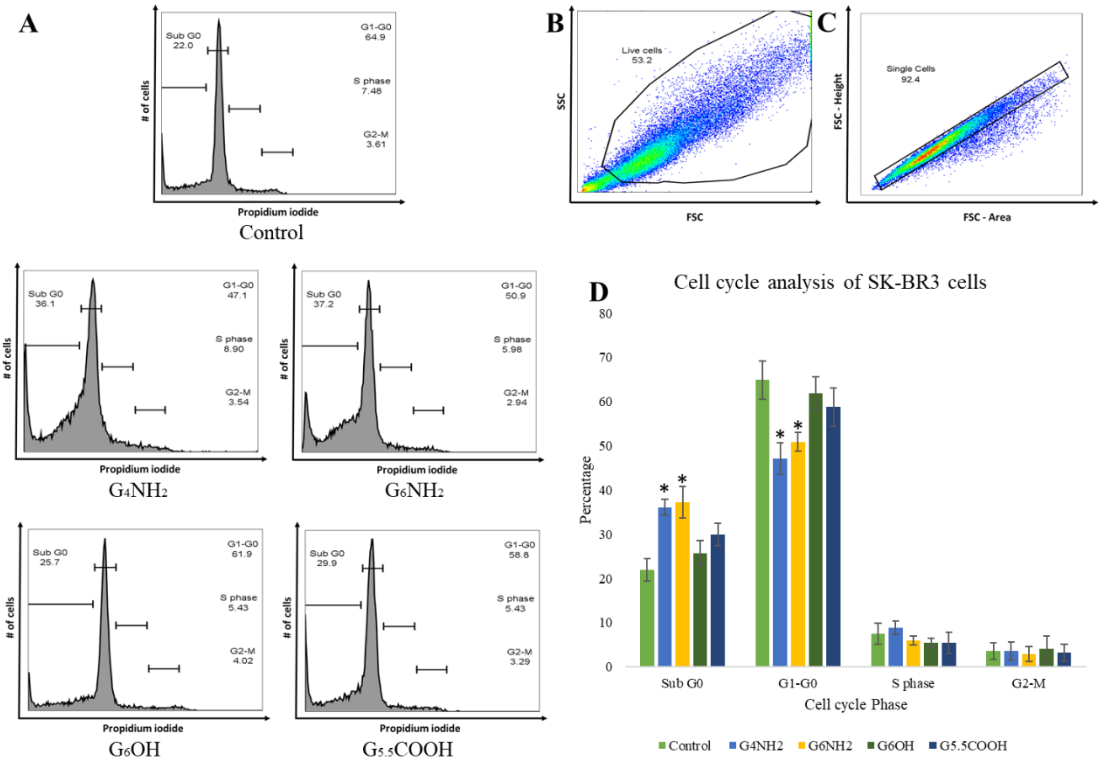

Figure 18. Cell cycle analysis by flow cytometer of SK-BR3 cells.
A) Percentage of cells in G1/G0, S, and G2/M phases, B) forward scatter (FSC) and side scatter (SSC) showed by flow cytometry, C) excluding doublets based on the dimensions of single cells calculated by the forward scatter, and D) quantification of the three phases. Results are presented as the Mean ± SEM; n=3. Statistical analysis was performed using one-way analysis of variance (ANOVA). Tukey's post-hoc test was conducted to compare treatment groups and results were stated as *statistically significant when $p<0.05$ compared to the control.

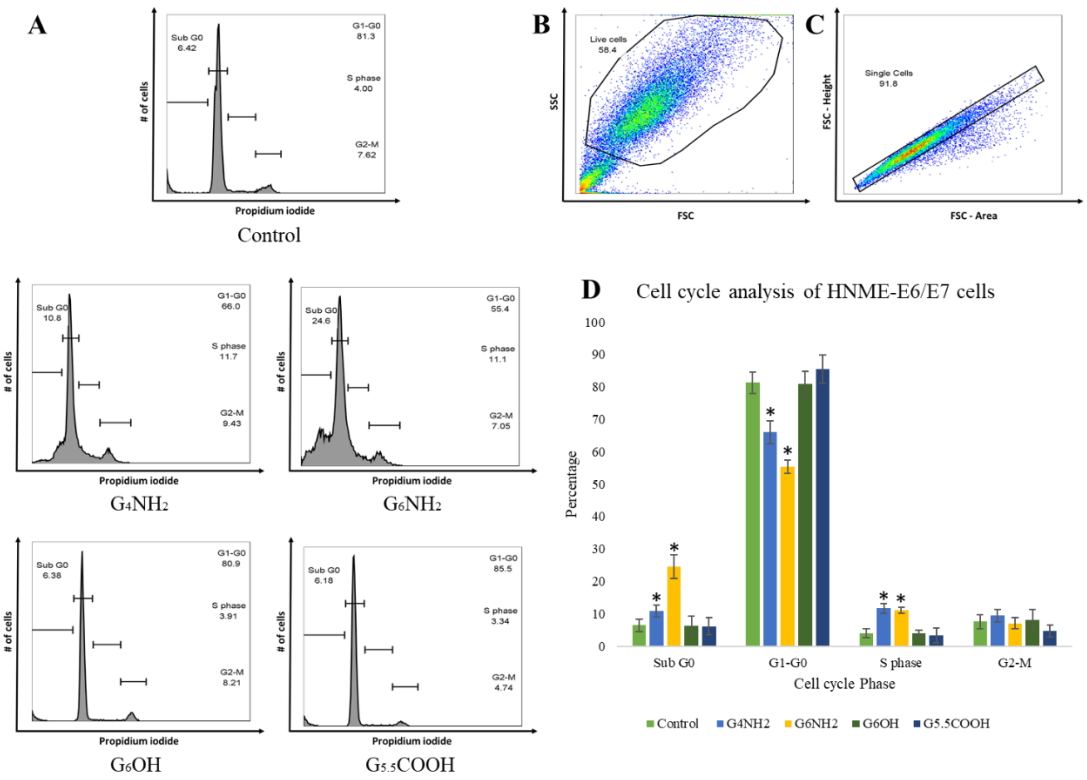

Figure 19. Cell cycle analysis by flow cytometer of HNME-E6/E7 cells.
A) Percentage of cells in G1/G0, S, and G2/M phases, B) forward scatter (FSC) and side scatter (SSC) showed by flow cytometry, C) excluding doublets based on the dimensions of single cells calculated by the forward scatter, and D) quantification of the three phases. Results are presented as the Mean ± SEM; n=3. Statistical analysis was performed using one-way analysis of variance (ANOVA). Tukey's post-hoc test was conducted to compare treatment groups and results were stated as *statistically significant when $p<0.05$ compared to the control.

3.1.4. Colony formation assay

Soft agar (colony formation) assay is a robust and valid *in vitro* test that can be comparable to *in vivo* tests. The importance of this experiment is that it helps in estimating the adhesion-independent growth ability of cancer cells since they lose contact inhibition. This results in an uncontrolled proliferation for cancer cells (130,131). Herein, each single cancer cell can form a colony in a soft agar plate within a few weeks, leading to uncontrolled tumor formation (132).

HER2-positive breast cancer cell lines; SK-BR3 and ZR-75 were treated for three weeks with PAMAM dendrimers at 4.62 and 4.21 μM (IC50s of G_6NH_2), respectively. Microscopic examination revealed that both of the examined cell lines produced a smaller number of colonies in wells treated with G_6NH_2 PAMAMs compared to controls, followed by wells treated with G_4NH_2 PAMAMs. The size of observed colonies varied between control and treatment, and it was very noticeable in the third week (Figures 20 and 21).

Quantification of colonies after three weeks of treatment revealed that colony number and size were significantly lower in wells treated with cationic polymers in both cell lines ($p<0.05$), while colonies in wells treated with G_6OH and $G_{5.5}COOH$ PAMAMs didn't differ significantly from controls in terms of number and size ($p>0.05$) (Figure 22).

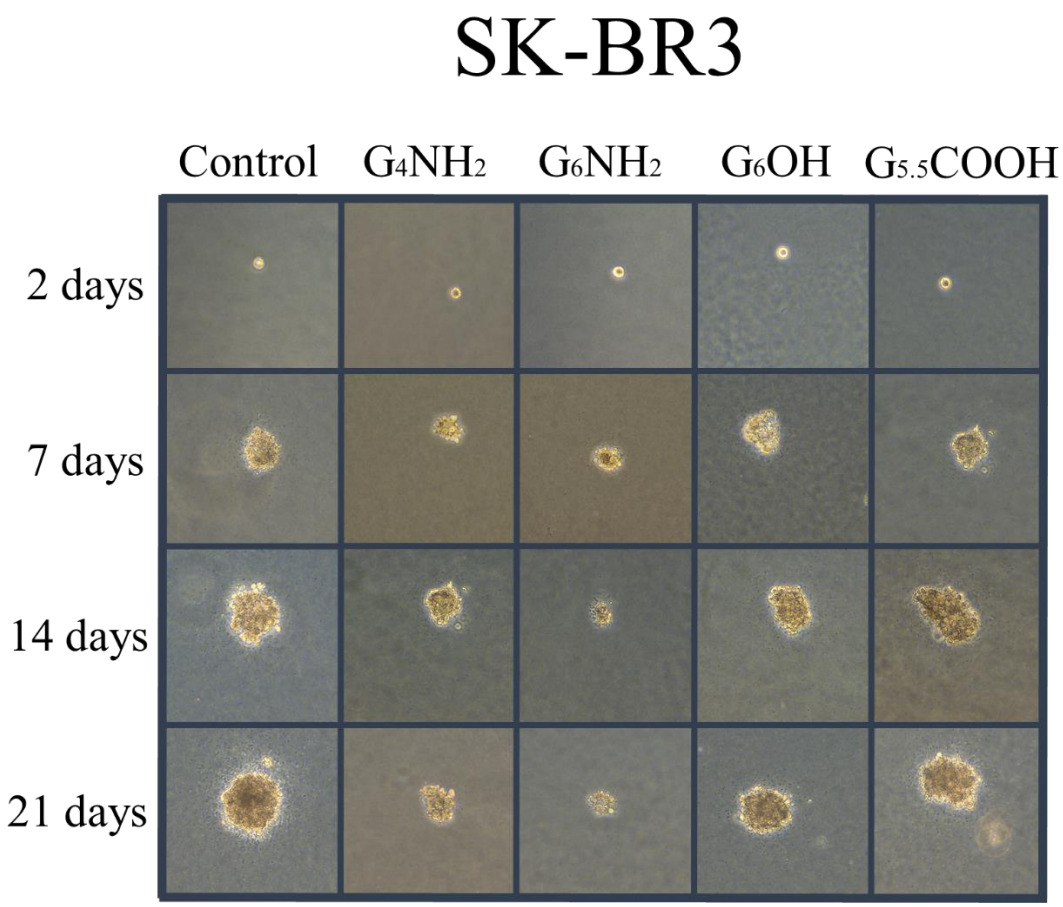

Figure 20. Colony formation in SK-BR3 cells upon treatment with PAMAM dendrimers.
Cells were treated with G_4NH_2, G_6NH_2, G_6OH, and $G_{5.5}COOH$ PAMAMs at concentrations equal to the IC50 of G_6NH_2 PAMAMs. Images were taken at a magnification scale of 10X at different time intervals post-treatment (N=3)[6].

[6] The captured colony per treatment group is not necessarily the same colony followed throughout time.

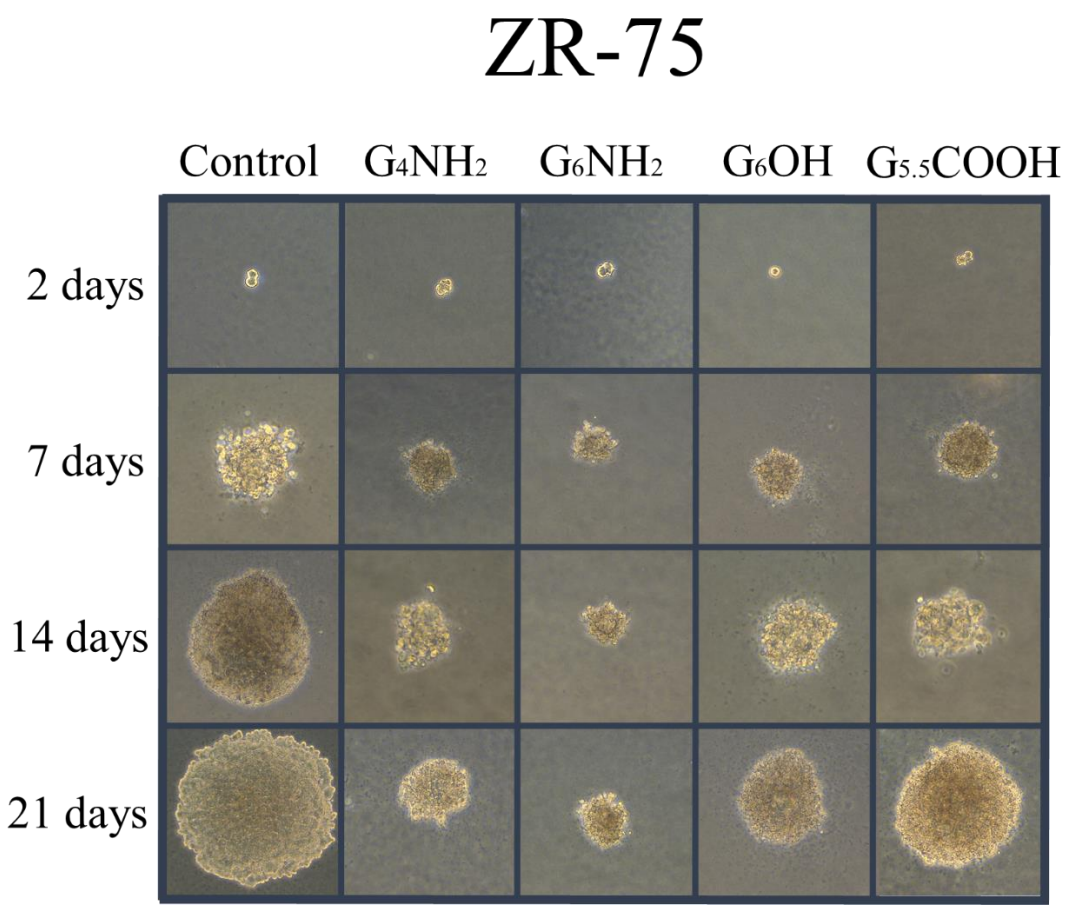

Figure 21. Colony formation in ZR-75 cells upon treatment with PAMAM dendrimers. Cells were treated with G_4NH_2, G_6NH_2, G_6OH, and $G_{5.5}COOH$ PAMAMs at concentrations equal to the IC50 of G_6NH_2 PAMAMs. Images were taken at a magnification scale of 10X at different time intervals post-treatment (N=3)[7].

[7] The captured colony per treatment group is not necessarily the same colony followed throughout time.

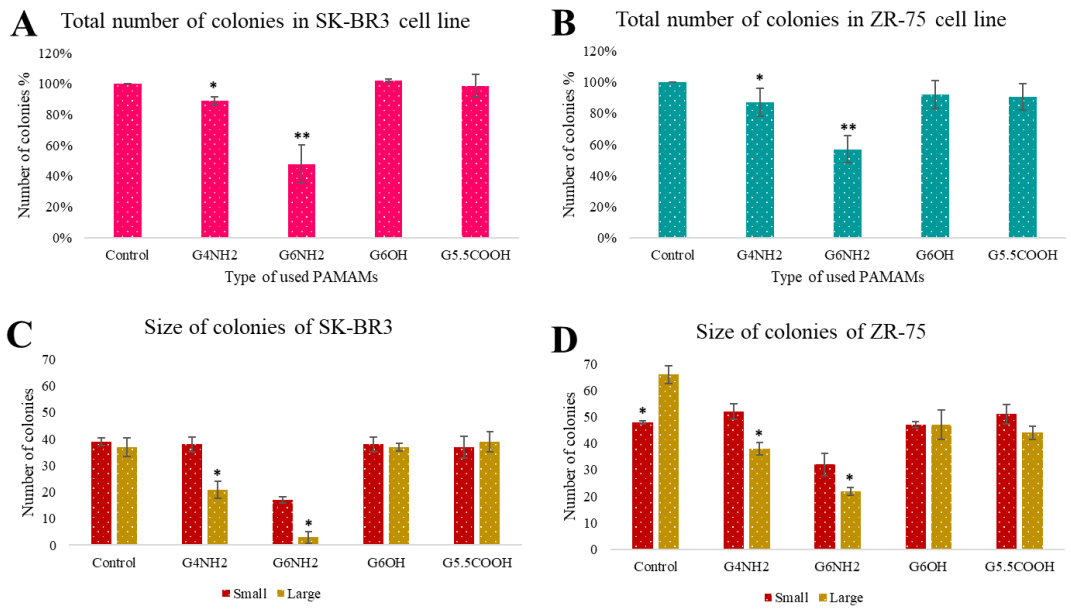

Figure 22. Quantitative results of colony formation assay obtained at 21 days post-treatment.
A) and B) represent the manually counted number of colonies in SK-BR3 and ZR-75 cells, respectively. This number was presented as percentage of treated cells relative to the control. C) and D) represent categorized colonies based on their size into either small or large. Results are presented as the Mean ± SEM; n=3. Statistical analysis was performed using one-way analysis of variance (ANOVA). Tukey's post-hoc test was conducted to compare treatment groups and results were stated as *statistically significant when $p<0.05$ compared to the control. * *$p<0.05$, **$p<0.01$, and *** $p<0.001$.*

3.1.5. RT-PCR of SK-BR3, ZR-75, and HNME-E6/E7 cells lines

3.1.5.1. Expression of VEGF Ligand

RT-PCR was performed to analyze the impact of PAMAM dendrimers on gene expression of HER2-positive breast cancer cell lines (SK-BR3 and ZR-75). Analysis showed that in breast cancer cell lines, treatment with G_6NH_2 and G_6OH PAMAMs had a significant impact on the VEGF expression, followed by G_4NH_2 and $G_{5.5}COOH$ PAMAMs. Treatment with lapatinib showed considerable inhibition of VEGF expression, while combining lapatinib and G_6NH_2 PAMAMs exceeded the effect of lapatinib alone in reducing the expression of VEGF (Figures 23 and 24).

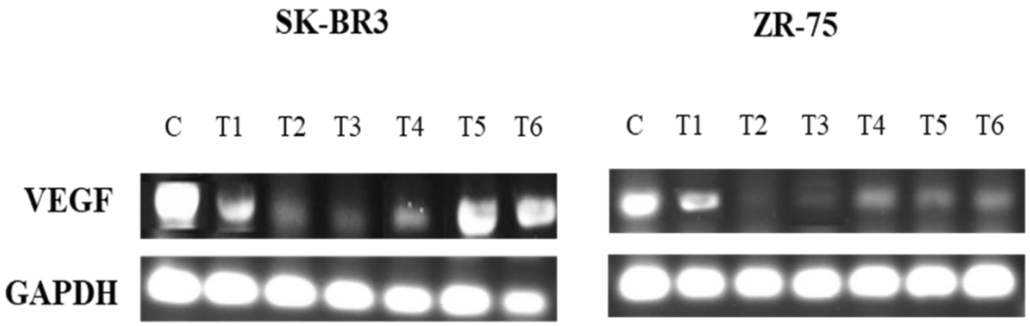

Figure 23. RT-PCR analysis of VEGF expression in SK-BR3, ZR-75, and HNME-E6/E7 cell lines.
Cells were treated with: T1-T4) G_4NH_2, G_6NH_2, G_6OH, and $G_{5.5}COOH$ PAMAMs at concentrations equal to the IC50 of G_6NH_2 PAMAMs, T5) lapatinib at concentrations equal to its corresponding IC50 in SK-BR3 and ZR-75 cells, T6) a combination of lapatinib (IC50) and G_6NH_2 PAMAMs (IC50). GAPDH gene amplified from the same tissue samples indicates similar loading in each group and used for expression quantification.

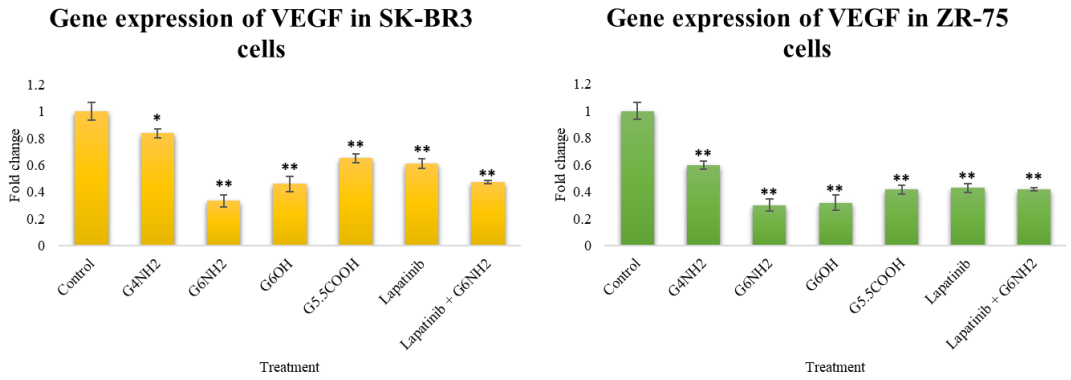

Figure 24. Quantification of the VEGF expression in SK-BR and ZR-75 cell lines.
Results are presented as the Mean ± SEM; n=3. Results were normalized using the housekeeping gene GAPDH. Statistical analysis was performed using one-way analysis of variance (ANOVA). Tukey's post-hoc test was conducted to compare treatment groups and results were stated as *statistically significant when $p<0.05$ compared to the control. * *$p<0.05$, **$p<0.01$, and *** $p<0.001$.*

3.1.5.2. Expression of apoptotic markers

RT-PCR analysis revealed that in comparison to HNME-E6/E7 cells, both HER2-positive cell lines (SK-BR3 and ZR-75) showed a significant increase in the expression of the pro-apoptotic key controller genes; Bax, Caspase-3, Caspase-8, Caspase-9, and p53. On the other hand, the expression of BCL-2 was lost when treated with PAMAM dendrimers, particularly G_6NH_2 (Figure 25).

Quantification of bands using ImageJ showed that while BCL-2 expression is lost in treated cells, expression of Bax, Caspases- 3, -8, -9 and p53 is upregulated in treated HER2-positive cell lines in comparison with HNME-E6/E7 and with control. Cationic PAMAMs showed the most significant effects (p<0.01), particularly G_6, followed by neutral and anionic PAMAMs, respectively.

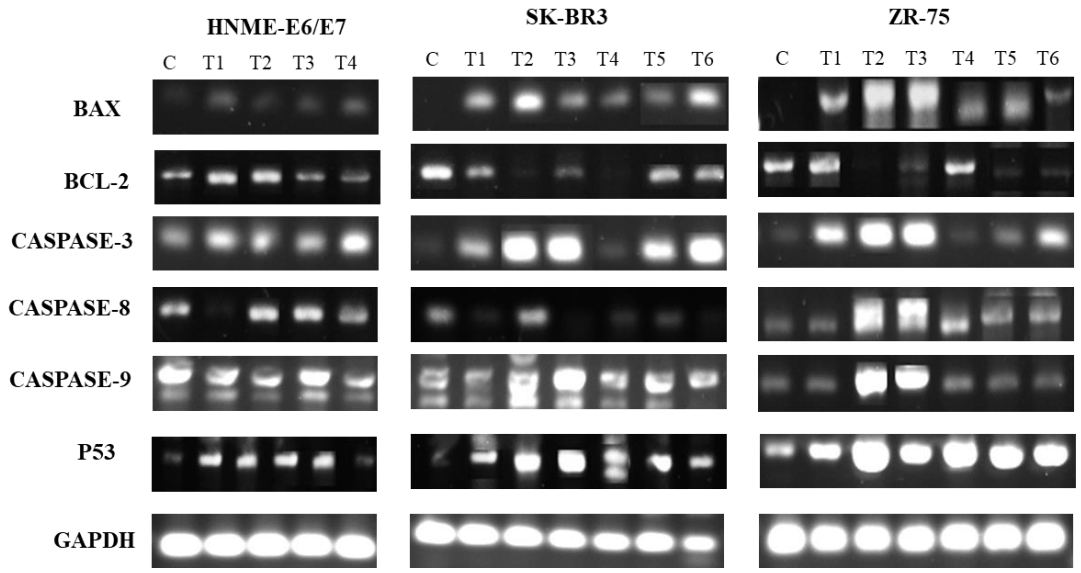

Figure 25. RT-PCR analysis of Bax, BCL-2, Caspase-3, Caspase-8, Caspase-9 and p53 genes in SK-BR3, ZR-75, and HNME-E6/E7 cell lines.
Cells were treated with T1-T4) G_4NH_2, G_6NH_2, G_6OH, and $G_{5.5}COOH$ PAMAMs at concentrations equal to the IC50 of G_6NH_2 PAMAMs, T5) lapatinib at concentrations equal to its corresponding IC50 in SK-BR3 and ZR-75 cells, T6) a combination of lapatinib (IC50) and G_6NH_2 PAMAMs (IC50). GAPDH gene amplified from the same cell samples indicates similar loading in each group.

Lapatinib was used as a positive control and resulted in increasing the expression of the pro-apoptotic markers compared to controls. It also reduced the expression of the anti-apoptotic marker BCL-2. However, its effect was less significant compared to PAMAM dendrimers. On the other hand, a combination treatment between G_6 cationic PAMAMs and lapatinib resulted in significant results compared to lapatinib alone, but not to G_6NH_2 alone (Figure 26).

3.1.6. Western blotting analysis

In order to investigate the underlying mechanisms of action responsible for PAMAMs anti-cancer effect, the expression levels of specific proteins involved in different molecular pathways such as apoptosis were analyzed by Western blot analysis. To obtain a relative quantification of protein expression, images acquired from Western blotting were analyzed using ImageJ software. The intensity of the bands relative to the GAPDH bands were used to calculate a relative expression of proteins in each cell line (Figure 27).

Our results revealed that PAMAM dendrimers reduced the expression of total and phosphorylated ErbB2 (HER2) compared to controls in a surface chemistry and generation-dependent manner. The phosphorylation of EGFR and ERK1/2 was downregulated as well upon treatment with cationic PAMAMs in comparison to controls. We also observed a significant upregulation in the expression of JNK1/JNK2/JNK3 in samples treated with cationic PAMAMs but not in other samples. A major decrease in the protein expression of the anti-apoptotic marker BCL-2 and a raise in the expression of the pro-apoptotic proteins BAX and cleaved Caspase-3 (17 kDa) were also observed. These effects were seen in both HER2-positive breast cancer cell lines; SK-BR3 and ZR-75 (Figures 28 and 29).

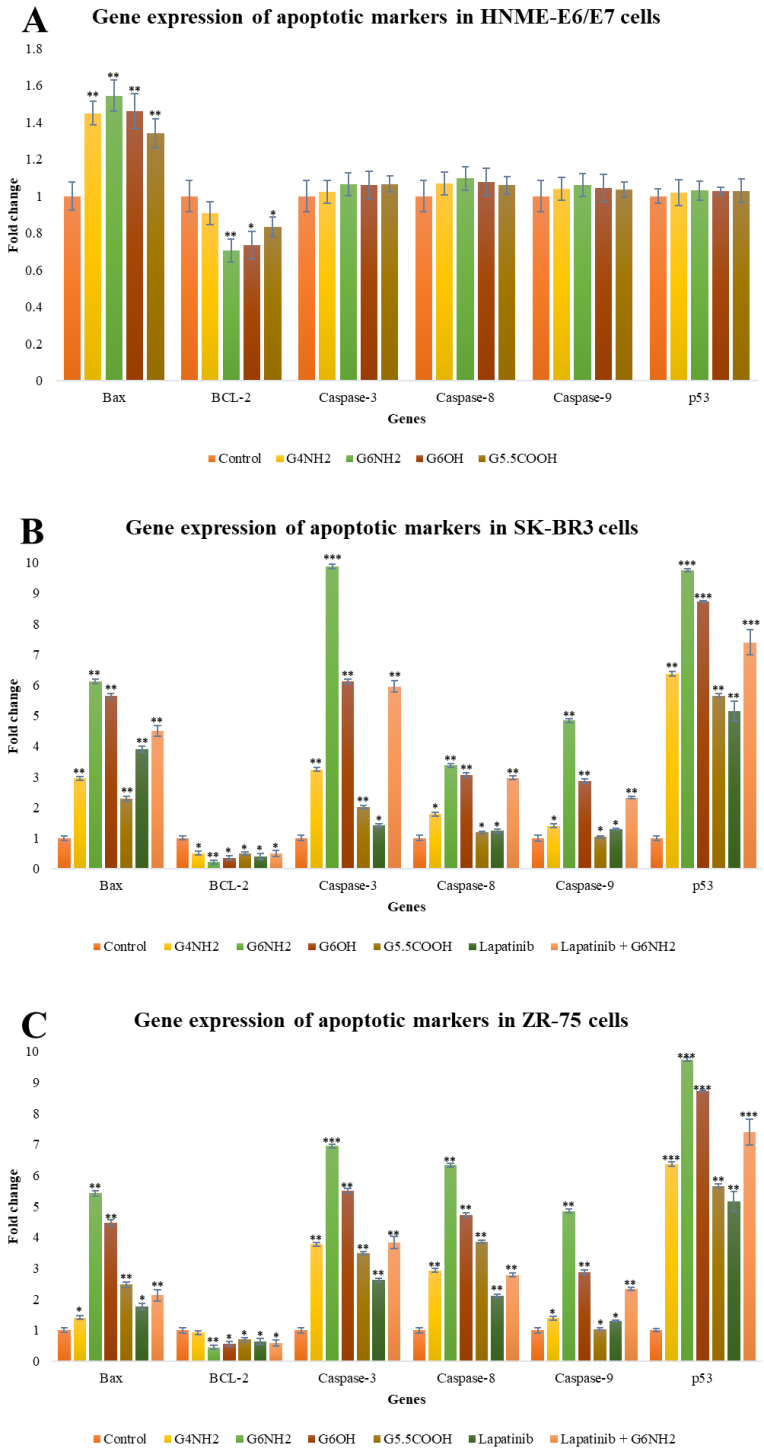

Figure 26. Quantification of the expression of Bax, BCL-2, Caspase-3, Caspase-8, Caspase-9, and p53 genes in SK-BR3, ZR-75, and HNME-E6/E7 cell lines.
A) Gene expression in HNME-E6/E7 cells, B) gene expression in SK-BR3 cells, and C) gene expression in ZR-75 cells. Results are presented as the Mean ± SEM; n=3. Results were normalized using the housekeeping gene GAPDH. Statistical analysis was performed using one-way analysis of variance (ANOVA). Tukey's post-hoc test was conducted to compare treatment groups and results were stated as *statistically significant when $p<0.05$ compared to the control. * *$p<0.05$, **$p<0.01$, and* *** *$p<0.001$*.

Treatment with lapatinib, on the other hand, produced similar effects to PAMAM dendrimers in terms of modulating the protein expression, but they were less significant compared to G_6NH_2. Moreover, combining lapatinib with G_6NH_2 PAMAMs exceeded the effect of lapatinib alone, but not the effect of G_6NH_2.

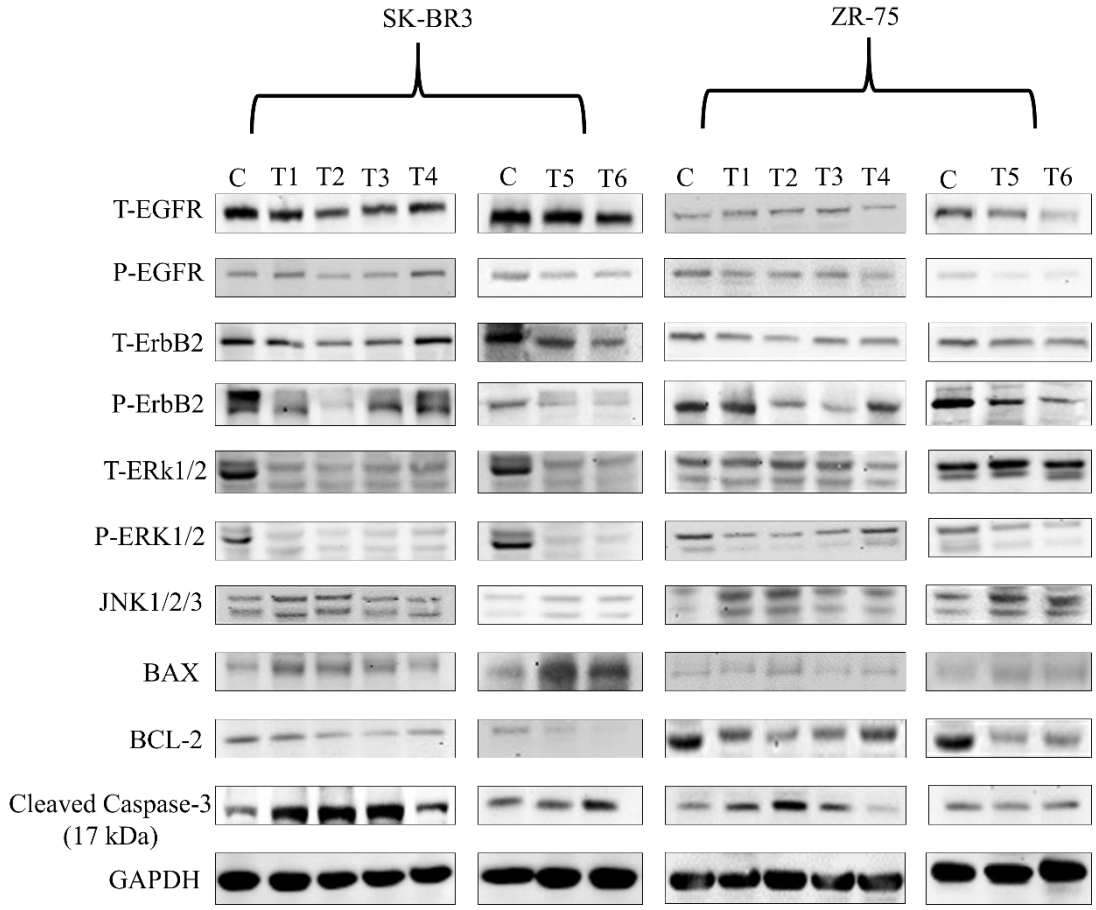

Figure 27. Effect of PAMAM dendrimers on the expression of different proteins in SK-BR3 and ZR-75 cell lines.
Cells were treated with: T1-T4) G_4NH_2, G_6NH_2, G_6OH, and $G_{5.5}COOH$ PAMAMs at concentrations equal to the IC50 of G_6NH_2 PAMAMs, T5) lapatinib at concentrations equal to its corresponding IC50 in SK-BR3 and ZR-75 cells, T6) a combination of lapatinib (IC50) and G_6NH_2 PAMAMs (IC50). GAPDH[8] protein expression from the same samples indicates similar loading in each group.

[8] The displayed GAPDH is representative and not necessarily extracted from the same blot as the bands above.

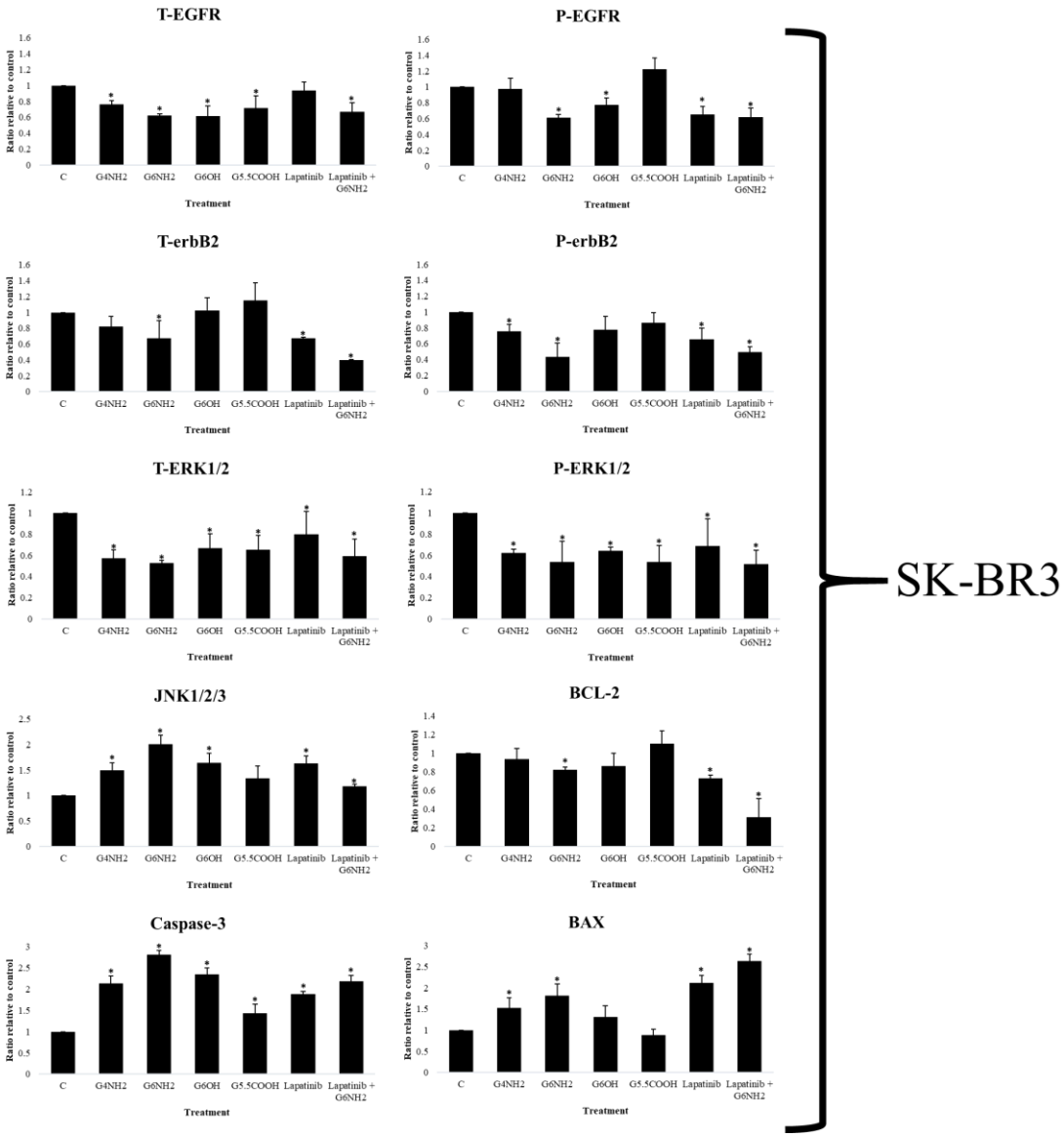

Figure 28. Quantification of the expression of proteins of interest in Western blotting in SK-BR3 cell line.

Results are presented as a ratio relative to the control (Mean ± SEM); n=3. Results were normalized using the housekeeping protein GAPDH. Statistical analysis was performed using one-way analysis of variance (ANOVA). Tukey's post-hoc test was conducted to compare treatment groups and results were stated as *statistically significant when $p<0.05$ compared to the control.

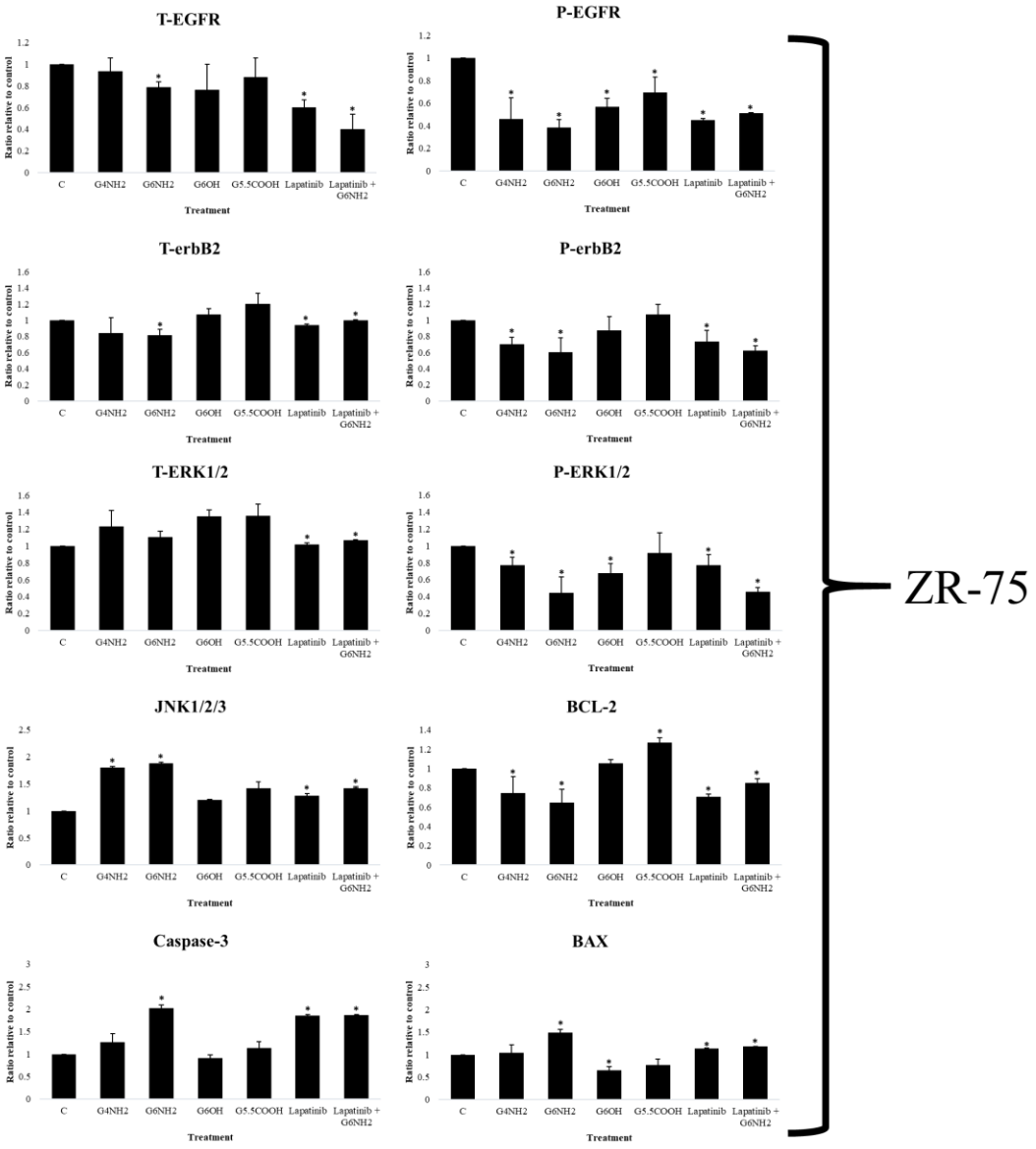

Figure 29. Quantification of the expression of proteins of interest in Western blotting in ZR-75 cell line.

Results are presented as a ratio relative to the control (Mean ± SEM); n=3. Results were normalized using the housekeeping protein GAPDH. Statistical analysis was performed using one-way analysis of variance (ANOVA). Tukey's post-hoc test was conducted to compare treatment groups and results were stated as *statistically significant when $p<0.05$ compared to the control.

3.2. Angiogenesis and embryogenesis studies using the chicken embryo model

3.2.1. Effect of PAMAM dendrimers on angiogenesis

3.2.1.1. Visual inspection

The effect of PAMAM dendrimers on angiogenesis was evaluated in the CAM of the chicken embryo model, which is a good model for such purpose. Visual inspection under the stereomicroscope of chicken embryos CAM revealed that both G_4 and G_6 cationic PAMAMs inhibited angiogenesis in the exposed area compared to the unexposed area and controls, in a dose-dependent manner. G_6 exhibited a more visually noticeable inhibitory effect than G_4 at similar doses (Figure 30). However, the effect of other types of PAMAMs on CAM was not visually noticed.

3.2.1.2. AngioTool quantification

The values of blood vessel parameters obtained from AngioTool analysis (Figure 31) were assessed for each group and were compared to external and internal controls. It was found that treatment with G_6 cationic PAMAMs caused a statistically significant reduction in the total number of junctions and vessel length in the exposed area compared to the unexposed area and controls ($p<0.05$), in a concentration-dependent fashion. G_6NH_2 PAMAMs decreased the studied blood vessel parameters down to 70.56%±0.38% and 67.96%±4.97% for the total number of junctions and average vessel length, respectively. On the other hand, treatment with G_4 cationic PAMAMs significantly reduced only the vessel length ($p<0.05$) but not the number of junctions ($p>0.05$). This inhibitory effect was higher upon treatment with G_6NH_2 PAMAMs compared to G_4NH_2 PAMAMs at similar concentrations ($p<0.05$). However, the effect of neutral (G_6OH) and anionic ($G_{5.5}COOH$) PAMAMs on the measured parameters was less than cationic PAMAMs and was not statistically significant ($p>0.05$) (Figures 32 and 33).

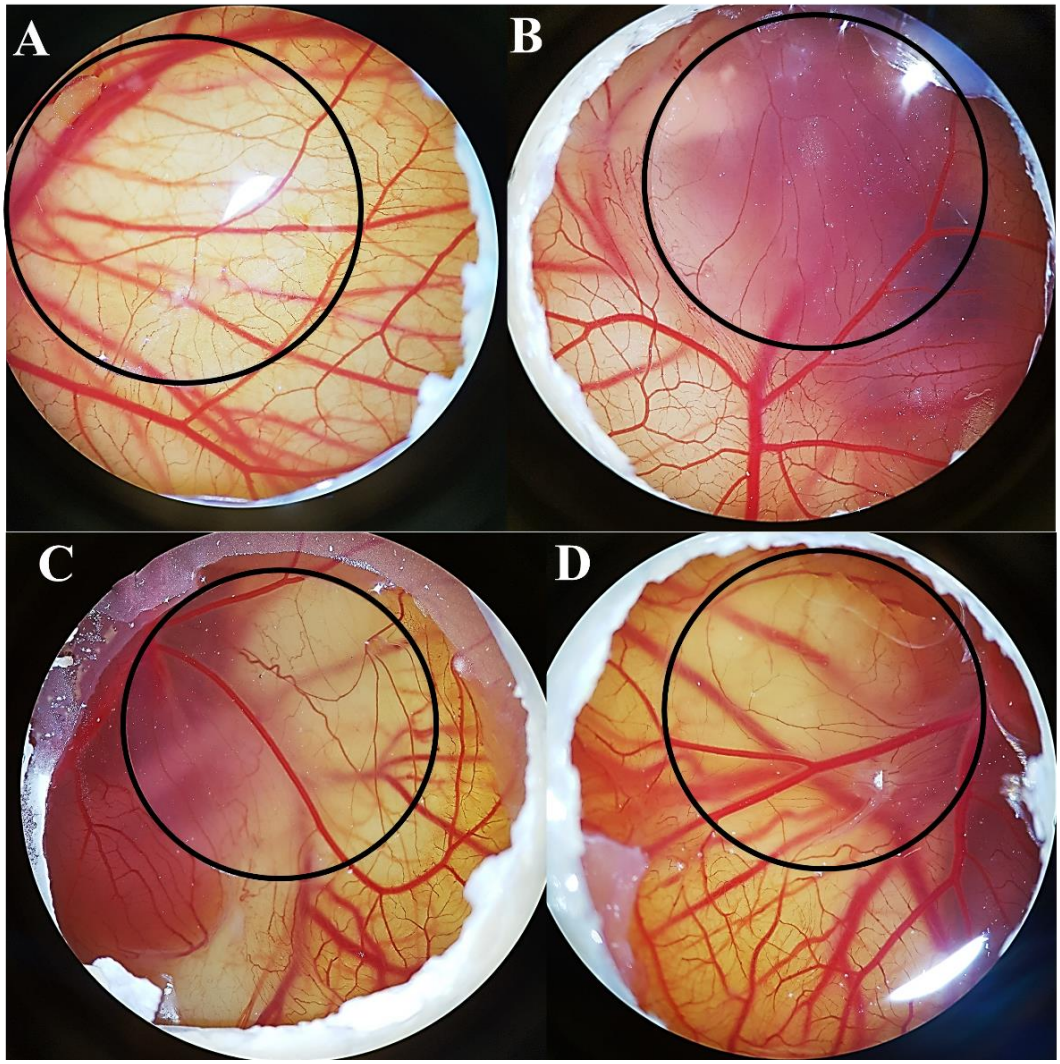

Figure 30. Visual inspection of chicken embryos upon treatment with PAMAM dendrimers for 48 hours.
Embryos were treated with: A) Control, B) 5 µM of G_6NH_2 PAMAMs, C) 10 µM of G_6NH_2 PAMAMs, D) 20 µM of G_6NH_2 PAMAMs. Images were taken using stereomicroscope 48 hours post-treatment (n=3).

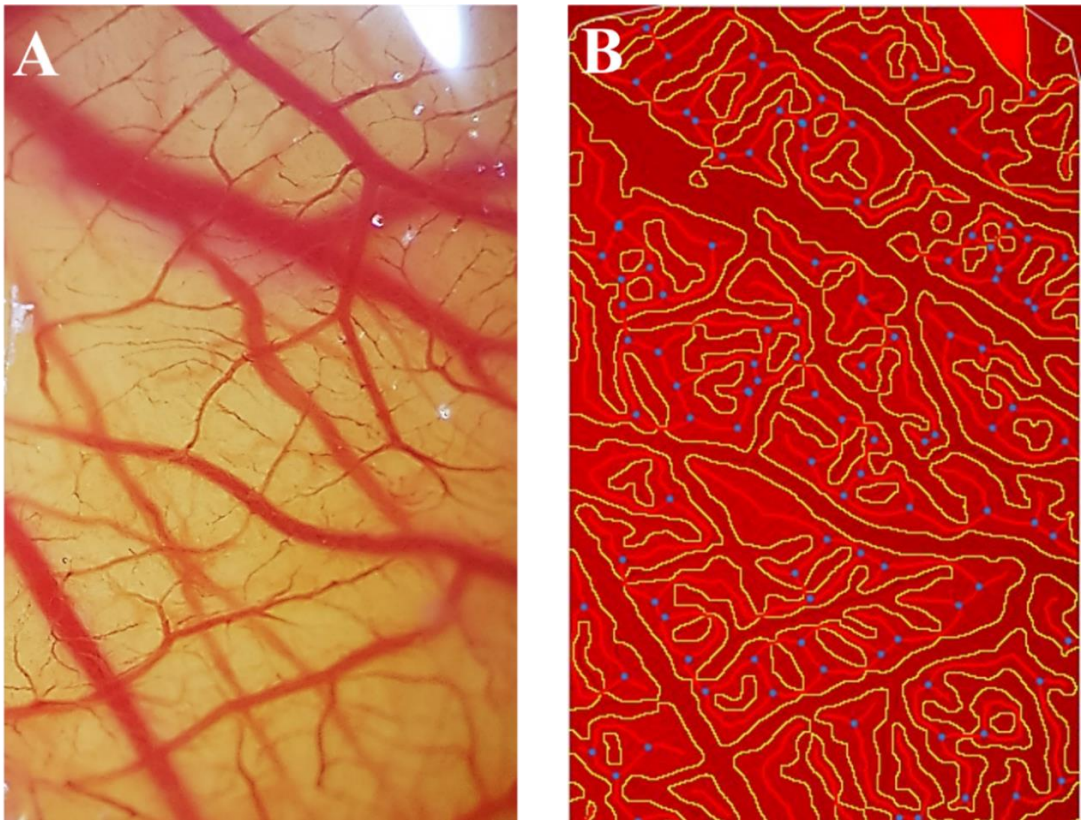

Figure 31. AngioTool analysis of CAM images.
Similar inputs were selected for all images as follows: Detection threshold (0-255), vessel thickness (0-10), small particles (20), and fill holes at 151.

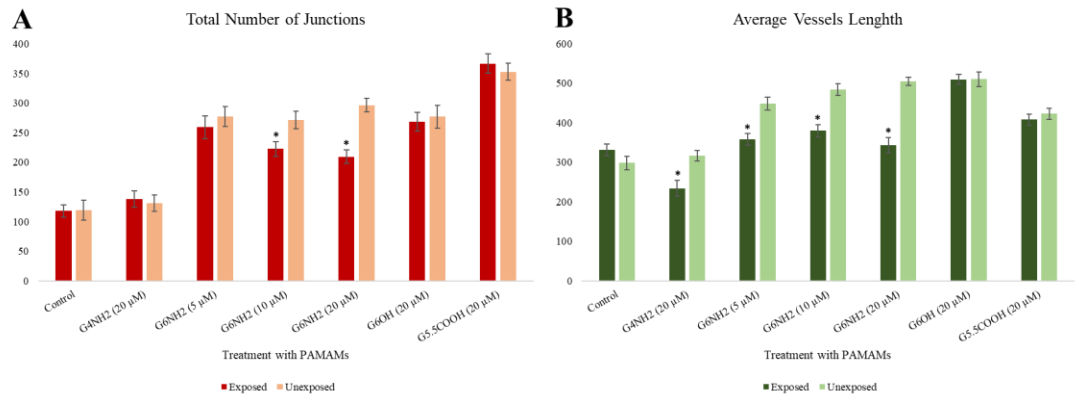

Figure 32. Comparing exposed area and unexposed area of the CAM of the chicken embryos upon treatment with PAMAM dendrimers.
Embryos were treated with: G_4NH_2 (20 µM), G_6NH_2 (5, 10, 20 µM), G_6OH (20µM), and $G_{5.5}COOH$ (20µM). Results are presented as the Mean ± SEM; n=3. Statistical analysis was performed using student's t-test to compare treatment groups and results were stated as *statistically significant when $p<0.05$ compared to the control.

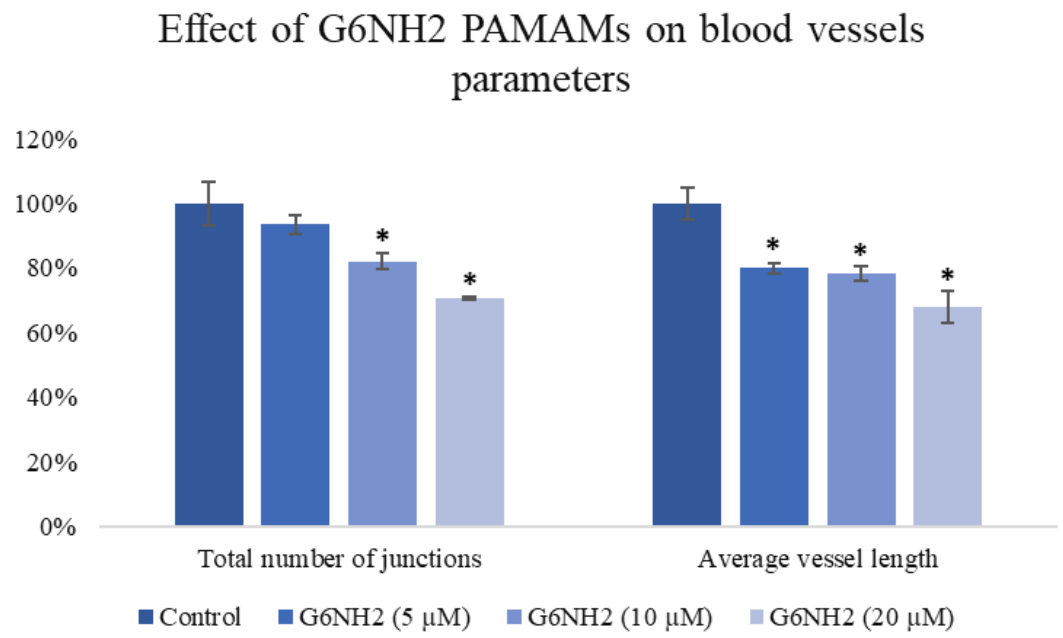

Figure 33. Percentage of reduction in blood vessel parameters upon treatment with G_6NH_2 PAMAMs.
Embryos were treated with different doses of G_6NH_2 PAMAMs (5, 10, and 20 µM). Results are presented as the Mean ± SEM; n=3. Statistical analysis was performed using one-way analysis of variance (ANOVA). Tukey's post-hoc test was conducted to compare treatment groups and results were stated as *statistically significant when $p<0.05$ compared to the control.

3.2.2. Effect of PAMAMs on the early stage of embryogenesis

To explore the impact of PAMAM dendrimers on the early stages of the normal embryonic development, chicken embryos were treated with G_4NH_2 and G_6NH_2 as described in the methods section. After 24 hours of treatment, it was found that approximately 10% and 26% of the embryos treated with G_4NH_2 and G_6NH_2 PAMAMs died, respectively, compared to the control groups which did not show death incidences. On the last day, before the autopsy was performed, around 50% of embryos treated with G_4NH_2 PAMAMs were dead, while in embryos treated with G_6NH_2 PAMAMs, the death rate was higher, and it reached up to 57% ($p<0.05$) (Figure 34).

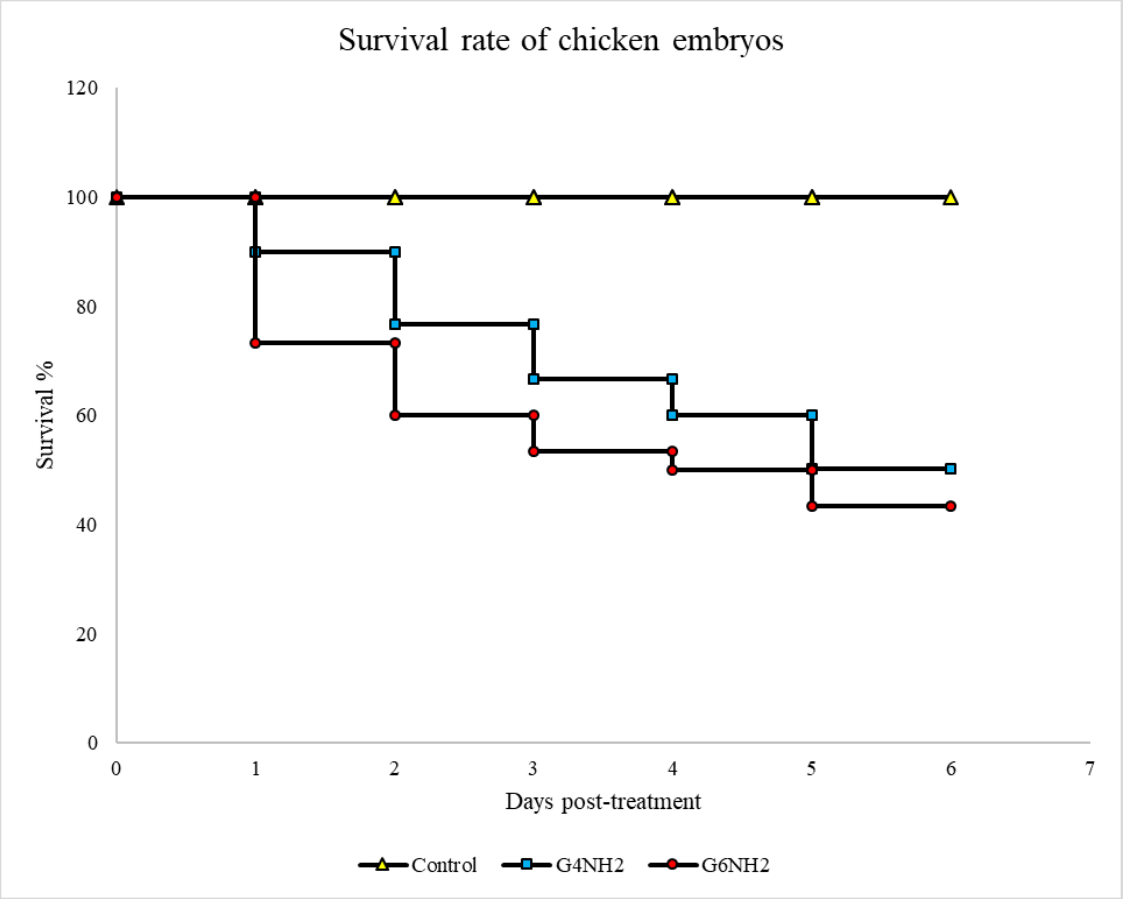

Figure 34. The calculated survival rate for chicken embryos treated with PAMAM dendrimers.

3.2.3. RT-PCR of tissues isolated from chicken embryos

The expression of ATF-3, BCL2, Caspase-8, FOXA-2, INHB-A, MAPRE-2, RIPK-1, SERPINA-4, and VEGFC genes was evaluated in the brain, heart and liver tissues derived from PAMAMs-treated embryos and their corresponding controls using RT-PCR analysis. It was shown that ATF-3, Caspase-8, FOXA-2, INHB-A, MAPRE-2, and RIPK-1 genes were upregulated in brain, heart and liver tissues in PAMAM-treated embryos compared to control tissues; while BCL-2, SERPINA-4, and VEGFC genes are downregulated in tissues from PAMAM-exposed embryo (Figures 35 and 36).

Quantification of the resulted bands showed that G_6NH_2 PAMAMs resulted in higher upregulation of ATF-3, Caspase-8, FOXA-2, INHB-A, MAPRE-2, and RIPK-1 genes, while it resulted in downregulating of BCL-2, SERPINA-4, and VEGFC in a significant manner compared to G_4NH_2 PAMAMs and to control tissues (p<0.01) (Figure 36).

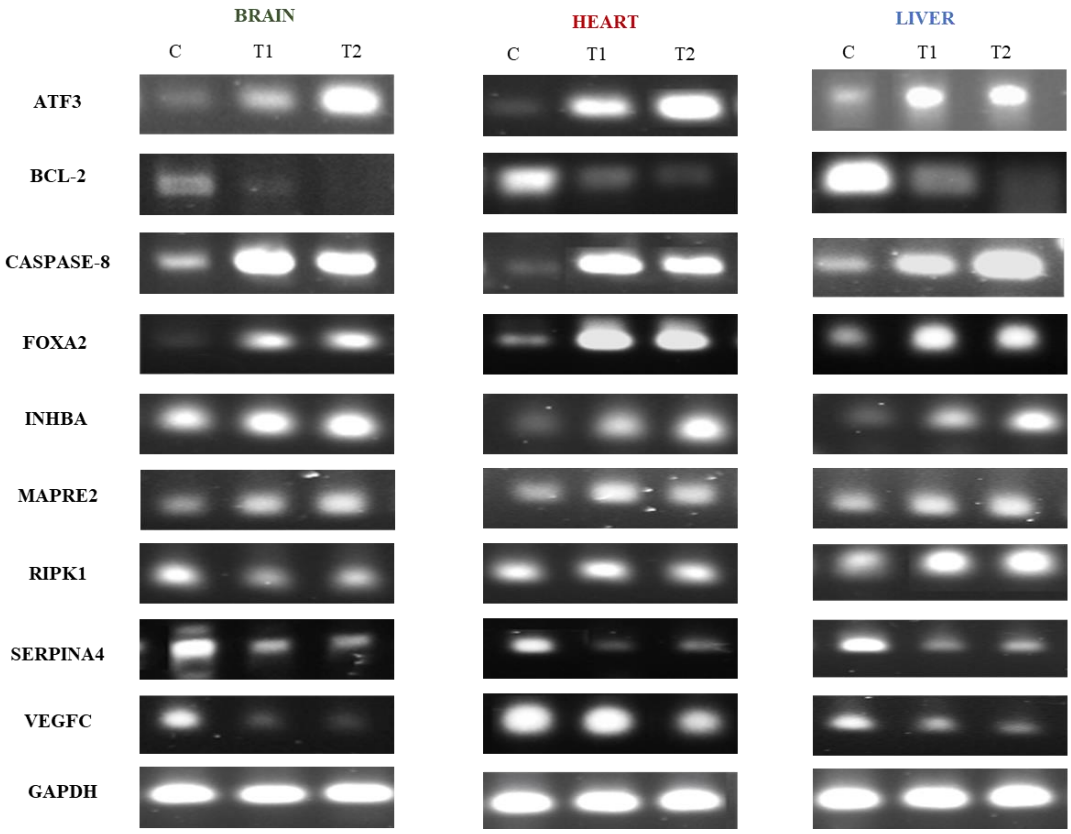

Figure 35. RT-PCR analysis of ATF-3, BCL-2, Caspase-8, FOXA-2, INHB-A, MAPRE-2, RIPK-1, SERPINA-4 and VEGFC genes in brain, heart and liver tissues derived from treated and control chicken embryos.
Embryos were treated with: T1) G_4NH_2 (20μM) and T2) G_6NH_2 (20μM). GAPDH gene amplified from the same tissue samples indicates similar loading in each group.

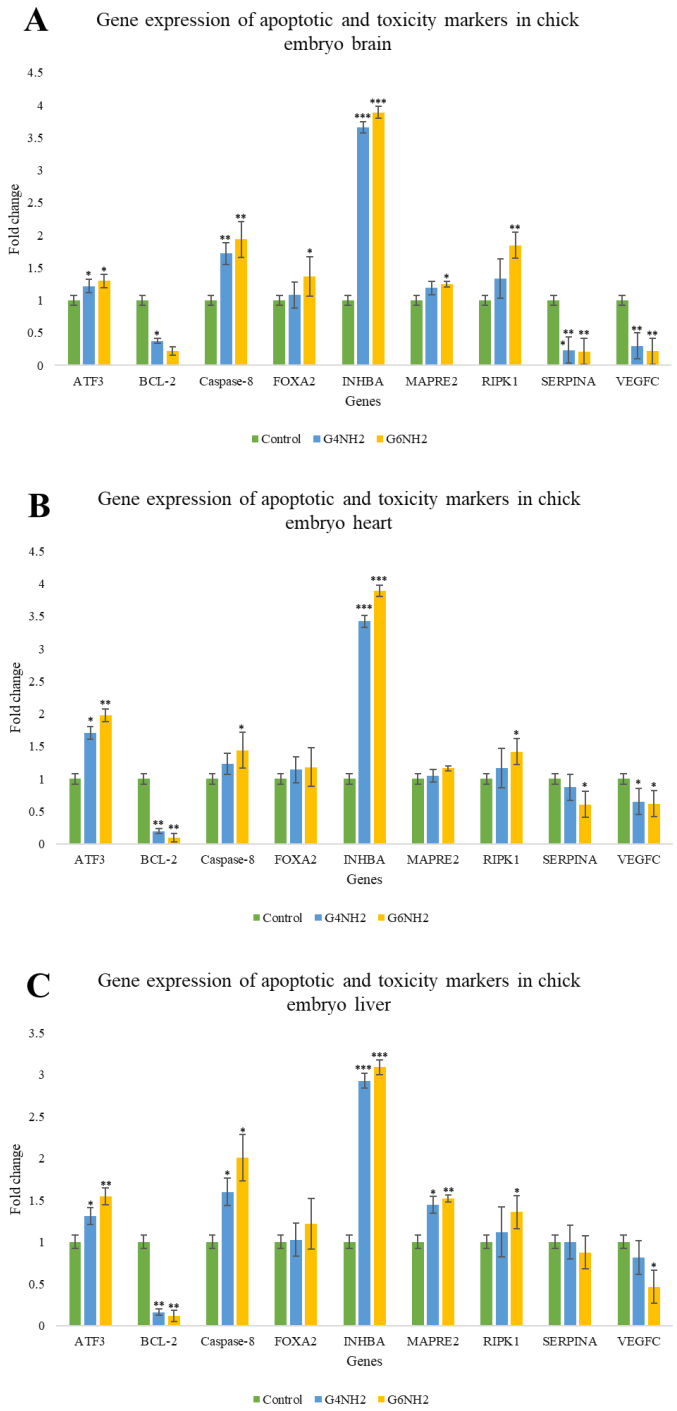

Figure 36. Quantification of the expression of ATF-3, BCL-2, Caspase-8, FOXA-2, INHB-A, MAPRE-2, RIPK-1, SERPINA-4 and VEGFC genes in brain, heart and liver tissues derived from treated and control chicken embryos.
A) Gene expression pattern in the brain of the chicken embryo, B) gene expression in the heart of the chicken embryo, and C) gene expression in the liver of chicken embryo. Results are presented as the Mean ± SEM; n=3. Results were normalized using the housekeeping gene GAPDH. Statistical analysis was performed using one-way analysis of variance (ANOVA). Tukey's post-hoc test was conducted to compare treatment groups and results were stated as *statistically significant when $p<0.05$ compared to the control.

CHAPTER 4: DISCUSSION

Approximately 15%-20% of breast cancers overexpress HER2 (EebB2) gene (133), which is closely related to epidermal growth factor receptors family (134). In this case, an excess amount of HER2 protein exists in the malignant cells. It was shown by many studies that overexpression of HER2 is the major contributor to the pathogenicity of HER2-positive breast cancer (135–139). Thus, targeting HER2 became a strategy in the treatment of this disease. Although anti-HER2 therapies such as trastuzumab are effective in managing the disease, they exhibit several limitations, mainly regarding their safety profile. Additionally, this type of breast cancer can develop resistance towards treatment, which was observed in over 50% of HER2-positive patients (78,87,140). These limitations emphasize the need of developing new therapeutic agents that can overcome drug resistance.

PAMAM dendrimers are widely used in gene transfection and delivery systems as carriers for nucleic acids and small molecular weight drugs. These polymers can be tailor-made to meet the needs of nanomedical applications, as their surface chemistry can be modified to be either cationic, anionic or neutral. Recently, these polymers drew attention to them due to their various pharmacological actions, such as altering gene expression, modulating inflammatory responses and interfering with signal transduction pathways without any drug cargo (11,12,15,17,46,57). They also can trigger cellular death through different mechanisms, autophagy, apoptosis, and necrosis (40–44). These biological effects caused by PAMAM dendrimers showed a specific trend, depending on their surface chemistry, generation, and dose.

A previous study demonstrated that G_5 cationic PAMAM dendrimers were able to inhibit the transactivation of EGFR and ErbB2 (HER2) signaling pathways mediated by Angiotensin II in primary aortic vascular smooth muscle cells (19). However, the

impact of PAMAM dendrimers on cancer cells that overexpress ErbB2 (HER2) is an unanswered question. To the best of our knowledge, this is the first study that focuses on the potential anti-cancer effects of naked PAMAMs dendrimers in HER2-positive breast cancer. Therefore, we hypothesized that naked PAMAM dendrimers, particularly cationic, might possess anti-cancer properties against HER2-positive breast cancer.

In this study, we explored a novel pharmacological actions of PAMAM dendrimers *in vitro* against two HER2-positive breast cancer cell lines; SK-BR3 and ZR-75. Human normal mammary epithelial cells immortalized by E6/E7 were used as a control (141). We examined four types of PAMAMs; G_4NH_2, G_6NH_2, G_6OH, $G_{5.5}COOH$, to see the impact of their surface chemistry and generation on their biological effects. The *in vitro* anti-cancer screening included cell viability assay, colony formation assay, and cell cycle analysis. The mechanisms of action were investigated by RT-PCR analysis and Western blotting. Besides, we monitored for the first time the effect of PAMAMs on the angiogenesis using the CAM of the chicken embryo, which is an extraembryonic membrane created after 4 days of incubation (142). It has been a favored method to study tumor angiogenesis and metastasis (143,144), mainly because it is a fast, easy to maintain, economical and reliable method (145). Furthermore, chicken embryos were also employed in studying the impact of PAMAMs on the early stages of embryonic development, as there are no studies regarding this matter.

The anti-cancer screening of PAMAM dendrimers revealed that G_6 cationic PAMAMs induced the most significant growth inhibition in SK-BR3 cells compared to the other types of PAMAMs. Also, we used another HER2-positive breast cancer cell line, which is ZR-75 to confirm the ability of G_6 cationic PAMAMs in reducing cell viability of this type of breast cancer cells. Interestingly; a similar potent IC50 value of

G_6NH_2 PAMAMs was found in both cell lines; 4.62±0.29 µM and 4.21±0.38 µM in SK-BR3 and ZR-75 cells, respectively. The inhibition of cancer cell viability was found to be in a dose and time-dependent fashion. As expected, other types of PAMAMs (neutral and anionic) had a less anti-cancer effect on the SK-BR3 cell line, nonetheless, it was statistically significant at 1 µM and 5 µM upon treatment of G_6OH and $G_{5.5}COOH$, respectively. Furthermore, the lower generation of cationic PAMAMs (G_4) did not show anti-cancer effects similar to G_6NH_2 in SK-BR3, implying the role of PAMAMs generation in reducing cell viability. This difference can be due to the highly branched structure of G_6NH_2 PAMAMs compared to G_4NH_2 PAMAMs and their higher number of terminal amino groups, as they contain 256 surface amino groups. A similar study by Kuo et al. looked into the impact of naked PAMAM dendrimers on the viability of cervical cancer cell line, HeLa and concluded that neutralizing surface charge of cationic polymers resulted in a loss of the anti-cancer action, confirming the major role of cationic surface in this effect (17).

As a control of this study, we used HNME cells immortalized by HPV E6/E7 type 16 to test the safety of PAMAMs. However, treatment with G_6NH_2 PAMAM dendrimers expressed a lower IC50 in HNME-E6/E7 cells compared to breast cancer cell lines; 1.5±0.86 µM. Thus, safety assessment using primary normal mammary cells is a must to balance between the desired effects and the toxicity of PAMAMs. In fact, the toxic effects of cationic polymers and nanomaterials are common in delivery systems due to their interaction with the negatively charged cellular membranes (13,146,147). Nevertheless, several methods have been proposed to diminish this toxicity, such as PEGylation, i.e. covalent bonding to polyethylene glycol (PEG). Many studies proposed that linking the PEG chain with cationic polymers results in decreasing their toxicity (148,149). Moreover, PEG can increase the biocompatibility

of PAMAMs and their half-life (148,150). Other molecules were found to also diminish the toxicity of PAMAMs, like lauryl groups and acetyl groups, when they are linked to PAMAMs surface (151,152). The previous methods reduced PAMAMs toxicity through masking the surface cationic charge, which in our case may not be desired due to an expected loss of the anti-cancer activity. Thus, a balance between the desired effects and the safety profile is needed. Other methods proposed in the literature can be used as a solution for this issue with preserving the cationic surface, such as choosing the optimum route of administration. A study by Wangpradit et al demonstrated that the intra-tracheal pathway is safe to avoid inflammatory response caused by G_5 cationic PAMAM dendrimers in rats (60). Furthermore, intraperitoneal administration of PAMAM dendrimers in rats was found to be favored over the intravenous route, where PAMAMs can cause hemolysis. Herein, PAMAMs will be slowly released from the peritoneum resulting in minimal hemolysis with cationic PAMAMs (21). Thus, we expect that injecting PAMAM dendrimers directly in the site of action may eliminate their intrinsic toxicity. Moreover, a targeted delivery of PAMAMs was also proposed by different studies, as they linked trastuzumab to the surface of PAMAMs creating a selectivity towards HER2-positive breast cancer cells rather than other cells (153–155).

The morphological changes induced by cationic PAMAMs in the examined cell lines (SK-BR3, ZR-75, and HNME-E6/E7) revealed a membrane loss, as it is well known that PAMAMs can interact with cellular membranes leading to cell lysis (156). Morphological examination also showed a high number of cell death in wells treated with G_6NH_2 PAMAMs compared to other PAMAMs and to controls, which was confirmed by cell cycle analysis.

Cationic PAMAMs deregulated the cell cycle control in SK-BR3 and HNME-E6/E7 cell lines, mainly the sub G0 and G1/G0 phases, while other types of PAMAMs

did not. Cationic PAMAMs resulted in cellular arrest in the sub G0 phase, which is an extended sub G1 phase that can be considered as an indicator of apoptosis. These data are in accordance with another study that showed the effect of cationic PAMAMs dendrimers in inhibiting the cell cycle and triggering cell death through different mechanisms (22). In another study, cationic PAMAM dendrimers were able to add benefit to cancer treatment by altering gene expression of several genes related to cell cycle arrest in HeLa cancer cells (17), which is consistent with our findings.

Based on our cell viability results, we hypothesized that cationic PAMAMs may be able to prevent anchorage-independent tumor growth of SK-BR3 and ZR-75 cells in soft agar. We treated cells with the same dose, which is the IC50 of G_6NH_2 to get a fair comparison between all PAMAMs types. Our results were consistent with our viability study and cell cycle analysis, confirming that G_6NH_2 PAMAMs play a role in counteracting tumor growth *in vitro*. This experiment provides a clear idea about tumor mass growth in semi-solid matrices and can be comparable to *in vivo* tests (157). Therefore, we can suggest that cationic polymers play a role in reducing carcinogenicity and preventing colony formation in these two cell lines.

Several studies discussed the mechanisms of cell death produced by PAMAM dendrimers, particularly apoptosis. Our RT-PCR analysis for apoptotic markers in SK-BR3 and ZR-75 cell lines treated with PAMAM dendrimers revealed that PAMAMs increased the expression of the pro-apoptotic markers; Bax, cleaved Caspase-3, Caspase-8, Caspase-9, and p53 in a significant manner ($p<0.01$), whereas the expression of BCL-2; an anti-apoptotic marker was lost. These effects were maximum in samples treated with G_6NH_2 PAMAMs followed by G_6OH and G_4NH_2 PAMAMs respectively, confirming the role of cationic surface and generation in inducing apoptosis. These findings are consistent with our cell cycle analysis data, as the

observed cellular arrest in the sub G0 phase caused by cationic PAMAMs may be an indicator of DNA fragmentation due to apoptosis. Our Western blotting analysis validated the results of RT-PCR regarding PAMAMs apoptotic effects in SK-BR3 and ZR-75 cells. Cells treated with our positive control; lapatinib were subjected to apoptotic death as well but to a less extent than cells treated with G_6NH_2 PAMAMs. A combination of G_6NH_2 PAMAMs and lapatinib induced apoptosis significantly higher than lapatinib alone, suggesting that PAMAMs can add benefit to the anti-cancer effect of the latter. Other studies suggested different mechanisms mediating apoptosis induction by PAMAM dendrimers, such as disruption of mitochondrial membrane potential (MMP) and activation of ATM-mediated DNA damage. Cationic PAMAMs were also capable of triggering apoptosis in oxidative stress-dependent mechanisms, such as increasing production of intracellular ROS (16,48,50,51). These pathways were not explored in our study; however, future investigation may determine whether they mediate PAMAMs apoptotic effects in HER2-positive breast cancer cells. Other proposed mechanisms were through lysosomal/mitochondrial pathways in a Caspase-dependent manner (45–47,52). Herein, we noticed an overexpression of the pro-apoptotic genes; Caspase-3, Caspase-8, and Caspase-9 in RT-PCR, mainly after treatment with G_6NH_2 PAMAMs. We also found an increase in cleaved Caspase-3 protein expression, which is consistent with the previous findings. These data emphasize that PAMAMs cationic surface chemistry plays a significant role in inducing apoptotic cell death.

To get further insights regarding the pathways of action in which PAMAMs produce anti-cancer effects in HER2-positive breast cancer cells, we looked at several molecular pathways using Western blotting analysis. As expected, PAMAM dendrimers reduced the phosphorylation of HER2 and EGFR proteins in SK-BR3 and

ZR-75 cell line, in a surface chemistry and generation-dependent fashion. We also noticed a reduction in ERK1/2 phosphorylation in accordance with what was stated by Akhtar et al., as their study showed an inhibition of transactivation of HER2, EGFR, and ERK1/2 caused by treatment with cationic PAMAMs *in vitro* and *in vivo* (16). Lapatinib, on the other hand, decreased the phosphorylation of HER2, EGFR, and ERK1/2 to a similar extent to G_6NH_2 PAMAMs.

A new pathway; JNK1/2/3, was discovered by this study in which PAMAMs exhibit anti-cancer effects. We found that cationic PAMAM dendrimers resulted in the upregulation of JNK1/2/3 in SK-BR3 and ZR-75 cells, in a similar manner to lapatinib. This protein is found to significantly increase tumor formation when it is downregulated (158). The upregulation of JNK1/2/3 was also associated with increasing the cancer cells sensitivity of many anti-cancer agents (159).

A combination of lapatinib and G_6NH_2 PAMAMs was used to treat HER2-positive cell lines, and protein expression was explored. Our data states that the combination expresses a higher reduction of the phosphorylation of HER2, EGFR, and ERK1/2 in comparison with treatment with lapatinib alone but not with G_6NH_2 alone. Regarding this matter, it was previously stated that PAMAM dendrimers enhance tumor inhibitory effects when co-administered with other anti-cancer compounds (17,160,161). Altogether, PAMAM dendrimers may become a new class of nanomedicines as candidates for future cancer treatment.

Throughout this study, we also noticed that the impact of a combination of lapatinib and G_6NH_2 PAMAMs on HER2-positive breast cancer cells was less than G_6NH_2 PAMAMs alone. This may be explained by partial neutralization of PAMAMs surface charge upon mixing with lapatinib, which can be avoided by applying each compound solely with an appropriate time interval.

Angiogenesis is a tightly controlled process mediated by endogenous inducers and inhibitors, which results in forming new blood capillaries from nearby endothelial cells (162). In cancer, angiogenesis supply the tumor cells with the oxygen and nutrients they need to progress, invade, and form metastasis. Recently, targeting tumor angiogenesis has resulted in high clinical benefits in cancer treatment (162). Moreover, angiogenesis can be activated during other pathological conditions, such as diabetic retinopathy, inflammatory, infectious and immune disorders (163,164). In this study, we monitored changes in angiogenesis using the CAM of the chicken embryo, which is an extraembryonic membrane created after 4 days of incubation (142). It represents a favored tool to investigate tumor angiogenesis and metastasis (143,144), mainly because it is fast, easy to maintain, economical and reliable (145). The main drawback of this method is the nonspecific inflammatory reactions that may occur as a result of manipulation which may induce blood vessel formation. This may interfere with the quantification of the investigated anti-angiogenic response (145). To our knowledge, this is the first study to evaluate the impact of PAMAM dendrimers on the angiogenesis using the CAM of a chicken embryo model. Several generations, surface chemistries and doses of PAMAM dendrimers were examined to establish a relationship between the outcomes and PAMAMs physiochemical properties. PAMAMs were applied to small round-shaped coverslips to avoid injuring the embryos. This method allows comparing angiogenesis inhibition within the same embryo and thus, eliminating variations. Results of visual inspection indicated that the inhibitory effect of PAMAM dendrimers is surface chemistry-dependent, as there was a clear difference between the exposed area and unexposed area after 48 hours of applying G_6 and G_4 cationic PAMAMs, with more obvious effect with G_6NH_2 compared to other types of PAMAMs. This indicates the role of PAMAMs surface chemistry and generation in the

anti-angiogenic effect.

AngioTool program was developed by Zudaire et al. (122). It is a validated method that permits quick and reproducible quantification of several blood vessel parameters in microscopic images. This software computes many morphological and spatial parameters such as the area covered by a vascular network, the number of vessels, vessel length, and vascular density. In this study, we focused on the total number of junctions and average vessel length which can give a clear idea about PAMAMs impact on angiogenesis. Our results revealed that cationic PAMAMs significantly inhibited angiogenesis after 48 hours of exposure compared to anionic and neutral PAMAMs and to controls, where no significant effects were noticed. Therefore, it is fair to say that surface chemistry or charge of PAMAMs may be the key to inhibiting angiogenesis. These results correspond with previous findings that demonstrated the impact of the cationic surface of polyethyleneimine and dextran polymers in promoting anti-tumor immunity and inhibiting angiogenesis (165). Moreover, the inhibition of angiogenesis increased upon dose increasing. It was also higher when a higher generation of PAMAMs was used (G_6) compared to the lower generation (G_4). This dose and generation-dependent trend was also proved to be essential in the extent of other biological effects of PAMAM dendrimers (42,55).

Cancer cells tend to produce many proteins to maintain their growth and progression. Among those proteins, the VEGFs have the main role in triggering angiogenesis (166–169). Thus, RT-PCR analysis was used to explore changes in the gene expression of VEGF ligand in SK-BR3 and ZR-75 cells upon treatment with PAMAM dendrimers. Interestingly, our results were correlated with visual inspection and AngioTool analysis, as PAMAM dendrimers, particularly G_6NH_2 reduced the expression of VEGF in a significant manner compared to controls. Moreover, G_6NH_2

produced more significant reduction of VEGF expression compared to the positive control; lapatinib. However, other mechanisms behind PAMAMs anti-angiogenesis effect need to be investigated at the genetic and molecular levels. As mentioned previously, many studies showed that cationic PAMAM dendrimers can modulate EGFR signaling pathways *in vitro* and *in vivo* (9,16,20), which can be related to their anti-angiogenesis effects.

The variety of naked PAMAM dendrimers biomedical applications shows the urgent need to gain more knowledge on their safety profile. In this study, their effects on the early stages of embryogenesis were explored for two reasons; first, the embryogenesis process can be highly comparable to tumorigenesis since cells behave in a similar manner (112,113). The second reason is related to getting further insights on PAMAMs potential toxicity during the early stages of pregnancy, which are very critical. For this purpose, we used chicken embryos, which represent a rapid cost-effective model. As we mentioned previously, cationic PAMAM dendrimers are known to possess certain toxic, but manageable effects (13,146–152). Herein, we reported that cationic PAMAM dendrimers can cause a substantial toxic effect on 3-day old chicken embryos. The survival rate decreased dramatically to less than 50% after 5 days of treatment, illustrating the toxicity of cationic PAMAMs on the exposed embryos compared to their matched controls. RT-PCR of tissues derived from treated chicken embryos revealed a deregulation in many key controller genes responsible for cell proliferation and apoptosis compared to controls; such as ATF-3, BCL-2, caspase-8, FOXA-2, INHB-A, MAPRE-2, RIPK-1, SERPINA-4, and VEGFC. This effect was generation-dependent supporting our findings in angiogenesis analysis. These results are in accordance with what was found by other studies regarding the toxicity of cationic but not anionic PAMAMs in the zebrafish embryos model (32,53,170–172).

Cationic PAMAMs attenuated the development of zebrafish embryos (170), and they activated innate immune response (172). They also were teratogenic to zebrafish larvae, in a generation-dependent manner (171). Moreover, a study reported that apoptosis was induced only by cationic PAMAMs in zebrafish embryos and it was concentration-dependent (53). PAMAMs with other surface chemistries (anionic and neutral) did not exhibit embryonic cytotoxicity, suggesting the safety of these compounds during the early stages of embryogenesis in comparison with cationic PAMAMs. Therefore, cationic PAMAMs should be excluded from administrating during pregnancy. However, since toxicity may differ based on the used model, further *in vivo* investigation is required.

One of the drawbacks of our study was the use of immortalized human normal mammary epithelial cells (HNME-E6/E7) as a control instead of primary mammary cells due to the unavailability of the latter. Our comparison with HNME-E6/E7 may not reflect the real toxicology of PAMAM dendrimers on normal cells, which warrants further assessment of PAMAMs safety using a primary mammary cell line.

Combined together, our findings suggest that PAMAM dendrimers, particularly cationic represent potentially effective compounds for the management of HER2-positive breast cancer and should be subjected to subsequent developmental stages.

CHAPTER 5: CONCLUSION AND FUTURE DIRECTIONS

HER2-positive breast cancer is a serious illness that can lead to death in women around the world with many challenges related to tumor behavior and current treatments. PAMAM dendrimers were proposed as candidates in an attempt to find novel therapies for HER2-positive breast cancer. Among their considerable pharmacological effects, their impact on HER2-positive breast cancer is unknown. Anti-cancer screening identified PAMAM dendrimers as promising compounds due to their significant inhibition of the viability of breast cancer cells and triggering many morphological changes in them. The most effective type of PAMAMs was found to be G_6NH_2, corresponding with the general trend regarding the extent of PAMAMs activities; surface chemistry and generation-dependency. PAMAM dendrimers induced apoptosis in HER2-positive breast cancer cells through different mechanisms. They also inhibited the phosphorylation of HER2 and EGFR, along with other proteins related to cancer progression. Additionally, cationic PAMAMs had anti-angiogenesis effects *in ovo*, in a generation-dependent manner, while other types of PAMAMs (anionic and neutral) did not result in significant changes. Their safety profile during embryogenesis reveals a substantial toxicity through upregulating several toxicity markers in this model. Thus, they should be excluded from using during pregnancy. Comparison of PAMAM dendrimers with lapatinib; an anti-HER2 agent, indicated that G_6NH_2 exhibit similar effects. Taken together, PAMAM dendrimers may become a new potential class of anti-HER2 agents, either to act solely or to add benefit to current treatments.

Further studies are planned to assess the safety of PAMAMs in primary normal mammary cells, which is a necessity to ensure a safe application of these compounds. Additional anti-cancer studies are required, and exploring other pathways will assist in

the potential employment of PAMAM dendrimers in cancer therapy. The underlying molecular pathways mediating PAMAMs' anti-angiogenic effect are planned to be investigated in human umbilical vein endothelial cells (HUVECs), which will provide deeper understanding of this effect. In conclusion, PAMAM dendrimers are promising compounds that have a potential role in cancer treatment through interfering with different molecular pathways.

REFERENCES

1. Duncan R. The dawning era of polymer therapeutics. Nat Rev Drug Discov. 2003 May;2(5):347–60.
2. Vicent MJ, Dieudonné L, Carbajo RJ, Pineda-Lucena A. Polymer conjugates as therapeutics: future trends, challenges and opportunities. Expert Opin Drug Deliv. 2008 May;5(5):593–614.
3. Kannan RM, Nance E, Kannan S, Tomalia DA. Emerging concepts in dendrimer-based nanomedicine: from design principles to clinical applications. J Intern Med. 2014 Dec 1;276(6):579–617.
4. Tomalia DA, Reyna LA, Svenson S. Dendrimers as multi-purpose nanodevices for oncology drug delivery and diagnostic imaging. Biochem Soc Trans. 2007 Feb;35(1):61–7.
5. Duncan R, Izzo L. Dendrimer biocompatibility and toxicity. Adv Drug Deliv Rev. 2005;57(15):2215–37.
6. Araújo RV de, Santos S da S, Igne Ferreira E, Giarolla J. New Advances in General Biomedical Applications of PAMAM Dendrimers. Molecules. 2018 Nov 2;23(11):2849.
7. Tomalia DA, Baker H, Dewald J, Hall M, Kallos G, Martin S, et al. A New Class of Polymers: Starburst-Dendritic Macromolecules. Polym J. 1985 Jan 15;17:117.
8. Tang MX, Szoka FC. The influence of polymer structure on the interactions of cationic polymers with DNA and morphology of the resulting complexes. Gene Therapy. 1997 Aug;4(8):823–32.
9. Akhtar S, Al-Zaid B, El-Hashim AZ, Chandrasekhar B, Attur S, Benter IF. Impact of PAMAM delivery systems on signal transduction pathways in vivo: Modulation of ERK1/2 and p38 MAP kinase signaling in the normal and diabetic

kidney. Int J Pharm. 2016 Dec;514(2):353–63.

10. PAMAM Dendrimers [Internet]. Dendritech, Inc. 2015 [cited 2019 Apr 25]. p. 2–4. Available from: http://www.dendritech.com/pamam.html

11. Akhtar S. Cationic nanosystems for the delivery of small interfering ribonucleic acid therapeutics: a focus on toxicogenomics. Expert Opin Drug Metab Toxicol. 2010 Nov;6(11):1347–62.

12. Akhtar S, Benter IF. Nonviral delivery of synthetic siRNAs in vivo. J Clin Invest. 2007 Dec 3;117(12):3623–32.

13. Labieniec-Watala M, Watala C. PAMAM dendrimers: destined for success or doomed to fail? Plain and modified PAMAM dendrimers in the context of biomedical applications. J Pharm Sci. 2015 Jan;104(1):2–14.

14. Vögtle F, Richardt G, Werner N. Dendritic Molecules: Concepts, Syntheses, Properties, Applications. 1st ed. 2007.

15. Hollins AJ, Omidi Y, Benter IF, Akhtar S. Toxicogenomics of drug delivery systems: Exploiting delivery system-induced changes in target gene expression to enhance siRNA activity. J Drug Target. 2007 Jan;15(1):83–8.

16. Akhtar S, Al-Zaid B, El-Hashim AZ, Chandrasekhar B, Attur S, Yousif MHM, et al. Cationic Polyamidoamine Dendrimers as Modulators of EGFR Signaling In Vitro and In Vivo. PLoS One. 2015 Jul 13;10(7):e0132215–e0132215.

17. Kuo JS, Liou M, Chiu H. Evaluating the gene-expression profiles of HeLa cancer cells treated with activated and nonactivated poly(amidoamine) dendrimers, and their DNA complexes. Mol Pharm. 2010 Jun;7(3):805–14.

18. Janaszewska A, Gorzkiewicz M, Ficker M, Petersen JF, Paolucci V, Christensen JB, et al. Pyrrolidone Modification Prevents PAMAM Dendrimers from Activation of Pro-Inflammatory Signaling Pathways in Human Monocytes. Mol

Pharm. 2018 Jan;15(1):12–20.

19. Akhtar S, El-Hashim AZ, Chandrasekhar B, Attur S, Benter IF. Naked Polyamidoamine Polymers Intrinsically Inhibit Angiotensin II-Mediated EGFR and ErbB2 Transactivation in a Dendrimer Generation- and Surface Chemistry-Dependent Manner. Mol Pharm. 2016 May 2;13(5):1575–86.

20. Akhtar S, Chandrasekhar B, Attur S, Yousif MHM, Benter IF. On the nanotoxicity of PAMAM dendrimers: Superfect(R) stimulates the EGFR-ERK1/2 signal transduction pathway via an oxidative stress-dependent mechanism in HEK 293 cells. Int J Pharm. 2013 May;448(1):239–46.

21. Akhtar S, Chandrasekhar B, Yousif MH, Renno W, Benter IF, El-Hashim AZ. Chronic administration of nano-sized PAMAM dendrimers in vivo inhibits EGFR-ERK1/2-ROCK signaling pathway and attenuates diabetes-induced vascular remodeling and dysfunction. Nanomedicine. 2019 Jun;18:78–89.

22. Feliu N, Kohonen P, Ji J, Zhang Y, Karlsson HL, Palmberg L, et al. Next-Generation Sequencing Reveals Low-Dose Effects of Cationic Dendrimers in Primary Human Bronchial Epithelial Cells. ACS Nano. 2015 Jan 27;9(1):146–63.

23. Tang Y, Han Y, Liu L, Shen W, Zhang H, Wang Y, et al. Protective effects and mechanisms of G5 PAMAM dendrimers against acute pancreatitis induced by caerulein in mice. Biomacromolecules. 2015 Jan;16(1):174–82.

24. Fischer D, Li Y, Ahlemeyer B, Krieglstein J, Kissel T. In vitro cytotoxicity testing of polycations: influence of polymer structure on cell viability and hemolysis. Biomaterials. 2003 Mar;24(7):1121–31.

25. Chen H-T, Neerman MF, Parrish AR, Simanek EE. Cytotoxicity, hemolysis, and acute in vivo toxicity of dendrimers based on melamine, candidate vehicles for

drug delivery. J Am Chem Soc. 2004 Aug;126(32):10044–8.

26. Malik N, Wiwattanapatapee R, Klopsch R, Lorenz K, Frey H, Weener JW, et al. Dendrimers: relationship between structure and biocompatibility in vitro, and preliminary studies on the biodistribution of 125I-labelled polyamidoamine dendrimers in vivo. J Control Release. 2000 Mar;65(1–2):133–48.

27. Domanski DM, Klajnert B, Bryszewska M. Influence of PAMAM dendrimers on human red blood cells. Bioelectrochemistry. 2004 Jun;63(1–2):189–91.

28. Thiagarajan G, Greish K, Ghandehari H. Charge affects the oral toxicity of poly(amidoamine) dendrimers. Eur J Pharm Biopharm. 2013 Jun;84(2):330–4.

29. Han M-H, Chen J, Wang J, Chen S-L, Wang X-T. Blood compatibility of polyamidoamine dendrimers and erythrocyte protection. J Biomed Nanotechnol. 2010 Feb;6(1):82–92.

30. Wang W, Xiong W, Zhu Y, Xu H, Yang X. Protective effect of PEGylation against poly(amidoamine) dendrimer-induced hemolysis of human red blood cells. J Biomed Mater Res B Appl Biomater. 2010 Apr;93(1):59–64.

31. Jones CF, Campbell RA, Franks Z, Gibson CC, Thiagarajan G, Vieira-de-Abreu A, et al. Cationic PAMAM dendrimers disrupt key platelet functions. Mol Pharm. 2012 Jun;9(6):1599–611.

32. Jones CF, Campbell RA, Brooks AE, Assemi S, Tadjiki S, Thiagarajan G, et al. Cationic PAMAM dendrimers aggressively initiate blood clot formation. ACS Nano. 2012 Nov;6(11):9900–10.

33. Dobrovolskaia MA, Patri AK, Simak J, Hall JB, Semberova J, De Paoli Lacerda SH, et al. Nanoparticle size and surface charge determine effects of PAMAM dendrimers on human platelets in vitro. Mol Pharm. 2011/11/10. 2012 Mar 5;9(3):382–93.

34. Greish K, Thiagarajan G, Herd H, Price R, Bauer H, Hubbard D, et al. Size and surface charge significantly influence the toxicity of silica and dendritic nanoparticles. Nanotoxicology. 2012 Nov;6(7):713–23.

35. Lin J, Hua W, Zhang Y, Li C, Xue W, Yin J, et al. Effect of poly(amidoamine) dendrimers on the structure and activity of immune molecules. Biochim Biophys Acta. 2015 Feb;1850(2):419–25.

36. Gurzov EN, Wang B, Pilkington EH, Chen P, Kakinen A, Stanley WJ, et al. Inhibition of hIAPP Amyloid Aggregation and Pancreatic β-Cell Toxicity by OH-Terminated PAMAM Dendrimer. Small. 2016 Mar 1;12(12):1615–26.

37. Avaritt BR, Swaan PW. Intracellular Ca2+ release mediates cationic but not anionic poly(amidoamine) (PAMAM) dendrimer-induced tight junction modulation. Pharm Res. 2014 Sep;31(9):2429–38.

38. Forstner P, Bayer F, Kalu N, Felsen S, Fortsch C, Aloufi A, et al. Cationic PAMAM dendrimers as pore-blocking binary toxin inhibitors. Biomacromolecules. 2014 Jul;15(7):2461–74.

39. Otto DP, de Villiers MM. Poly(amidoamine) Dendrimers as a Pharmaceutical Excipient. Are We There yet? J Pharm Sci. 2018 Jan;107(1):75–83.

40. Li C, Liu H, Sun Y, Wang H, Guo F, Rao S, et al. PAMAM nanoparticles promote acute lung injury by inducing autophagic cell death through the Akt-TSC2-mTOR signaling pathway. J Mol Cell Biol. 2009 Oct;1(1):37–45.

41. Li Y, Wang S, Wang Z, Qian X, Fan J, Zeng X, et al. Cationic poly(amidoamine) dendrimers induced cyto-protective autophagy in hepatocellular carcinoma cells. Nanotechnology. 2014 Sep;25(36):365101.

42. Wang S, Li Y, Fan J, Wang Z, Zeng X, Sun Y, et al. The role of autophagy in the neurotoxicity of cationic PAMAM dendrimers. Biomaterials. 2014

Aug;35(26):7588–97.

43. Li Y, Zeng X, Wang S, Sun Y, Wang Z, Fan J, et al. Inhibition of autophagy protects against PAMAM dendrimers-induced hepatotoxicity. Nanotoxicology. 2015 May;9(3):344–55.

44. Li Y, Zhu H, Wang S, Qian X, Fan J, Wang Z, et al. Interplay of Oxidative Stress and Autophagy in PAMAM Dendrimers-Induced Neuronal Cell Death. Theranostics. 2015 Oct 8;5(12):1363–77.

45. Choi YJ, Kang SJ, Kim YJ, Lim Y-B, Chung HW. Comparative studies on the genotoxicity and cytotoxicity of polymeric gene carriers polyethylenimine (PEI) and polyamidoamine (PAMAM) dendrimer in Jurkat T-cells. Drug Chem Toxicol. 2010 Oct;33(4):357–66.

46. Lee J-H, Cha KE, Kim MS, Hong HW, Chung DJ, Ryu G, et al. Nanosized polyamidoamine (PAMAM) dendrimer-induced apoptosis mediated by mitochondrial dysfunction. Toxicol Lett. 2009 Oct;190(2):202–7.

47. Thomas TP, Majoros I, Kotlyar A, Mullen D, Holl MMB, Baker Jr JR. Cationic poly(amidoamine) dendrimer induces lysosomal apoptotic pathway at therapeutically relevant concentrations. Biomacromolecules. 2009 Dec 14;10(12):3207–14.

48. Kuo J-HS, Jan M-S, Chiu HW. Mechanism of cell death induced by cationic dendrimers in RAW 264.7 murine macrophage-like cells. J Pharm Pharmacol. 2005 Apr;57(4):489–95.

49. Mukherjee SP, Lyng FM, Garcia A, Davoren M, Byrne HJ. Mechanistic studies of in vitro cytotoxicity of poly(amidoamine) dendrimers in mammalian cells. Toxicol Appl Pharmacol. 2010 Nov;248(3):259–68.

50. Naha PC, Byrne HJ. Generation of intracellular reactive oxygen species and

genotoxicity effect to exposure of nanosized polyamidoamine (PAMAM) dendrimers in PLHC-1 cells in vitro. Aquat Toxicol. 2013 May;132–133:61–72.

51. Naha PC, Davoren M, Lyng FM, Byrne HJ. Reactive oxygen species (ROS) induced cytokine production and cytotoxicity of PAMAM dendrimers in J774A.1 cells. Toxicol Appl Pharmacol. 2010 Jul;246(1–2):91–9.

52. Patel M, De Paoli SH, Elhelu OK, Farooq S, Simak J. Cell membrane disintegration and extracellular vesicle release in a model of different size and charge PAMAM dendrimers effects on cultured endothelial cells. Nanotoxicology. 2019 Feb;1–18.

53. Bodewein L, Schmelter F, Di Fiore S, Hollert H, Fischer R, Fenske M. Differences in toxicity of anionic and cationic PAMAM and PPI dendrimers in zebrafish embryos and cancer cell lines. Toxicol Appl Pharmacol. 2016 Aug;305:83–92.

54. Janaszewska A, Mączyńska K, Matuszko G, Appelhans D, Voit B, Klajnert B, et al. Cytotoxicity of PAMAM, PPI and maltose modified PPI dendrimers in Chinese hamster ovary (CHO) and human ovarian carcinoma (SKOV3) cells. New J Chem. 2012;36(2):428–37.

55. Naha PC, Mukherjee SP, Byrne HJ. Toxicology of Engineered Nanoparticles: Focus on Poly(amidoamine) Dendrimers. Int J Environ Res Public Health. 2018 Feb;15(2).

56. Fruchon S, Poupot R. Pro-Inflammatory Versus Anti-Inflammatory Effects of Dendrimers: The Two Faces of Immuno-Modulatory Nanoparticles. Nanomater (Basel, Switzerland). 2017 Sep;7(9).

57. Chauhan AS, Diwan P V, Jain NK, Tomalia DA. Unexpected in vivo anti-inflammatory activity observed for simple, surface functionalized

poly(amidoamine) dendrimers. Biomacromolecules. 2009 May;10(5):1195–202.

58. Durocher I, Girard D. In vivo proinflammatory activity of generations 0-3 (G0-G3) polyamidoamine (PAMAM) nanoparticles. Inflamm Res. 2016 Sep;65(9):745–55.

59. Mukherjee SP, Byrne HJ. Polyamidoamine dendrimer nanoparticle cytotoxicity, oxidative stress, caspase activation and inflammatory response: experimental observation and numerical simulation. Nanomedicine. 2013 Feb;9(2):202–11.

60. Wangpradit O, Adamcakova-Dodd A, Heitz K, Robertson L, Thorne PS, Luthe G. PAMAM dendrimers as nano carriers to investigate inflammatory responses induced by pulmonary exposure of PCB metabolites in Sprague-Dawley rats. Environ Sci Pollut Res Int. 2016 Feb;23(3):2128–37.

61. Rastegar A, Nazari S, Allahabadi A, Falanji F, Akbari Dourbash FAD, Rezai Z, et al. Antibacterial activity of amino- and amido- terminated poly (amidoamine)-G6 dendrimer on isolated bacteria from clinical specimens and standard strains. Med J Islam Repub Iran. 2017;31:64.

62. Gholami M, Mohammadi R, Arzanlou M, Akbari Dourbash F, Kouhsari E, Majidi G, et al. In vitro antibacterial activity of poly (amidoamine)-G7 dendrimer. BMC Infect Dis. 2017 Jun;17(1):395.

63. Calabretta MK, Kumar A, McDermott AM, Cai C. Antibacterial activities of poly(amidoamine) dendrimers terminated with amino and poly(ethylene glycol) groups. Biomacromolecules. 2007 Jun;8(6):1807–11.

64. Labena A, Kabel KI, Farag RK. One-pot synthesize of dendritic hyperbranched PAMAM and assessment as a broad spectrum antimicrobial agent and anti-biofilm. Mater Sci Eng C Mater Biol Appl. 2016 Jan;58:1150–9.

65. Holmes AM, Heylings JR, Wan K-W, Moss GP. Antimicrobial efficacy and

mechanism of action of poly(amidoamine) (PAMAM) dendrimers against opportunistic pathogens. Int J Antimicrob Agents. 2019 Apr;53(4):500–7.

66. Wang B, Navath RS, Menjoge AR, Balakrishnan B, Bellair R, Dai H, et al. Inhibition of bacterial growth and intramniotic infection in a guinea pig model of chorioamnionitis using PAMAM dendrimers. Int J Pharm. 2010 Aug;395(1–2):298–308.

67. Ataollahi MR, Sharifi J, Paknahad MR, Paknahad A. Breast cancer and associated factors: a review. J Med Life. 2015;8(Spec Iss 4):6–11.

68. Breast Cancer Awareness Campaign. Hamad Medical Corporation [Internet] 2019 [cited 2019 November 25]. Available from: https://www.hamad.qa/EN/your health/bcac/Pages/default.aspx

69. Yarden Y, Sliwkowski MX. Untangling the ErbB signalling network. Nat Rev Mol Cell Biol. 2001 Feb;2(2):127–37.

70. Gschwind A, Fischer OM, Ullrich A. The discovery of receptor tyrosine kinases: Targets for cancer therapy. Vol. 4, Nature Reviews Cancer. England; 2004. p. 361–70.

71. Harbeck N, Gnant M. Breast cancer. Lancet (London, England). 2017 Mar;389(10074):1134–50.

72. Makki J. Diversity of breast carcinoma: Histological subtypes and clinical relevance. Clin Med Insights Pathol. 2015 Dec 21;8(1):23–31.

73. Shen Z, Chen J, Ding Y, Hou J, Shalchi Amirkhiz B, Chan K, et al. Role of interfacial reaction on the mechanical performance of Al/steel dissimilar refill friction stir spot welds. Sci Technol Weld Join. 2018 Jan;23(6):462–77.

74. Slamon DJ, Godolphin W, Jones LA, Holt JA, Wong SG, Keith DE, et al. Studies of the HER-2/neu proto-oncogene in human breast and ovarian cancer. Science

(80-). 1989 May;244(4905):707–12.

75. Vernieri C, Milano M, Brambilla M, Mennittoa A, Maggia C, Conaa MS, et al. Resistance mechanisms to anti-HER2 therapies in HER2-positive breast cancer: Current knowledge, new research directions and therapeutic perspectives. Crit Rev Oncol / Hematol. 2019;139:53–66.

76. Seshadri R, Firgaira FA, Horsfall DJ, McCaul K, Setlur V, Kitchen P. Clinical significance of HER-2/neu oncogene amplification in primary breast cancer. J Clin Oncol. 1993 Oct;11(10):1936–42.

77. Gabos Z, Sinha R, Hanson J, Chauhan N, Hugh J, Mackey JR, et al. Prognostic significance of human epidermal growth factor receptor positivity for the development of brain metastasis after newly diagnosed breast cancer. J Clin Oncol. 2006 Dec;24(36):5658–63.

78. Perez EA, Romond EH, Suman VJ, Jeong JH, Sledge G, Geyer CE, et al. Trastuzumab plus adjuvant chemotherapy for human epidermal growth factor receptor 2 - Positive breast cancer: Planned joint analysis of overall survival from NSABP B-31 and NCCTG N9831. J Clin Oncol. 2014 Nov;32(33):3744–52.

79. Arteaga CL, Sliwkowski MX, Osborne CK, Perez EA, Puglisi F, Gianni L. Treatment of HER2-positive breast cancer: Current status and future perspectives. Nat Rev Clin Oncol. 2012 Nov 29;9(1):16–32.

80. Larionov AA. Current Therapies for Human Epidermal Growth Factor Receptor 2-Positive Metastatic Breast Cancer Patients. Front Oncol. 2018 Apr 3;8:89.

81. Rimawi MF, De Angelis C, Schiff R. Resistance to Anti-HER2 Therapies in Breast Cancer. Am Soc Clin Oncol Educ B. 2015;35:e157–64.

82. Padmanabhan R, Kheraldine HS, Meskin N, Vranic S, Al Moustafa A-E. Crosstalk between HER2 and PD-1/PD-L1 in Breast Cancer: From Clinical

Applications to Mathematical Models. Cancers (Basel). 2020 Mar;12(3).

83. Rexer BN, Arteaga CL. Intrinsic and acquired resistance to HER2-targeted therapies in HER2 gene-amplified breast cancer: mechanisms and clinical implications. Crit Rev Oncog. 2012;17(1):1–16.

84. Ruprecht B, Zaal EA, Zecha J, Wu W, Berkers CR, Kuster B, et al. Lapatinib Resistance in Breast Cancer Cells Is Accompanied by Phosphorylation-Mediated Reprogramming of Glycolysis. Cancer Res. 2017 Apr 15;77(8):1842 LP – 1853.

85. Eustace AJ, Conlon NT, McDermott MSJ, Browne BC, O'Leary P, Holmes FA, et al. Development of acquired resistance to lapatinib may sensitise HER2-positive breast cancer cells to apoptosis induction by obatoclax and TRAIL. BMC Cancer. 2018;18(1):965.

86. Seidman AD, Fornier MN, Esteva FJ, Tan L, Kaptain S, Bach A, et al. Weekly trastuzumab and paclitaxel therapy for metastatic breast cancer with analysis of efficacy by HER2 immunophenotype and gene amplification. J Clin Oncol. 2001 May;19(10):2587–95.

87. Slamon DJ, Leyland-Jones B, Shak S, Fuchs H, Paton V, Bajamonde A, et al. Use of chemotherapy plus a monoclonal antibody against HER2 for metastatic breast cancer that overexpresses HER2. N Engl J Med. 2001 Mar;344(11):783–92.

88. Esteva FJ, Valero V, Booser D, Guerra LT, Murray JL, Pusztai L, et al. Phase II study of weekly docetaxel and trastuzumab for patients with HER-2-overexpressing metastatic breast cancer. J Clin Oncol. 2002 Apr;20(7):1800–8.

89. Brandao M, Ponde NF, Poggio F, Kotecki N, Salis M, Lambertini M, et al. Combination therapies for the treatment of HER2-positive breast cancer: current and future prospects. Expert Rev Anticancer Ther. 2018 Jul;18(7):629–49.

90. Viale G, Morganti S, Ferraro E, Zagami P, Marra A, Curigliano G. What therapies are on the horizon for HER2 positive breast cancer? Expert Rev Anticancer Ther. 2019 Sep 2;19(9):811–22.

91. de Azambuja E, Procter MJ, van Veldhuisen DJ, Agbor-Tarh D, Metzger-Filho O, Steinseifer J, et al. Trastuzumab-associated cardiac events at 8 years of median follow-up in the Herceptin Adjuvant trial (BIG 1-01). J Clin Oncol. 2014 Jul;32(20):2159–65.

92. Joensuu H, Bono P, Kataja V, Alanko T, Kokko R, Asola R, et al. Fluorouracil, epirubicin, and cyclophosphamide with either docetaxel or vinorelbine, with or without trastuzumab, as adjuvant treatments of breast cancer: Final results of the FinHer trial. J Clin Oncol. 2009 Dec;27(34):5685–92.

93. Slamon D, Eiermann W, Robert N, Pienkowski T, Martin M, Rolski J, et al. Phase III Randomized Trial Comparing Doxorubicin and Cyclophosphamide Followed by Docetaxel (AC→T) with Doxorubicin and Cyclophosphamide Followed by Docetaxel and Trastuzumab (AC→TH) with Docetaxel, Carboplatin and Trastuzumab (TCH) in Her2neu Positive Early Breast Cancer Patients: BCIRG 006 Study. Cancer Res. 2009 Dec 15;69(24 Supplement):62 LP – 62.

94. Guan Z, Xu B, DeSilvio ML, Shen Z, Arpornwirat W, Tong Z, et al. Randomized trial of lapatinib versus placebo added to paclitaxel in the treatment of human epidermal growth factor receptor 2-overexpressing metastatic breast cancer. J Clin Oncol. 2013 Jun;31(16):1947–53.

95. Untch M, Loibl S, Bischoff J, Eidtmann H, Kaufmann M, Blohmer J-U, et al. Lapatinib versus trastuzumab in combination with neoadjuvant anthracycline-taxane-based chemotherapy (GeparQuinto, GBG 44): a randomised phase 3 trial.

Lancet Oncol. 2012 Feb;13(2):135–44.

96. Di Leo A, Gomez HL, Aziz Z, Zvirbule Z, Bines J, Arbushites MC, et al. Phase III, double-blind, randomized study comparing lapatinib plus paclitaxel with placebo plus paclitaxel as first-line treatment for metastatic breast cancer. J Clin Oncol. 2008 Dec;26(34):5544–52.

97. Ponde N, Brandao M, El-Hachem G, Werbrouck E, Piccart M. Treatment of advanced HER2-positive breast cancer: 2018 and beyond. Cancer Treat Rev. 2018 Jun;67:10–20.

98. Escriva-de-Romani S, Arumi M, Bellet M, Saura C. HER2-positive breast cancer: Current and new therapeutic strategies. Breast. 2018 Jun;39:80–8.

99. Welslau M, Hartkopf AD, Muller V, Wockel A, Lux MP, Janni W, et al. Update Breast Cancer 2019 Part 5 - Diagnostic and Therapeutic Challenges of New, Personalised Therapies in Patients with Advanced Breast Cancer. Geburtshilfe Frauenheilkd. 2019 Oct;79(10):1090–9.

100. Menderes G, Bonazzoli E, Bellone S, Black J, Altwerger G, Masserdotti A, et al. SYD985, a novel duocarmycin-based HER2-targeting antibody-drug conjugate, shows promising antitumor activity in epithelial ovarian carcinoma with HER2/Neu expression. Gynecol Oncol. 2017/05/01. 2017 Jul;146(1):179–86.

101. Doi T, Iwata H, Tsurutani J, Takahashi S, Park H, Redfern CH, et al. Single agent activity of DS-8201a, a HER2-targeting antibody-drug conjugate, in heavily pretreated HER2 expressing solid tumors. J Clin Oncol. 2017 May 20;35(15_suppl):108.

102. Adaire T, Montani J. Overview of Angiogenesis. In: Angiogenesis. San Rafael (CA): Morgan & Claypool Life Sciences; 2010.

103. Karamysheva AF. Mechanisms of Angiogenesis. Biochemistry. 2008;73:751–62.

104. Nishida N, Yano H, Nishida T, Kamura T, Kojiro M. Angiogenesis in cancer. Vasc Health Risk Manag. 2006/09/. 2006 Sep;2(3):213–9.

105. Bottaro DP, Liotta LA. Cancer: Out of air is not out of action. Vol. 423, Nature. England; 2003. p. 593–5.

106. Niu G, Carter WB. Human epidermal growth factor receptor 2 regulates angiopoietin-2 expression in breast cancer via AKT and mitogen-activated protein kinase pathways. Cancer Res. 2007 Feb;67(4):1487–93.

107. Rico-Varela J, Ho D, Wan LQ. In Vitro Microscale Models for Embryogenesis. Adv Biosyst. 2018/05/07. 2018 Jun;2(6):1700235.

108. Mark Hill. Models of Human Development. Embryology [Internet]. 2020 [cited 2020 January 15]. Available from: https://embryology.med.unsw.edu.au/embryology/index.php/Models_of_Human_Development

109. Roman D, Yasmeen A, Mireuta M, Stiharu I, Al Moustafa A-E. Significant toxic role for single-walled carbon nanotubes during normal embryogenesis. Nanomedicine. 2013 Oct;9(7):945–50.

110. Ashour AA, Haik MY, Sadek KW, Yalcin HC, Bitharas J, Aboulkassim T, et al. Substantial Toxic Effect of Water-Pipe Smoking on the Early Stage of Embryonic Development. Nicotine Tob Res. 2018 Mar;20(4):502–7.

111. Al-Qahdi SS, Alzohari N, Alsaid AY, Ashour AA, Aboulkassim T, Vranic S, et al. Teucrium Polium Plant Extract Provokes Substantial Cytotoxicity at the Early Stage of Embryonic Development. Bosn J basic Med Sci. 2019 Feb;19(1):67–71.

112. Ma Y, Zhang P, Wang F, Yang J, Yang Z, Qin H. The relationship between early

embryo development and tumourigenesis. J Cell Mol Med. 2010 Dec;14(12):2697–701.

113. Manzo G. Similarities Between Embryo Development and Cancer Process Suggest New Strategies for Research and Therapy of Tumors: A New Point of View. Front Cell Dev Biol. 2019;7:20.

114. Wu F, Stutzman A, Mo Y-Y. Notch signaling and its role in breast cancer. Front Biosci. 2007 May;12:4370–83.

115. Wang Y. Wnt/Planar cell polarity signaling: a new paradigm for cancer therapy. Mol Cancer Ther. 2009 Aug;8(8):2103–9.

116. Lloyd JR, Jayasekara PS, Jacobson KA. Characterization of Polyamidoamino (PAMAM) Dendrimers Using In-Line Reversed Phase LC Electrospray Ionization Mass Spectrometry. Anal Methods. 2015/12/07. 2016 Jan 14;8(2):263–9.

117. Yasmeen A, Zhang L, Al Moustafa A-E. Does the vesicular stomatitis virus really have a selective oncolytic effect in human cancer? Vol. 126, International journal of cancer. United States; 2010. p. 2509–10.

118. Chu B, Liu F, Li L, Ding C, Chen K, Sun Q, et al. A benzimidazole derivative exhibiting antitumor activity blocks EGFR and HER2 activity and upregulates DR5 in breast cancer cells. Cell Death Dis. 2015 Mar;6:e1686.

119. Kalous O, Conklin D, Desai AJ, O'Brien NA, Ginther C, Anderson L, et al. Dacomitinib (PF-00299804), an irreversible Pan-HER inhibitor, inhibits proliferation of HER2-amplified breast cancer cell lines resistant to trastuzumab and lapatinib. Mol Cancer Ther. 2012 Sep;11(9):1978–87.

120. Konecny GE, Pegram MD, Venkatesan N, Finn R, Yang G, Rahmeh M, et al. Activity of the dual kinase inhibitor lapatinib (GW572016) against HER-2-

overexpressing and trastuzumab-treated breast cancer cells. Cancer Res. 2006 Feb;66(3):1630–9.

121. Tazawa H. Adverse effect of failure to turn the avian egg on the embryo oxygen exchange. Respir Physiol. 1980 Aug;41(2):137–42.

122. Zudaire E, Gambardella L, Kurcz C, Vermeren S. A computational tool for quantitative analysis of vascular networks. PLoS One. 2011;6(11):e27385.

123. Kittappa R, Chang WW, Awatramani RB, McKay RDG. The foxa2 gene controls the birth and spontaneous degeneration of dopamine neurons in old age. PLoS Biol. 2007 Dec;5(12):e325–e325.

124. Pruitt KD, Tatusova T, Brown GR, Maglott DR. NCBI Reference Sequences (RefSeq): current status, new features and genome annotation policy. Nucleic Acids Res. 2011/11/24. 2012 Jan;40(Database issue):D130–5.

125. Chai KX, Chen LM, Chao J, Chao L. Kallistatin: a novel human serine proteinase inhibitor. Molecular cloning, tissue distribution, and expression in Escherichia coli. J Biol Chem. 1993 Nov;268(32):24498–505.

126. Barber RD, Harmer DW, Coleman RA, Clark BJ. GAPDH as a housekeeping gene: analysis of GAPDH mRNA expression in a panel of 72 human tissues. Physiol Genomics. 2005 May;21(3):389–95.

127. Rampersad SN. Multiple Applications of Alamar Blue as an Indicator of Metabolic Function and Cellular Health in Cell Viability Bioassays. Sensors. 2012 Sep;12(9):12347–60.

128. Kreft S, Kreft M. Quantification of dichromatism: a characteristic of color in transparent materials. J Opt Soc Am A Opt Image Sci Vis. 2009 Jul;26(7):1576–81.

129. Page B, Page M, Noel C. A new fluorometric assay for cytotoxicity

measurements in-vitro. Int J Oncol. 1993 Sep;3(3):473–6.

130. Du F, Zhao X, Fan D. Soft Agar Colony Formation Assay as a Hallmark of Carcinogenesis. Bio-protocol. 2017;7(12):e2351.

131. Pavel M, Renna M, Park SJ, Menzies FM, Ricketts T, Füllgrabe J, et al. Contact inhibition controls cell survival and proliferation via YAP/TAZ-autophagy axis. Nat Commun. 2018;9(1):2961.

132. Todaro GJ, Fryling C, De Larco JE. Transforming growth factors produced by certain human tumor cells: polypeptides that interact with epidermal growth factor receptors. Proc Natl Acad Sci U S A. 1980 Sep;77(9):5258–62.

133. Slamon DJ, Clark GM, Wong SG, Levin WJ, Ullrich A, McGuire WL. Human breast cancer: correlation of relapse and survival with amplification of the HER-2/neu oncogene. Science. 1987 Jan;235(4785):177–82.

134. Coussens L, Yang-Feng TL, Liao YC, Chen E, Gray A, McGrath J, et al. Tyrosine kinase receptor with extensive homology to EGF receptor shares chromosomal location with neu oncogene. Science. 1985 Dec;230(4730):1132–9.

135. Hudziak RM, Schlessinger J, Ullrich A. Increased expression of the putative growth factor receptor p185HER2 causes transformation and tumorigenesis of NIH 3T3 cells. Proc Natl Acad Sci U S A. 1987 Oct;84(20):7159–63.

136. Di Fiore PP, Pierce JH, Kraus MH, Segatto O, King CR, Aaronson SA. erbB-2 is a potent oncogene when overexpressed in NIH/3T3 cells. Science. 1987 Jul;237(4811):178–82.

137. Guy CT, Webster MA, Schaller M, Parsons TJ, Cardiff RD, Muller WJ. Expression of the neu protooncogene in the mammary epithelium of transgenic mice induces metastatic disease. Proc Natl Acad Sci U S A. 1992

Nov;89(22):10578–82.

138. Chazin VR, Kaleko M, Miller AD, Slamon DJ. Transformation mediated by the human HER-2 gene independent of the epidermal growth factor receptor. Oncogene. 1992 Sep;7(9):1859–66.

139. Pietras RJ, Arboleda J, Reese DM, Wongvipat N, Pegram MD, Ramos L, et al. HER-2 tyrosine kinase pathway targets estrogen receptor and promotes hormone-independent growth in human breast cancer cells. Oncogene. 1995 Jun;10(12):2435–46.

140. Cobleigh MA, Vogel CL, Tripathy D, Robert NJ, Scholl S, Fehrenbacher L, et al. Multinational study of the efficacy and safety of humanized anti-HER2 monoclonal antibody in women who have HER2-overexpressing metastatic breast cancer that has progressed after chemotherapy for metastatic disease. J Clin Oncol. 1999 Sep;17(9):2639–48.

141. Al Moustafa A-E, Foulkes WD, Benlimame N, Wong A, Yen L, Bergeron J, et al. E6/E7 proteins of HPV type 16 and ErbB-2 cooperate to induce neoplastic transformation of primary normal oral epithelial cells. Oncogene. 2004 Jan;23(2):350–8.

142. Ribatti D. The Chick Embryo Chorioallantoic Membrane as an In Vivo Assay to Study Antiangiogenesis. Pharmaceuticals (Basel). 2010 Mar 8;3(3):482–513.

143. Auerbach R, Auerbach W, Polakowski I. Assays for angiogenesis: a review. Pharmacol Ther. 1991;51(1):1–11.

144. Quigley JP, Armstrong PB. Tumor cell intravasation alu-cidated: the chick embryo opens the window. Cell. 1998 Aug;94(3):281–4.

145. Ribatti D. Chick embryo chorioallantoic membrane as a useful tool to study angiogenesis. Int Rev Cell Mol Biol. 2008;270:181–224.

146. Lv H, Zhang S, Wang B, Cui S, Yan J. Toxicity of cationic lipids and cationic polymers in gene delivery. J Control Release. 2006 Aug;114(1):100–9.

147. Knudsen KB, Northeved H, Kumar PEK, Permin A, Gjetting T, Andresen TL, et al. In vivo toxicity of cationic micelles and liposomes. Nanomedicine. 2015 Feb;11(2):467–77.

148. Kim Y, Klutz AM, Jacobson KA. Systematic investigation of polyamidoamine dendrimers surface-modified with poly(ethylene glycol) for drug delivery applications: synthesis, characterization, and evaluation of cytotoxicity. Bioconjug Chem. 2008 Aug;19(8):1660–72.

149. Yang H, Lopina ST. Stealth dendrimers for antiarrhythmic quinidine delivery. J Mater Sci Mater Med. 2007 Oct;18(10):2061–5.

150. Harris JM, Chess RB. Effect of pegylation on pharmaceuticals. Nat Rev Drug Discov. 2003 Mar;2(3):214–21.

151. Jevprasesphant R, Penny J, Jalal R, Attwood D, McKeown NB, D'Emanuele A. The influence of surface modification on the cytotoxicity of PAMAM dendrimers. Int J Pharm. 2003 Feb;252(1–2):263–6.

152. Kolhatkar RB, Kitchens KM, Swaan PW, Ghandehari H. Surface acetylation of polyamidoamine (PAMAM) dendrimers decreases cytotoxicity while maintaining membrane permeability. Bioconjug Chem. 2007;18(6):2054–60.

153. Kulhari H, Pooja D, Shrivastava S, Kuncha M, Naidu VGM, Bansal V, et al. Trastuzumab-grafted PAMAM dendrimers for the selective delivery of anticancer drugs to HER2-positive breast cancer. Sci Rep. 2016 Apr;6:23179.

154. Marcinkowska M, Stanczyk M, Janaszewska A, Sobierajska E, Chworos A, Klajnert-Maculewicz B. Multicomponent Conjugates of Anticancer Drugs and Monoclonal Antibody with PAMAM Dendrimers to Increase Efficacy of HER-

2 Positive Breast Cancer Therapy. Pharm Res. 2019 Sep 3;36(11):154.

155. Marcinkowska M, Stanczyk M, Janaszewska A, Gajek A, Ksiezak M, Dzialak P, et al. Molecular Mechanisms of Antitumor Activity of PAMAM Dendrimer Conjugates with Anticancer Drugs and a Monoclonal Antibody. Polymers (Basel). 2019 Aug 29;11(9):1422.

156. Fox LJ, Richardson RM, Briscoe WH. PAMAM dendrimer - cell membrane interactions. Adv Colloid Interface Sci. 2018 Jul;257:1–18.

157. Horibata S, Vo T V, Subramanian V, Thompson PR, Coonrod SA. Utilization of the Soft Agar Colony Formation Assay to Identify Inhibitors of Tumorigenicity in Breast Cancer Cells. J Vis Exp. 2015 May 20;(99):e52727–e52727.

158. Gkouveris I, Nikitakis NG. Role of JNK signaling in oral cancer: A mini review. Tumour Biol. 2017 Jun;39(6):1010428317711659.

159. Ashenden M, van Weverwijk A, Murugaesu N, Fearns A, Campbell J, Gao Q, et al. An In Vivo Functional Screen Identifies JNK Signaling As a Modulator of Chemotherapeutic Response in Breast Cancer. Mol Cancer Ther. 2017 Sep;16(9):1967–78.

160. Gajbhiye V, Palanirajan VK, Tekade RK, Jain NK. Dendrimers as therapeutic agents: a systematic review. J Pharm Pharmacol. 2009 Aug;61(8):989–1003.

161. Mollazade M, Nejati-Koshki K, Akbarzadeh A, Zarghami N, Nasiri M, Jahanban-Esfahlan R, et al. PAMAM dendrimers augment inhibitory effects of curcumin on cancer cell proliferation: possible inhibition of telomerase. Asian Pac J Cancer Prev. 2013;14(11):6925–8.

162. El-Kenawi AE, El-Remessy AB. Angiogenesis inhibitors in cancer therapy: mechanistic perspective on classification and treatment rationales. Br J Pharmacol. 2013/10/01. 2013 Oct;170(4):712–29.

163. Carmeliet P. Angiogenesis in health and disease. Nat Med. 2003 Jun;9(6):653–60.

164. Willis LM, El-Remessy AB, Somanath PR, Deremer DL, Fagan SC. Angiotensin receptor blockers and angiogenesis: clinical and experimental evidence. Clin Sci (Lond). 2011 Apr;120(8):307–19.

165. Huang Z, Yang Y, Jiang Y, Shao J, Sun X, Chen J, et al. Anti-tumor immune responses of tumor-associated macrophages via toll-like receptor 4 triggered by cationic polymers. Biomaterials. 2013 Jan;34(3):746–55.

166. Siveen KS, Prabhu K, Krishnankutty R, Kuttikrishnan S, Tsakou M, Alali FQ, et al. Vascular Endothelial Growth Factor (VEGF) Signaling in Tumour Vascularization: Potential and Challenges. Curr Vasc Pharmacol. 2017;15(4):339–51.

167. Karaman S, Leppanen V-M, Alitalo K. Vascular endothelial growth factor signaling in development and disease. Development. 2018 Jul;145(14).

168. de Aguiar RB, de Moraes JZ. Exploring the Immunological Mechanisms Underlying the Anti-vascular Endothelial Growth Factor Activity in Tumors. Front Immunol. 2019;10:1023.

169. Ceci C, Atzori MG, Lacal PM, Graziani G. Role of VEGFs/VEGFR-1 Signaling and its Inhibition in Modulating Tumor Invasion: Experimental Evidence in Different Metastatic Cancer Models. Int J Mol Sci. 2020 Feb;21(4).

170. Heiden TCK, Dengler E, Kao WJ, Heideman W, Peterson RE. Developmental toxicity of low generation PAMAM dendrimers in zebrafish. Toxicol Appl Pharmacol. 2007 Nov;225(1):70–9.

171. Calienni MN, Feas DA, Igartua DE, Chiaramoni NS, Alonso SDV, Prieto MJ. Nanotoxicological and teratogenic effects: A linkage between dendrimer surface

charge and zebrafish developmental stages. Toxicol Appl Pharmacol. 2017 Dec;337:1–11.

172. Oliveira E, Casado M, Faria M, Soares AMVM, Navas JM, Barata C, et al. Transcriptomic response of zebrafish embryos to polyaminoamine (PAMAM) dendrimers. Nanotoxicology. 2014 Aug;8 Suppl 1:92–9.